

UC Berkeley

UC Berkeley Electronic Theses and Dissertations

Title

Biogeochemical response to hurricanes and droughts: indicators of climate change impacts on tropical forest ecosystems

Permalink

<https://escholarship.org/uc/item/0cq3r37z>

Author

Gutierrez del Arroyo, Omar

Publication Date

2021

Peer reviewed|Thesis/dissertation

Biogeochemical response to hurricanes and droughts:
indicators of climate change impacts on tropical forest ecosystems

By

Omar Gutiérrez del Arroyo

A dissertation submitted in partial satisfaction of the
requirements for the degree of

Doctor of Philosophy

in

Environmental Science, Policy, and Management

in the

Graduate Division

of the

University of California, Berkeley

Committee in charge:

Professor Whendee L. Silver

Professor Mary Firestone

Professor Jeffrey Chambers

Summer 2021

Abstract

Biogeochemical responses to hurricanes and droughts:
indicators of climate change impacts on tropical forest ecosystems

By

Omar Gutiérrez del Arroyo

Doctor of Philosophy in Environmental Science, Policy, and Management

University of California, Berkeley

Professor Whendee L. Silver, Chair

The effects of climate change are causing widespread changes in forest disturbance regimes, with significant implications for ecosystem carbon (C) and nutrient cycles in wet tropical forests. These humid ecosystems are faced with multiple types of natural disturbances, including hurricanes and drought, both of which are projected to increase in frequency due to climate change. Understanding future trajectories of wet tropical forests exposed to novel disturbance regimes requires the study of belowground biogeochemical responses to disturbance at multiple temporal and spatial scales. In this dissertation, I focused on studying the responses of soil biogeochemistry to hurricanes and drought in a wet tropical forest in Puerto Rico. In the first chapter, I present the soil biogeochemical responses to a long-term (10 yr) ecosystem manipulation experiment called the Canopy Trimming Experiment, which revealed the significant impact of hurricane-induced debris deposition on soil biogeochemistry throughout the soil profile. In the second chapter, I make use of an ecosystem biogeochemical model (DayCent) to study the long-term (decades to centuries) effects of changes in the hurricane disturbance regime on soil biogeochemistry, demonstrating the significance of changes in live biomass and soil C pools due to increases in hurricane frequency for ecosystem-scale C fluxes. In the third chapter, I present the results of a throughfall exclusion experiment that demonstrated the rapid and significant effects of drought on soil microclimate and biogeochemical cycling, even within the context of a Category 4 hurricane that had a major impact on the site. This unexpected event gave me the opportunity to study the interaction between these two major disturbances in the field, revealing important insights for better understanding the consequences of changing disturbance regimes for soil biogeochemical cycling and the implications for wet tropical forests.

Table of Contents

Abstract.....	1
Table of Contents.....	i
Dedication.....	ii
List of Figures.....	iii
List of Tables.....	vi
Introduction.....	vii
Acknowledgements.....	viii
Chapter 1: Disentangling the long-term effects of disturbance on soil biogeochemistry in a wet tropical forest ecosystem.....	1
Introductory section.....	1
Abstract.....	2
Introduction.....	3
Materials and Methods.....	4
Results.....	6
Discussion.....	14
References.....	16
Transitional section.....	21
Chapter 2: Modeling the effects of increased hurricane frequency on the tropical forest carbon cycle.....	22
Abstract.....	22
Introduction.....	23
Methods.....	24
Results.....	26
Discussion.....	32
References.....	34
Chapter 3: Soil biogeochemical responses to throughfall exclusion in a wet tropical forest in Puerto Rico.....	41
Abstract.....	41
Introduction.....	42
Materials and Methods.....	43
Results.....	45
Discussion.....	62
References.....	66
Supplementary Figures.....	73
Concluding section.....	81

Dedication

To the world that surrounds me, especially the *Homo sapiens*, for being the reason behind all this process and for being the eternal source of answers to the questions that are yet to come.

Al mundo que me rodea, especialmente a los *Homo sapiens*, por ser la razón de ser de todo este proceso y por ser la eterna fuente de respuestas a las preguntas que vendrán.

List of Figures

Figure 1. (a) Depth profiles of gravimetric soil moisture by treatment; (b) depth profiles of soil pH by treatment (error bars indicate ± 1 SE; $n = 3$; $*p < 0.05$).....	8
Figure 2. Depth profiles of total soil carbon (a) and nitrogen (b) concentrations by treatment (error bars indicate ± 1 SE; $n = 3$; $*p < 0.05$).....	9
Figure 3. Surface (0 to 10 cm) soil carbon (C) concentrations (a) and soil C pools (b) by density fraction for control and debris only treatments (FLF, free-light fraction; OLF, occluded-light fraction; HF, heavy fraction; error bars indicate ± 1 SE; $n = 3$; $*p < 0.10$).....	11
Figure 4. Deep (50 to 60 cm) soil carbon (C) concentrations (a) and soil C pools (b) by density fraction for control and debris only treatments (FLF, free-light fraction; OLF, occluded-light fraction; HF, heavy fraction; error bars indicate ± 1 SE; $n = 3$).....	11
Figure 5. Depth profiles of NaOH-extractable total phosphorus (a), organic phosphorus (b), and inorganic phosphorus (c) (error bars indicate ± 1 SE; $n = 3$; $*p < 0.05$).....	13
Figure 6. Time-series of live forest biomass C (mean ± 1 SEM; $n=8$) by hurricane frequency...26	26
Figure 7. Time-series of leaf area index (mean ± 1 SEM; $n=8$) by hurricane frequency.....28	28
Figure 8. Time-series of total soil C (mean ± 1 SEM; $n=8$) by hurricane frequency treatment (note inset with shortened y-axis that allows for improved visualization of patterns during treatment period).....28	28
Figure 9. Time-series of soil C fractions (mean ± 1 SEM; $n=8$) across hurricane frequency treatments: a) active soil C b) slow soil C c) passive soil C (note differences in ranges and increasing magnitudes of y-axes from a-c).....30	30
Figure 10. Boxplot of the cumulative hurricane debris inputs showing the significant increase in magnitude at the highest hurricane frequencies ($p < 0.001$).....30	30
Figure 11. Forest ecosystem C fluxes (Mg C/ha) across hurricane frequency treatments including heterotrophic respiration (HET; red), net primary productivity (NPP; green), and net ecosystem productivity (NEP; blue; calculated as the difference between NPP and HET, such that negative NEP indicates the ecosystem is a C source).....32	32
Figure 12a-c. Mean daily volumetric soil moisture (\pm SE, $n = 5$) by treatment for a) 0-15 cm, b) 15-30 cm, c) 30-45 cm. Black vertical dashed lines indicate start/end of throughfall exclusion period (March 2017 and November 2018, respectively), and red vertical dashed lines indicate Hurricanes Irma and María in September 2017.....47	47

Figure 13a-c. Mean daily soil oxygen concentrations (\pm SE, n = 5 per depth) by treatment for a) 0-15 cm, b) 15-30 cm, c) 30-45 cm. Black vertical dashed lines indicate start/end of throughfall exclusion period (March 2017 and November 2018, respectively), and red vertical dashed lines indicate Hurricanes Irma and María in September 2017.....49

Figure 14a-c. Mean daily soil temperature (\pm SE, n = 5) by treatment for a) 0-15 cm, b) 15-30 cm, and c) 30-45 cm. Black vertical dashed lines indicate start/end of throughfall exclusion period (March 2017 and November 2018, respectively), and red vertical dashed lines indicate Hurricanes Irma and María in September 2017.....51

Figure 15a-c. Mean gravimetric soil moisture (\pm SE, n = 5) by treatment at a) 0-15 cm, b) 15-30 cm, and c) 30-45 cm. Sampling dates are arranged chronologically and include the pre-treatment and post-treatment samplings (Jan-17 and Jan-19, respectively), and the post-hurricane sampling (Oct-17). Other three samplings (Jun-17, Apr-18, Sep-18) occurred with throughfall exclusion. Red and black asterisks denote significance at $p < 0.05$ and $p < 0.1$, respectively.....52

Figure 16a-c. Mean soil pH (\pm SE, n = 5) by treatment at a) 0-15 cm, b) 15-30 cm, and c) 30-45 cm. Sampling dates are arranged chronologically and include the pre-treatment and post-treatment samplings (Jan-17 and Jan-19, respectively), and the post-hurricane sampling (Oct-17). Other three samplings (Jun-17, Apr-18, Sep-18) occurred with throughfall exclusion.....53

Figure 17. Mean NaHCO₃-extractable total soil phosphorus (+ SE, n = 5) at 0-15 cm by treatment. Red and black asterisk indicate significance at $p < 0.05$ or $p < 0.1$, respectively.....55

Figure 18a-c. Mean KCl-extractable soil ammonium (+ SE, n = 5) by treatment at a) 0-15 cm, b) 15-30 cm, and c) 30-45 cm. Red and black asterisk indicate significance at $p < 0.05$ or $p < 0.1$, respectively.....56

Figure 19a-b. Mean total soil carbon (\pm SE, n = 5) by treatment and depth at the a) pre-treatment sampling in January 2017 and b) post-treatment sampling in January 2019. Red asterisk indicates significance at $p < 0.05$57

Figure 20a-b. Mean total soil carbon (\pm SE, n = 5) by sampling date and depth in the a) control plots and b) drought plots. Red and black asterisks indicate significance at $p < 0.05$ and $p < 0.1$, respectively.....59

Figure 21. Mean surface soil CO₂ efflux (\pm SE, n = 5) by treatment and sampling date. Red and black asterisks indicate significance at $p < 0.05$ and $p < 0.1$, respectively.....61

Figure 22a-b. Mean surface a) soil CH₄ and b) soil N₂O fluxes (\pm SE, n = 5) by treatment and sampling date. Black dashed lines indicate start/end of throughfall exclusion treatments and red dashed lines indicate Hurricanes Irma and María in September 2017.....61

Figure 23a-c. Mean surface soil greenhouse gas fluxes (\pm SE, n = 28) of a) CO₂, b) CH₄, and c) N₂O during the throughfall exclusion period from March 2017 to November 2018. Red asterisk indicates significance at $p < 0.05$62

Supplementary Figure 1a-c. Mean HCl-extractable Fe ²⁺ (+ SE, n = 5) by treatment at a) 0-15 cm, b) 15-30 cm, and c) 30-45 cm.....	73
Supplementary Figure 2a-c. Mean HCl-extractable total Fe (+ SE, n = 5) by treatment at a) 0-15 cm, b) 15-30 cm, and c) 30-45 cm.	74
Supplementary Figure 3a-c. Mean citrate ascorbate-extractable Fe (+ SE, n = 5) by treatment at a) 0-15 cm, b) 15-30 cm, and c) 30-45 cm.	75
Supplementary Figure 4a-c. Mean NaHCO ₃ -extractable soil phosphorus (+ SE, n = 5) by treatment at a) 0-15 cm, b) 15-30 cm, and c) 30-45 cm. Red and black asterisk indicate significance at p < 0.05 or p < 0.1, respectively.	76
Supplementary Figure 5a-c. Mean NaOH-extractable inorganic soil phosphorus (+ SE, n = 5) by treatment at a) 0-15 cm, b) 15-30 cm, and c) 30-45 cm.	77
Supplementary Figure 6a-c. Mean NaOH-extractable organic soil phosphorus (+ SE, n = 5) by treatment at a) 0-15 cm, b) 15-30 cm, and c) 30-45 cm.	78
Supplementary Figure 7a-c. Mean NaOH-extractable total soil phosphorus (+ SE, n = 5) by treatment at a) 0-15 cm, b) 15-30 cm, and c) 30-45 cm.	79
Supplementary Figure 8a-c. Mean KCl-extractable soil nitrate (+ SE, n = 5) by treatment at a) 0-15 cm, b) 15-30 cm, and c) 30-45 cm.	80

List of Tables

Table 1. Mean gravimetric soil moisture, soil pH, soil C and N, and Fe concentrations by soil depth and treatment (n/d = no data; S.E. in parentheses; n = 3).....	7
Table 2. Mean increases in soil C and N between control and debris deposition only treatments by soil depth (S.E. in parentheses; n = 3). Bolded values indicate statistically significant differences between treatments ($p < 0.05$). *At these depths in Block A (or Block B for soil N at 10 cm), control plots had higher soil C or N than debris deposition only plots.....	10
Table 3. NaHCO ₃ and NaOH soil phosphorus fractions by soil depth and treatment (units: $\mu\text{g P/g}$ dry soil; S.E. in parentheses; n = 3).....	12
Table 4. Soil mass and carbon concentration of free-light, occluded-light, and heavy fractions, separated from control and debris deposition only treatments using density fractionation (S.E. in parentheses; n = 3; *indicates statistical significance at $p < 0.10$).....	13
Table 5. Hurricane-induced percentage loss of each biomass fraction.....	25
Table 6. Forest C stocks and annual aboveground C inputs (mean \pm 1SEM; n = 8) for the Luquillo Experimental Forest by hurricane frequency (letters denote significant differences among treatments at $p < 0.05$).....	27
Table 7. Leaf area index (mean \pm 1SEM; n = 8) by hurricane frequency during the last 400 years of the simulations, which excludes the initial transition period (letters denote significant differences among treatments at $p < 0.05$).....	27
Table 8. Soil C pools (mean \pm 1SEM; n = 8) across hurricane frequency treatments (letters denote significant differences among treatments at $p < 0.05$).....	29
Table 9. Annual ecosystem C fluxes (mean \pm 1SEM; n = 8) for the Luquillo Experimental Forest across hurricane frequency treatments (negative NEP indicates ecosystem is a C source; letters denote significant differences among treatments at $p < 0.05$).....	31
Table 10. Mean daily volumetric soil moisture, soil oxygen concentration, and soil temperature (\pm SE) at 0-15 cm by treatment and time-period. Different capital letters denote significance between treatments for each variable at $p < 0.05$	46
Table 11. Mean soil greenhouse gas fluxes (\pm SE) for different periods during the experiment. Letters indicate significance at $p < 0.05$ between treatments within each period for each gas....	60

Introduction

Changing disturbance regimes due to climate change can have significant implications for biogeochemical cycles in forest ecosystems. Understanding the potential feedbacks between changing disturbance regimes and ecosystem carbon (C) and nutrient cycling is critical for constraining the future role of forests in the global C cycle, and thus their effects on the global climate system. The preeminent role of wet tropical forests for the global C cycle is well recognized, but there is a large gap of knowledge in terms of the varying timescales of response of different ecosystem components to disturbances, especially belowground in the soil matrix where plant-microbial interactions occur. The large uncertainties surrounding the disturbance response of soil biogeochemistry in wet tropical forests, where high productivity coincides with frequent exposure to disturbances, limit the ability to project potential changes in forest form and function that may occur in response to novel climate and disturbance regimes.

I aimed to address these uncertainties in this dissertation by taking advantage of experimental and modeling approaches that were all based on the Tabonuco Forest within the Luquillo Experimental Forest in Puerto Rico. By taking the approach of combining methods, I was able to address questions at different spatial and temporal scales providing a more comprehensive understanding of the disturbance-responses that occur within these dynamic ecosystems. Moreover, the long experimental history of this site affords the unique opportunity of having access to extensive complementary data that serves to contextualize the results presented here.

The structure of this dissertation begins with a chapter describing the soil biogeochemical response after ten years of the Canopy Trimming Experiment, which aimed to separate the individual and combined effects of the two main structural changes caused by hurricanes: canopy opening and debris deposition. This long-term field manipulation demonstrated that debris deposition has significant effects on soil biogeochemistry throughout the soil profile, and confirmed the resilience of soil C and nutrient pools to hurricane disturbances. While ten years can be considered long-term for field-based experiments, a modeling approach was advantageous for extending our question about the effects of changing disturbance regimes to longer time-scales (decadal to centennial). These results are presented in the second chapter, which revealed the importance of hurricane frequency for live biomass and soil C pools, as well as the future forest C balance. In combination, the two initial chapters serve to highlight the different time-scales at which hurricane disturbances can affect various ecosystem components (i.e., vegetation vs. soils), with significant long-term consequences for the forest form and function. The final chapter of this dissertation focuses on drought where I describe the Luquillo Throughfall Exclusion Experiment, which aimed to understand the effects of drought on soil microclimate and biogeochemical cycling throughout the soil profile. This experiment was initially designed to focus only on drought, but the impacts of Hurricanes Irma and María in 2017 added an additional component with the study of the hurricane effects in the field.

Acknowledgements

First off, I would like to thank my family, especially my wife Camille, for her invaluable support and the countless sacrifices made during this process. I am also grateful for my dissertation chair and advisor Whendee L. Silver believing in me as a young student and helping me become a better scientist. Similarly, I would like to thank my committee members Mary Firestone, Jeff Chambers, Dennis Baldocchi, and Todd Dawson for the time dedicated to my formation as a scientist.

I would like to thank Dr. Melannie Hartman at Colorado State University for her continued training with the DayCent model and support in the preparation of the second chapter. I want to specially thank Gisela González, Jordan Stark and Ryan Salladay from UC Berkeley and Sarah Stankavich from El Verde Field Station for collecting and shipping soils, as well as Heather Dang, Summer Ahmed, and Drs. Christine O’Connell and Yang Lin, among others in the Silver Lab for providing invaluable assistance with sample processing and data analyses. Drs. Steven J. Hall, Wenbo Yang, and Andrew Yang provided guidance and assisted with iron analyses at UC Berkeley. I am grateful to the Luquillo LTER, the International Institute of Tropical Forestry, and the University of Puerto Rico, Río Piedras for establishing and maintaining the ongoing Canopy Trimming Experiment for over a decade, and for the support with the throughfall exclusion experiment. Finally, I want to acknowledge an anonymous reviewer whose constructive criticism substantially improved the quality of the first chapter manuscript.

This work was supported by grants from the Department of Energy and National Science Foundation to W.L.S. as well as the NSF Luquillo Critical Zone Observatory to the University of New Hampshire and the NSF Luquillo LTER to the University of Puerto Rico. O.G.A. was supported by an NSF Graduate Research Fellowship, as well as the Berkeley Fellowship for Graduate Study.

Introductory Section

The structure of this dissertation will begin with an initial chapter where I present the responses of soil biogeochemistry after a decade of the Canopy Trimming Experiment in the Luquillo Experimental Forest. This manuscript, which has been co-authored with my advisor Dr. Whendee L. Silver and published in the peer-reviewed journal *Global Change Biology*, provides valuable insights into how soil biogeochemistry varies with depth in a wet tropical forest, as well as describing the individual and combined decadal effects of canopy trimming and debris deposition. These are the two main effects of hurricanes on forest structure, which I hypothesized had contrasting effects on soil biogeochemistry. The importance of this first chapter for the development of this dissertation is providing a comprehensive description of the context in which disturbance regime changes are ongoing. Further, the ability of separating the effects of debris deposition and canopy opening was essential for understanding the long-term response to repeated hurricane disturbances, as was evaluated in the second chapter.

Title: Disentangling the long-term effects of disturbance on soil biogeochemistry in a wet tropical forest ecosystem

Key words: tropical forest, hurricane, disturbance, soil nutrients, carbon sequestration, phosphorus, soil depth

Abstract

Climate change is increasing the intensity of severe tropical storms and cyclones (also referred to as hurricanes or typhoons), with major implications for tropical forest structure and function. These changes in disturbance regime are likely to play an important role in regulating ecosystem carbon (C) and nutrient dynamics in tropical and subtropical forests. Canopy opening and debris deposition resulting from severe storms have complex and interacting effects on ecosystem biogeochemistry. Disentangling these complex effects will be critical to better understand the long-term implications of climate change on ecosystem C and nutrient dynamics. In this study, we used a well-replicated, long-term (10 y) canopy and debris manipulation experiment in a wet tropical forest to determine the separate and combined effects of canopy opening and debris deposition on soil C and nutrients throughout the soil profile (1 m). Debris deposition alone resulted in higher soil C and N concentrations, both at the surface (0-10 cm) and at depth (50-80 cm). Concentrations of NaOH-organic P also increased significantly in the debris deposition only treatment (20-90 cm depth), as did NaOH-total P (20-50 cm depth). Canopy opening, both with and without debris deposition, significantly increased NaOH-inorganic P concentrations from 70-90 cm depth. Soil iron concentrations were a strong predictor of both C and P patterns throughout the soil profile. Our results demonstrate that both surface- and subsoils have the potential to significantly increase C and nutrient storage a decade after the sudden deposition of disturbance-related organic debris. Our results also show that these effects may be partially offset by rapid decomposition and decreases in litterfall associated with canopy opening. The significant effects of debris deposition on soil C and nutrient concentrations at depth (>50 cm), suggest that deep soils are more dynamic than previously believed, and can serve as sinks of C and nutrients derived from disturbance-induced pulses of organic matter inputs.

Introduction

Climate change is affecting the intensity of severe tropical storms, the most powerful of which are cyclones (also referred to as hurricanes or typhoons), with significant implications for ecosystem processes in near-coastal tropical forests (Knutson *et al.*, 2010, Lugo, 2000, Walsh *et al.*, 2016). These observed and projected changes in disturbance regime are likely to play an important role in regulating ecosystem carbon (C) and nutrient dynamics (Crausbay & Martin, 2016, Dale *et al.*, 2001, Lugo, 2000, Lugo, 2008, Xi, 2015). The major effects of severe storms on ecosystem structure, and feedbacks on multiple ecosystem processes, have been well documented in forests globally (Bellingham *et al.*, 1996, Boose *et al.*, 1994, Burslem *et al.*, 2000, Lin *et al.*, 2011, Lugo, 2008, Shaw, 1983, Tanner *et al.*, 1991, Webb, 1958, Wolfgang, 1985, Xi, 2015). However, the bulk of this research has focused on aboveground dynamics, and much less attention has been given to the effects on belowground processes such as soil C and nutrient cycling (Ostertag *et al.*, 2003, Parrotta & Lodge, 1991, Sanford *et al.*, 1991, Vargas, 2012, Vargas & Allen, 2008). Furthermore, despite the major implications of the belowground effects of severe tropical storms on the global C cycle, the long-term (> 5 y) effects on soil biogeochemistry have only rarely been studied in tropical forests.

Organic matter redistribution is likely to be a major driver of belowground responses to canopy disturbance associated with storm events (Lodge *et al.*, 2014, Sanford *et al.*, 1991, Silver *et al.*, 2014, Turton, 2008, Vargas, 2012). High velocity winds result in a large deposition of biomass from the canopy to the forest floor (Frangi & Lugo, 1991, Horng *et al.*, 1995, Lin *et al.*, 2003, Lodge *et al.*, 1991, Wang *et al.*, 2016, Whigham *et al.*, 1991, Xu *et al.*, 2004). The contribution of green leaves and live branches to total litterfall during these disturbances results in a pulse of C and nutrients to the soil (González *et al.*, 2014, Lin *et al.*, 2002, Lodge *et al.*, 1994, Lodge *et al.*, 1991, Silver *et al.*, 2014, Sullivan *et al.*, 1999). The effects of organic matter redistribution during storms on soil biogeochemistry may be varied and dependent on the time-scale considered (Scatena, 2013, Silver *et al.*, 1996). In the short-term, storm-associated pulses of organic debris can provide labile C, as well as N, phosphorus (P), and other essential nutrients for microbial and root uptake, potentially increasing rates of plant and microbial activity (Lodge *et al.*, 1994, Lodge *et al.*, 1991, Vargas, 2012, Vargas & Allen, 2008). Large inputs of woody debris with high C:N and C:P ratios can simultaneously lead to increased nutrient immobilization by microbial decomposers, which, in addition to leaching losses, results in a transient decrease in nutrient availability (Rice *et al.*, 1997, Zimmerman *et al.*, 1995). Rapid decomposition of storm-related debris may increase rates of ecosystem recovery from disturbance (Beard *et al.*, 2005). Ostertag *et al.* (2003) found that the forest floor mass returned to pre-disturbance levels in less than one year following a hurricane in Puerto Rico. They suggested that the rapid disappearance of leaf litter and associated nutrients was an indicator of a high degree of resilience of tropical forests to severe storms (Beard *et al.*, 2005, Ostertag *et al.*, 2003, Vogt *et al.*, 1996).

Partially decomposed organic materials can be translocated deeper into the soil profile. Most of the research on disturbance effects has been conducted in surface soils (< 50 cm), so little is known about if and how disturbance impacts are propagated through the soil profile (Xu *et al.*, 2004). Over time, a fraction of the C, N, and P in the deposited debris may be transported into the subsoil through a variety of physical and biological pathways (Cotrufo *et al.*, 2015, Leff *et al.*, 2012). The subsoil has the potential to become a major sink for soil C and nutrients derived from the disturbance-induced pulse of organic matter through increasing organ-mineral interactions or accumulating detritus. Thus, the legacy of storms and hurricanes on soil biogeochemistry is likely to occur throughout the entire soil profile, and not just near the surface.

In addition to the pulse of debris, changes in forest structure caused by severe storms can have complex and interacting effects on ecosystem C and nutrient cycling (Shiels *et al.*, 2015, Xi, 2015). For example, canopy opening can alter microclimate conditions (i.e., light, temperature, and humidity; Shiels & González, 2014), reduce litterfall inputs (Beard *et al.*, 2005, Silver *et al.*, 2014), cause fine root mortality (Beard *et al.*, 2005, Silver *et al.*, 1996, Silver & Vogt, 1993), and stimulate decomposition rates at the soil surface (Ostertag *et al.*, 2003). Changes in tree species composition following disturbance (i.e., an increase in light-demanding, low wood density pioneers such as *Cecropia sheberiana*) could alter the quantity and quality of C inputs, and affect subsequent rates of C and nutrient cycling (Shiels *et al.*, 2010). These changes in the quantity and quality of organic matter inputs associated with canopy opening can have major implications for the trajectories of ecosystem recovery, although this may also be a transient response as the pre-disturbance vegetation recovers. At longer time-scales, the recovery of organic matter inputs to pre-disturbance levels (both quantity and quality) may be an important factor in determining legacy effects on soil biogeochemistry (Scatena *et al.*, 1996, Silver *et al.*, 1996).

Disentangling the complex effects of canopy opening and debris deposition in tropical forests is critical to better understand the long-term implications of changing disturbance regimes on ecosystem C and nutrient dynamics. In this study, we used the long-term canopy trimming experiment (CTE) in a wet tropical forest in Puerto Rico (Shiels & González, 2014) to determine the separate and combined effects of canopy opening and debris deposition on soil C and nutrients throughout the soil profile. This design did not mimic all aspects of a severe storm event (e.g. high wind and rainfall and associated sheer stress impacts), but instead was a controlled experiment that facilitated the study of two important impacts common to all severe storm events that would not be possible during an actual storm. We tested the hypothesis that hurricane disturbances (combined canopy opening with debris deposition) have detectable long-term effects on soil organic C and nutrient concentrations, due primarily to the lasting impacts of debris deposition on the soil surface. We predicted that the large debris deposition associated with severe storms would dominate the biogeochemical responses, with greater C and nutrient concentrations than plots with canopy opening only. We also hypothesized that canopy opening alone would lead to long-term declines in soil C and N due to lower litterfall rates (Scatena *et al.* 1996, Silver *et al.* 2014), and an increase in soil P, due to lower plant P uptake from a damaged canopy, coupled with higher P retention in soils relative to the C and N released via decomposing litter (Mage & Porder, 2012, Sanford *et al.*, 1991). Finally, we predicted that the effects of debris deposition would lead to long-term C, N, P accumulation through the soil profile, and that when combined with canopy opening this effect would decline due to the higher decomposition rates and lower litterfall inputs associated with canopy disturbance (Ostertag *et al.* 2003).

Materials and Methods

Study site and experimental design

The study was conducted in the El Verde research area of the Luquillo Experimental Forest (LEF), Puerto Rico, as part of the NSF-sponsored Long Term Ecological Research program (18° 20' N, 65°49' W). This area of subtropical wet forest is dominated by the tabonuco forest type, which characterizes most of the lowlands within the LEF (~350 m a.s.l.; Ewel & Whitmore, 1973). Dominant tree species include *Dacryodes excelsa* (Vahl) (Burseraceae), *Sloanea berteriana* (Choisy) (Elaeocarpaceae), and *Manilkara bidentata* ((A.DC)A.Chev)

(Sapotaceae), as well as the palm *Prestoea acuminata* (Willdenow) H.E. Moore var. *montana* (Graham) Henderson and Galeano (Arecaceae). Mean air temperature from 2000 to 2017 was 24 °C, while mean annual precipitation is ~3,500 mm, both exhibiting only slight seasonality (Brown *et al.*, 1983, García-Martínó *et al.*, 1996). Soils are classified as highly weathered Oxisols derived from volcanoclastic sediments, with high clay content (Mage & Porder, 2012, Silver *et al.*, 1994).

Soils were collected from the Canopy Trimming Experiment (CTE), a long-term, ecosystem-scale study aimed at understanding the effects of severe disturbances on forest dynamics by separating the individual and interactive effects of canopy opening and debris deposition (Shiels & González, 2014). The CTE consisted of a randomized complete block design that imposed the following treatments replicated across three blocks: untreated control, canopy opening only, debris deposition only, and a combination of canopy opening and debris deposition. One soil core (2.5 inches in diameter) was collected from each of twelve 30 x 30 m plots, which resulted in three replicates per treatment per depth. Within each block, plots were separated by at least 20 m, and factors such as land-use history (>80% forest cover in 1936), soil type (Zarzal clay series), topography (average slope of 24°), and elevation (340-485 m) were similar across blocks (Shiels *et al.*, 2010).

Treatments were imposed between late 2004 and early 2005, and a range of ecological processes including plant succession, litterfall, and nutrient cycling was followed for nearly a decade afterwards (Shiels & González, 2014). In late 2014, soils were sampled in each plot at 10 cm intervals down to 1 m depth. Immediately after collection, soils were placed in labeled zip-lock bags (double-bagged to retain moisture) and shipped in coolers overnight from Puerto Rico to UC Berkeley for laboratory analyses.

Laboratory procedures

We measured soil pH in a 1:1 soil to water slurry, as well as gravimetric soil moisture by oven-drying subsamples at 105 °C to a constant weight. Total soil C and N content were measured on a CE Instruments NC 2100 Elemental Analyzer (Rodano, Milano, Italy) on soils that were air-dried and ground. To measure labile (i.e., soluble phosphate) and recalcitrant (i.e., bound to Fe or Al) P pools, we used a modified Hedley fractionation with NaHCO₃ and NaOH extractions, respectively (Tiessen & Moir, 1993). Briefly, we sequentially extracted approximately 1.5 g fresh soil with 0.5M NaHCO₃ and 0.1M NaOH. Both extracts were analyzed colorimetrically for inorganic P and total P after digestion with acid ammonium persulfate, while organic P was calculated as the difference between total and inorganic P (Murphy & Riley, 1962). We measured Fe species as these have been shown to be an important predictor of both C (Hall and Silver 2015) and P (Chacon *et al.* 2006) cycling in this ecosystem. Concentrations of reduced and oxidized iron (Fe(II) + Fe(III)) were measured with a 0.5 M HCl extraction and analyzed colorimetrically. Soils were extracted with 0.2 M sodium citrate/0.05M sodium ascorbate solution and analyzed on an inductively coupled plasma atomic emission spectrometer (Perkin-Elmer, USA) for poorly crystalline Fe. We were only able to analyze two treatments for citrate ascorbate-extractable Fe due to limited resources, and thus chose the controls and the opening+debris treatments as being most representative of a natural event.

Soil C density fractionation was used to compare free-light (FLF), occluded-light (OLF), and heavy (HF) fractions in surface and deep soils (0-10 and 50-60 cm, respectively) of the control and debris treatments (Marín-Spiotta *et al.*, 2008). We chose this comparison because the debris deposition only treatment was the only one that showed statistically significant changes in soil C concentrations along the depth profile. Depths were chosen based on statistically

significant patterns in the bulk soil C concentration data, with the 50-60 cm depth representing the top of the zone of accumulation in the subsoil. Using a sodium polytungstate solution (1.85 g/cm³) we separated each fraction from moist soils and determined their mass and C concentration after rising repeatedly with DI water (stopped when density reached 1.0 g/cm³). Bulk density measurements from the CTE (D.J. Lodge and A. Shiels, *unpublished data*) were used to calculate soil C pools in each fraction.

Statistical analyses

A linear mixed-effects model with treatment and depth as fixed factors, and block as a random factor, was used to test for significant differences in soil moisture, pH, bulk soil C and N concentrations, and P and Fe concentrations. To compare the soil density fractionation data from the control and debris deposition treatments we used students t-tests, while linear and non-linear regressions were used to determine relationships between the measured variables (i.e., C, P, Fe). All analyses were conducted in the open source software, R Studio (Version 1.0.136). Values reported in the text are means plus or minus one standard error. Statistical significance was determined at $p < 0.10$ unless otherwise noted.

Results

Soil moisture and pH

Gravimetric soil moisture decreased significantly with depth across all treatments ($p < 0.0001$; Figure 1a). Mean soil moisture at 0-10 cm was 42.7 ± 1.4 % and decreased linearly to 60 cm. Below this depth (60-100 cm), soil moisture showed little variation, with mean values ranging between 32.5 ± 0.5 and 34.2 ± 0.5 % (Figure 1a). There was no significant treatment effect on soil moisture.

Soil pH also decreased significantly with depth across all treatments ($p < 0.0001$; Figure 1b). Soil pH at 0-10 cm ranged from 4.62 ± 0.17 to 4.89 ± 0.08 (canopy opening only and debris deposition only treatments, respectively), while values at 90-100 cm ranged from 4.97 ± 0.11 to 5.16 ± 0.08 (debris deposition only and control treatments, respectively). There was a significant treatment effect of canopy opening only in surface soils (0-30 cm, $p < 0.05$), which resulted in the lowest pH values measured (< 4.75) and a steeper depth gradient than the other treatments (Figure 1b).

Table 1. Mean gravimetric soil moisture, soil pH, soil C and N, and Fe concentrations by soil depth and treatment (n/d = no data; S.E. in parentheses; n = 3).

Soil depth (cm)	Gravimetric soil moisture (%)			Soil pH			Soil C (%)			Soil N (%)			Citrate-ascorbate Fe (mg/g)			HCl Fe(II)+Fe(III) (mg/g)			
	Control	Opening only	Debris + debris only	Control	Opening only	Debris + debris only	Control	Opening only	Debris only	Control	Opening only	Debris only	Control	Opening only	Debris + debris only	Control	Opening only	Debris only	
10	42.1 (3.3)	42.7 (1.2)	41.5 (4.2)	4.89 (0.07)	4.62 (0.17)	4.89 (0.08)	5.27 (0.65)	5.63 (0.81)	6.72 (0.41)	5.37 (0.27)	0.40 (0.05)	0.48 (0.04)	1.89 (0.05)	0.43 (0.00)	1.97 (0.39)	1.70 (0.48)	1.43 (0.11)	1.35 (1.23)	2.32 (1.23)
20	38.3 (2.0)	40.4 (1.5)	37.5 (3.4)	5.07 (0.04)	4.77 (0.17)	5.02 (0.06)	2.83 (0.26)	3.29 (0.73)	3.69 (0.59)	3.04 (0.21)	0.24 (0.02)	0.25 (0.04)	1.50 (0.14)	0.25 (0.00)	1.41 (0.34)	0.95 (0.25)	0.90 (0.23)	1.03 (1.39)	1.91 (1.39)
30	36.8 (1.8)	38.8 (1.5)	36.3 (2.6)	5.03 (0.04)	4.73 (0.19)	5.03 (0.02)	2.33 (0.24)	2.51 (0.53)	2.99 (0.67)	2.40 (0.17)	0.19 (0.02)	0.19 (0.03)	1.15 (0.17)	0.20 (0.00)	1.05 (0.37)	0.68 (0.08)	0.73 (0.25)	0.84 (0.36)	0.82 (0.49)
40	35.1 (1.7)	37.0 (2.5)	36.7 (3.4)	4.99 (0.04)	4.92 (0.19)	4.92 (0.04)	1.65 (0.29)	1.99 (0.65)	2.64 (0.84)	1.71 (0.26)	0.14 (0.02)	0.14 (0.04)	0.84 (0.27)	0.14 (0.01)	0.56 (0.31)	0.39 (0.12)	0.39 (0.10)	0.59 (0.28)	0.35 (0.19)
50	33.6 (1.1)	35.9 (2.6)	35.8 (3.5)	5.05 (0.02)	4.94 (0.17)	4.96 (0.07)	1.11 (0.17)	1.66 (0.62)	2.24 (0.86)	1.49 (0.15)	0.08 (0.01)	0.11 (0.03)	0.42 (0.11)	0.12 (0.01)	0.27 (0.13)	0.24 (0.05)	0.23 (0.05)	0.55 (0.24)	0.17 (0.05)
60	32.8 (0.8)	34.2 (1.2)	35.8 (3.6)	5.09 (0.02)	5.00 (0.17)	4.95 (0.12)	0.79 (0.08)	1.11 (0.30)	1.80 (0.71)	1.00 (0.18)	0.06 (0.00)	0.14 (0.04)	0.26 (0.08)	0.08 (0.01)	0.16 (0.05)	0.14 (0.02)	0.17 (0.03)	0.47 (0.27)	0.11 (0.02)
70	32.6 (1.5)	32.3 (0.4)	35.1 (3.6)	5.03 (0.15)	5.02 (0.17)	4.88 (0.03)	0.62 (0.03)	0.66 (0.20)	1.50 (0.50)	0.81 (0.12)	0.05 (0.01)	0.11 (0.03)	0.12 (0.04)	0.07 (0.00)	0.10 (0.03)	0.11 (0.02)	0.12 (0.01)	0.22 (0.07)	0.10 (0.02)
80	33.4 (1.4)	32.7 (1.5)	33.6 (3.9)	5.06 (0.04)	4.99 (0.18)	4.99 (0.09)	0.62 (0.06)	0.48 (0.13)	1.26 (0.38)	0.70 (0.10)	0.05 (0.01)	0.04 (0.01)	0.12 (0.03)	0.06 (0.01)	0.08 (0.02)	0.09 (0.02)	0.13 (0.01)	0.27 (0.10)	0.08 (0.01)
90	33.7 (0.7)	31.2 (0.5)	33.4 (3.8)	5.20 (0.11)	4.99 (0.25)	4.92 (0.09)	0.54 (0.08)	0.39 (0.11)	0.81 (0.29)	0.67 (0.19)	0.04 (0.00)	0.06 (0.02)	0.08 (0.02)	0.06 (0.01)	0.09 (0.04)	0.08 (0.01)	0.27 (0.16)	0.13 (0.01)	0.09 (0.01)
100	34.0 (0.8)	32.0 (0.9)	33.1 (3.3)	5.16 (0.08)	5.14 (0.29)	4.97 (0.11)	0.52 (0.03)	0.37 (0.07)	0.80 (0.29)	0.61 (0.15)	0.04 (0.00)	0.03 (0.02)	0.10 (0.02)	0.06 (0.01)	0.08 (0.03)	0.08 (0.00)	0.35 (0.25)	0.14 (0.04)	0.08 (0.02)

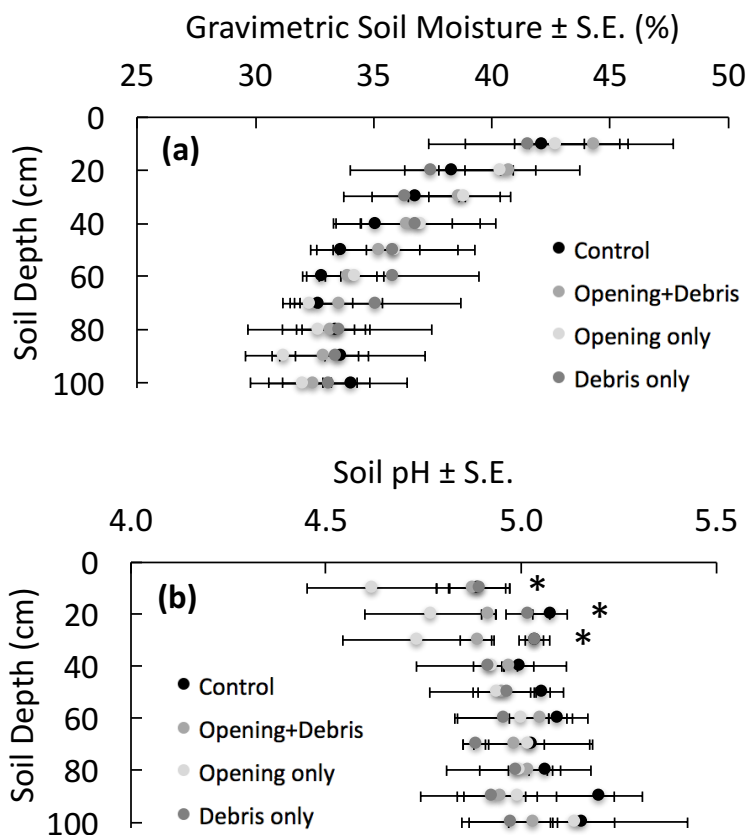


Figure 1. (a) Depth profiles of gravimetric soil moisture by treatment; (b) Depth profiles of soil pH by treatment (error bars indicate ± 1 S.E.; $n = 3$; * $p < 0.05$).

Iron species

The concentration of both HCl- and citrate ascorbate-extractable Fe species decreased significantly with depth across all treatments ($p < 0.001$; Table 1). Soil Fe concentrations decreased linearly from surface soils down to 60 cm, where concentrations stabilized at low values. The sum of HCl-extractable Fe(II) and Fe(III) decreased from 1.7 ± 0.3 mg/g at 0-10 cm (mean across treatments), to less than 0.5 mg/g below 50 cm for all treatments. Similarly, citrate ascorbate-extractable Fe showed strong depth gradients regardless of the treatment, decreasing from 1.9 ± 0.2 mg/g at 0-10 cm and stabilizing around 0.1 mg/g below 60 cm. There were no significant treatment effects on any of the forms of soil Fe measured.

Soil carbon and nitrogen concentrations

Across all treatments, there was a significant decrease in soil C concentration with depth ($p < 0.0001$; Figure 2a). Mean soil C concentrations across treatments decreased from 5.8 ± 0.3 % at 0-10 cm to 0.6 ± 0.1 % at 90-100 cm. There was a significant treatment effect of debris deposition only on soil C concentrations ($p < 0.05$; Figure 2a), both at the surface (0-10 cm) and at depth (50-80 cm). Notably, soil C concentrations below 60 cm were lower than 1 % for all treatments except debris deposition only, demonstrating the significant treatment effects on subsoil C concentrations. All other treatments (opening+debris and canopy opening only)

resulted in trends of increasing soil C across all depths, except deep soils (>80 cm) in the canopy opening only treatment, which showed a trend of lower soil C relative to the control. Including the data from all depths, soil C concentrations were significantly positively correlated with citrate ascorbate-extractable Fe in both control ($R^2 = 0.95$, $p < 0.05$) and canopy opening with debris deposition treatments ($R^2 = 0.85$, $p < 0.05$). Soil C concentrations also showed a significant positive correlation with HCl-extractable Fe ($R^2 = 0.79$, $p < 0.05$).

Soil N concentrations decreased significantly with depth across all treatments ($p < 0.05$; Figure 2b). Mean soil N concentrations ranged from 0.43 ± 0.02 to 0.05 ± 0.01 %, at 0-10 and 90-100 cm, respectively. There was a significant treatment effect of debris deposition only on soil N concentrations from 50-80 cm, where soil N concentrations were particularly low (<0.1 %) and showed a >100% increase in response to the treatment (Figure 2b).

Overall, debris deposition alone significantly increased soil C and N concentrations by 26 to 142 % and 16 to 123 % (calculated for each 10 cm sampling interval relative to the control treatment), respectively, with the greatest relative increases (i.e., >100 %) occurring deep in the soil profile at 60-70 cm (Table 2).

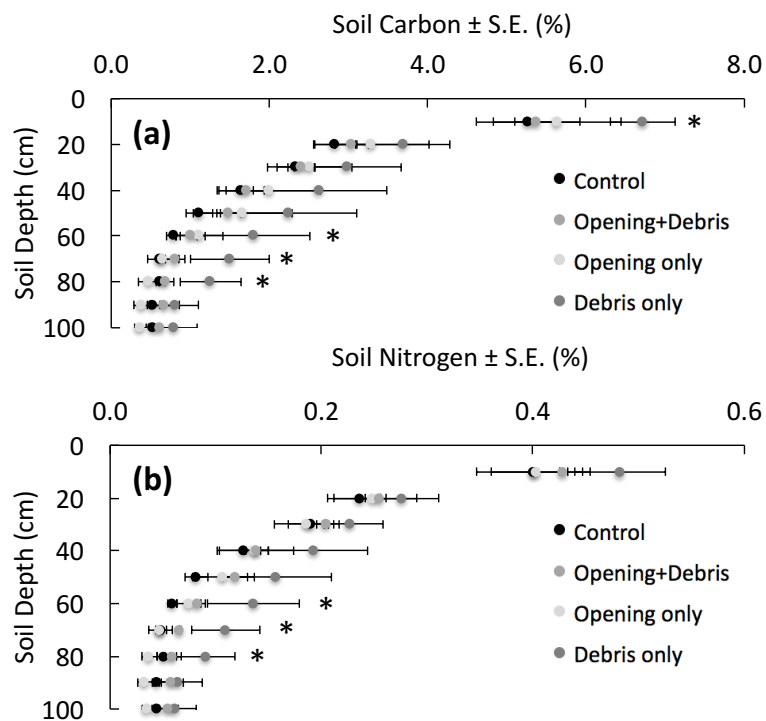


Figure 2. Depth profiles of total soil carbon (a) and nitrogen (b) concentrations by treatment (error bars indicate ± 1 S.E.; $n = 3$; * $p < 0.05$).

Table 2. Mean increases in soil C and N between control and debris deposition only treatments by soil depth (S.E. in parentheses; n = 3). Bolded values indicate statistically significant differences between treatments ($p < 0.05$). *At these depths in Block A (or Block B for soil N at 10 cm), control plots had higher soil C or N than debris deposition only plots.

Soil Depth (cm)	Soil Carbon (%)			Soil Nitrogen (%)		
	Control	Debris only	% Difference	Control	Debris only	% Difference
10	5.27 (0.65)	6.72 (0.41)	29.8 (9.4)	0.40 (0.05)	0.48 (0.04)	24.6 (18.5)*
20	2.83 (0.26)	3.69 (0.59)	28.7 (10.5)	0.24 (0.02)	0.28 (0.03)	16.4 (3.3)
30	2.33 (0.24)	2.99 (0.67)	26.2 (21.4)*	0.19 (0.02)	0.23 (0.03)	19.9 (14.0)
40	1.65 (0.29)	2.64 (0.84)	51.8 (32.3)*	0.13 (0.02)	0.19 (0.05)	47.8 (22.3)
50	1.11 (0.17)	2.24 (0.86)	85.7 (53.2)*	0.08 (0.01)	0.16 (0.05)	81.5 (44.6)*
60	0.79 (0.09)	1.80 (0.71)	116.5 (73.8)*	0.06 (0.00)	0.14 (0.04)	120.9 (61.4)*
70	0.62 (0.03)	1.50 (0.50)	142.0 (79.9)*	0.05 (0.01)	0.11 (0.03)	122.9 (60.0)
80	0.62 (0.06)	1.26 (0.38)	100.2 (55.7)*	0.05 (0.01)	0.09 (0.03)	73.2 (37.2)
90	0.54 (0.08)	0.81 (0.29)	58.2 (53.3)*	0.04 (0.00)	0.06 (0.02)	42.0 (40.8)*
100	0.52 (0.03)	0.80 (0.29)	58.2 (61.6)*	0.04 (0.00)	0.06 (0.02)	36.9 (39.8)*

Soil carbon density fractionation

Analyses of soil C fractions revealed that higher bulk C concentrations in the debris deposition only treatment (0-10 cm depth) was due to greater FLF and HF, although this was only marginally statistically detectable ($p < 0.17$); no change was observed in the OLF (Figure 3b). The increase in FLF C stocks at 0-10 cm likely resulted from an accumulation of particulate organic matter derived from the deposited debris (Table 4), as C concentrations were not significantly different from the control treatment (Figure 3a). Conversely, the trend of increased HF C stock at 0-10 cm in the debris deposition only treatment was likely driven by the significantly higher soil C concentrations of the HF (Figure 3a), as there were no significant differences in the mass of the HF between treatments (Table 4). The greater variability at 50-60 cm depth precluded the detection of statistically significant differences in soil C stocks (Figure 4b). In general, increases in the mass of the free-light and occluded-light fractions tended to be more important than C concentrations, while the opposite was true for the heavy fraction (Table 4).

Soil phosphorus fractionation

There was a significant exponential decline in NaOH-organic P with depth ($p < 0.05$; Table 3), which also resulted in a significant decrease in NaOH-total P with depth across all treatments ($p < 0.05$; Table 3). The NaOH-organic P pools was strongly positively correlated with organic C across treatments ($R^2 = 0.94$, $P < 0.01$). Similar to the pattern for soil C, NaOH-organic P was also strongly positively correlated with citrate ascorbate-extractable Fe ($R^2 = 0.92$, $P < 0.01$) and HCl-extractable Fe ($R^2 = 0.76$, $P < 0.05$).

There was a significant increase in NaOH-organic P in the debris deposition only treatment from 20-90 cm ($p < 0.05$; Figure 5b), as well as for NaOH-total P from 20-50 cm ($p < 0.05$; Figure 5a). There was also a treatment effect of canopy opening, both with and without debris deposition, which significantly increased NaOH-inorganic P concentrations from 70-90 cm ($p < 0.05$; Figure 5c). Although concentrations of NaOH-organic P made up most of the NaOH-total P found in surface soils, NaOH-inorganic P was of similar magnitude, or greater than NaOH-organic P at depth (i.e., below 80 cm) across all treatments. Overall, both the canopy

opening only and debris deposition only treatments had significant effects on NaOH-inorganic P and organic P, respectively, while the combined canopy opening and debris deposition treatment significantly increased NaOH-inorganic P at depth (Figure 5a-c).

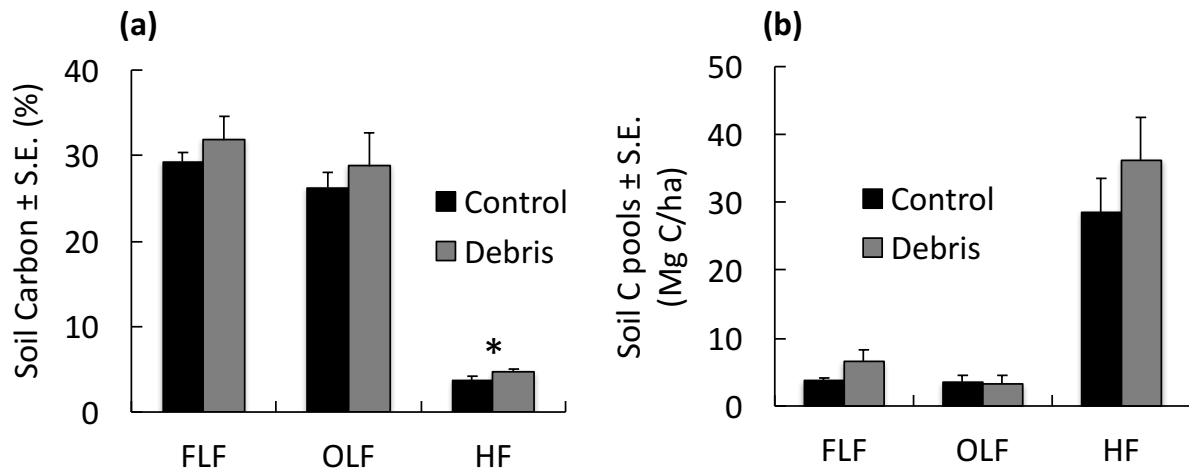


Figure 3. Surface (0 to 10 cm) soil carbon (C) concentrations (a) and soil C pools (b) by density fraction for control and debris only treatments (FLF, free-light fraction; OLF, occluded-light fraction; HF, heavy fraction; error bars indicate \pm 1SE; n = 3; *p < 0.10).

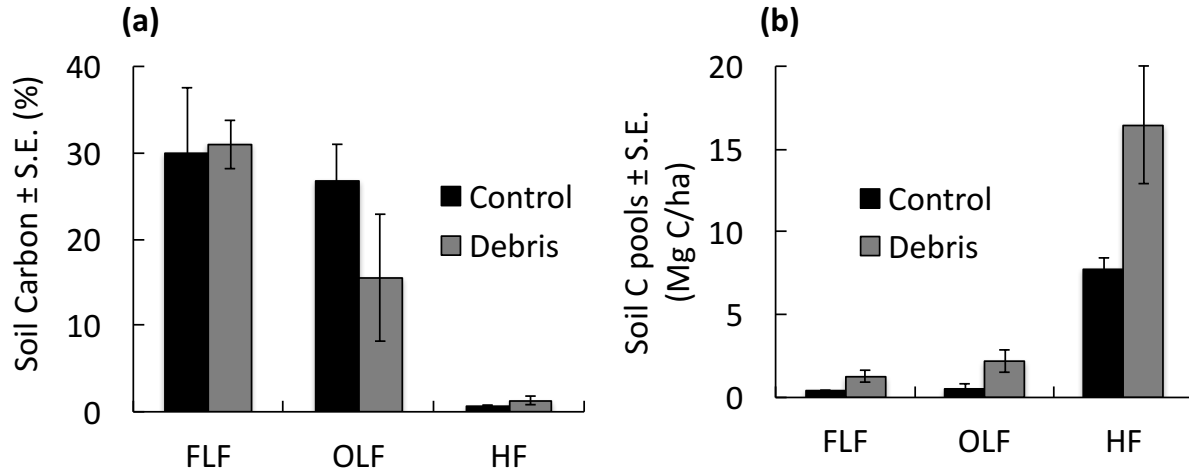


Figure 4. Deep (50 to 60 cm) soil carbon (C) concentrations (a) and soil C pools (b) by density fraction for control and debris only treatments (FLF, free-light fraction; OLF, occluded-light fraction; HF, heavy fraction; error bars indicate \pm 1SE; n = 3).

Table 3. NaHCO₃ and NaOH soil phosphorus fractions by soil depth and treatment (units: μg P/g dry soil; S.E. in parentheses; n = 3).

Soil depth (cm)	Inorganic NaHCO ₃ Phosphorus			Organic NaHCO ₃ Phosphorus			Total NaHCO ₃ Phosphorus			Inorganic NaOH Phosphorus			Organic NaOH Phosphorus			Total NaOH Phosphorus				
	Control	Opening only	Dabhis only	Control	Opening + Dabhis	Dabhis only	Control	Opening only	Dabhis only	Control	Opening + Dabhis	Dabhis only	Control	Opening only	Dabhis only	Control	Opening only	Dabhis only	Opening + Dabhis	
10	1.4 (0.0)	1.2 (0.2)	1.5 (0.1)	5.6 (1.7)	6.9 (1.1)	8.7 (3.2)	7.0 (1.7)	8.1 (1.2)	10.2 (3.3)	7.5 (2.1)	15.5 (1.1)	20.2 (2.2)	16.7 (1.8)	57.9 (12.2)	75.0 (13.1)	60.3 (15.2)	73.0 (10.7)	74.5 (15.2)	95.2 (9.1)	77.0 (8.1)
20	1.2 (0.0)	1.0 (0.0)	1.2 (0.1)	2.9 (1.7)	3.0 (1.5)	5.8 (2.2)	4.1 (1.7)	4.1 (1.5)	7.1 (2.2)	7.1 (1.6)	9.3 (0.1)	12.6 (0.8)	9.7 (0.8)	30.5 (6.4)	47.3 (6.7)	36.3 (7.7)	39.8 (7.7)	43.6 (6.2)	59.9 (8.0)	46.0 (6.5)
30	1.1 (0.0)	1.1 (0.0)	1.1 (0.1)	2.9 (1.6)	3.6 (1.7)	4.6 (1.5)	4.0 (1.6)	4.7 (1.6)	5.6 (1.6)	3.5 (1.8)	8.4 (0.5)	12.4 (2.0)	7.8 (0.8)	26.9 (4.3)	45.8 (8.5)	25.6 (0.7)	35.3 (4.9)	32.6 (3.3)	58.2 (10.3)	33.4 (1.2)
40	1.0 (0.0)	1.0 (0.0)	1.0 (0.1)	3.4 (0.6)	4.2 (1.8)	4.3 (2.9)	4.4 (0.6)	5.2 (1.8)	5.3 (2.9)	3.9 (1.5)	7.8 (0.7)	10.7 (2.1)	7.1 (1.4)	19.4 (3.2)	32.6 (7.6)	16.7 (2.2)	27.2 (3.0)	27.6 (4.1)	43.4 (9.7)	23.8 (2.4)
50	0.9 (0.0)	1.1 (0.1)	1.0 (0.0)	2.3 (1.7)	3.4 (1.6)	4.2 (2.2)	3.2 (1.7)	4.5 (1.6)	5.2 (2.2)	4.4 (1.1)	10.2 (3.1)	9.1 (2.0)	9.1 (1.4)	20.7 (3.5)	28.4 (6.5)	13.9 (1.0)	30.8 (2.0)	28.3 (4.2)	37.5 (7.8)	21.5 (1.6)
60	1.0 (0.0)	1.0 (0.1)	1.0 (0.0)	3.8 (1.9)	2.2 (0.9)	4.3 (2.9)	4.8 (1.9)	3.2 (1.0)	5.3 (2.9)	5.8 (2.2)	9.3 (2.1)	10.0 (2.1)	9.3 (3.9)	10.2 (1.8)	22.9 (4.3)	11.3 (2.0)	22.3 (1.4)	25.0 (1.1)	32.2 (5.2)	21.6 (2.9)
70	0.9 (0.0)	1.0 (0.1)	0.9 (0.0)	2.3 (1.0)	2.1 (0.9)	4.6 (2.2)	3.2 (1.0)	3.1 (0.9)	5.6 (2.2)	3.2 (1.0)	9.5 (1.8)	8.4 (1.5)	10.3 (3.4)	10.2 (3.1)	22.5 (4.4)	8.9 (0.6)	19.7 (1.9)	24.3 (1.5)	30.9 (5.1)	19.2 (2.8)
80	0.9 (0.0)	1.1 (0.1)	1.0 (0.0)	1.7 (0.5)	2.6 (0.5)	2.9 (1.7)	2.6 (0.5)	3.7 (0.6)	3.9 (1.7)	2.6 (0.6)	10.8 (2.9)	15.5 (1.3)	11.9 (3.5)	10.2 (2.5)	16.1 (3.2)	8.9 (1.5)	21.0 (2.5)	28.8 (2.1)	25.6 (2.7)	20.8 (2.9)
90	0.9 (0.0)	1.3 (0.2)	1.3 (0.0)	1.2 (0.5)	2.3 (0.5)	3.7 (2.2)	2.1 (0.6)	3.6 (0.5)	5.0 (2.0)	3.7 (0.6)	10.7 (1.3)	9.7 (2.2)	14.7 (4.4)	10.4 (2.8)	12.1 (3.9)	9.2 (2.5)	21.1 (1.8)	32.3 (2.6)	21.8 (3.0)	23.9 (2.7)
100	1.0 (0.1)	1.2 (0.2)	0.9 (0.1)	1.1 (0.6)	1.9 (1.0)	2.9 (1.7)	2.1 (0.6)	3.1 (0.9)	3.9 (1.7)	2.6 (0.6)	12.1 (2.6)	17.1 (3.1)	9.1 (1.9)	16.6 (6.6)	11.3 (4.6)	9.7 (2.1)	27.1 (9.2)	28.5 (1.7)	20.7 (5.1)	26.3 (5.3)

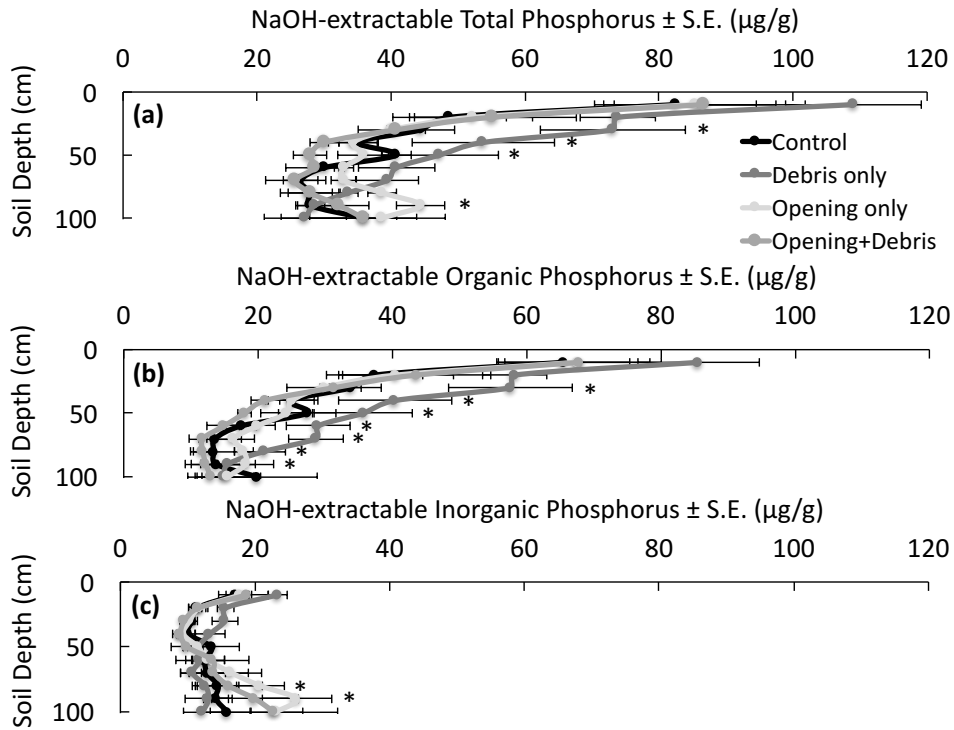


Figure 5. Depth profiles of NaOH-extractable total phosphorus (a), organic phosphorus (b), and inorganic phosphorus (c) (error bars indicate ± 1 SE; $n = 3$; * $p < 0.05$).

Table 4. Soil mass and carbon concentration of free-light, occluded-light, and heavy fractions, separated from control and debris deposition only treatments using density fractionation (S.E. in parentheses; $n = 3$; *indicates statistical significance at $p < 0.10$).

Soil depth (cm) and Treatment	Soil mass (g)			Soil carbon concentration (%)		
	FLF	OLF	HF	FLF	OLF	HF
0-10, Control	0.36 (0.06)	0.37 (0.10)	21.69 (1.11)	29.29 (1.07)	26.28 (1.75)	3.61 (0.59)
0-10, Debris	0.62 (0.16)	0.33 (0.11)	22.14 (1.55)	31.79 (2.80)	28.73 (3.93)	4.71 (0.32)*
50-60, Control	0.03 (0.01)	0.04 (0.02)	22.70 (0.76)	29.94 (7.59)	26.82 (4.16)	0.68 (0.09)
50-60, Debris	0.08 (0.04)	0.12 (0.07)	21.87 (1.07)	30.96 (2.80)	15.53 (7.35)	1.32 (0.50)

Discussion

The impacts of debris deposition

Canopy disturbance and associated debris deposition during severe storm events result in complex and interacting effects on ecosystem biogeochemistry. We hypothesized that debris deposition would be the dominant driver of biogeochemical responses to hurricane disturbance, due to the large direct impact of C and nutrient inputs to the forest floor (Lodge *et al.*, 1994, Lodge *et al.*, 1991, Sanford *et al.*, 1991). We found that the effects of debris deposition significantly increased C, N and P over a decadal time scale. The initial experiment deposited approximately 3 kg C m⁻² (dry mass) on the soil surface as part of the debris deposition treatments in 2005 (Shiels & González, 2014). In 2015, we measured a significant increase in soil C stocks in response to the debris deposition only treatment amounting to 1.02 ± 0.19 and 1.12 ± 0.71 kg C m⁻² at 0-10 and 50-60 cm, respectively. There was no significant increase in litterfall in this treatment (first five years only, Silver *et al.*, 2014), thus the greater soil C stocks likely resulted from an increased capacity to sequester C in soil, associated with the transport of dissolved and particulate organic matter from the debris into the subsoil (Cotrufo *et al.*, 2015). This may have been facilitated by an increase in mineral and organic bonding at depth (Vogel *et al.*, 2014). Clearly, debris deposition had long-term effects on soil biogeochemistry in this forest, a demonstration of the decadal legacy of hurricane disturbances on wet tropical forests.

Soil density fractionation allowed us to explore the mechanisms behind the significant increases in soil C stocks throughout the soil profile. We found that the FLF was relatively C-rich, while the HF accounted for much of the mass of C in these soils, similar to what has been described in other tropical (Marin Spiotta *et al.* 2009, Cusack *et al.* 2010) and temperate (Swanston *et al.* 2005) forests. In general, the FLF is thought to consist of more labile, and thus less stable materials, while the HF is thought to contain more stabilized organic material (Swanston *et al.* 2005, but see Schmidt *et al.* 2011). Ten years following debris deposition, we measured a marginally significant increase in the mass of the FLF and a significant increase in the C concentration of the HF in surface soils. While the increase in HF might be expected given the large initial inputs of C to the soil, the slight increase in the FLF over this time period was surprising given the rapid rates of decomposition in this ecosystem (Parton *et al.* 2007, Ostertag *et al.* 2003), and suggests that particulate C may persist in soils for longer than previously believed (Lodge *et al.*, 2016).

Soils at depth (50-60 cm) also showed a trend of increasing FLF and OLF mass, although the magnitude was lower than at the surface where particulate organic matter inputs dominate. Deeper soils were characterized by a low mass of the FLF and OF (<0.1 g), and despite the marked increases of the mass of these fractions, most of the enhancement in soil C stocks at depth could be attributed to the doubling of the C concentration of the HF (0.68 to 1.32 %), which made up more than 98% of the bulk soil mass. The increase in C concentration of this fraction suggests that deep soils were an important sink for the debris-C deposited. This is likely due to the abundance of free sites for C-mineral associations at depth (Coward *et al.* 2017), further supported by our Fe data. Deep soils may thus serve as a significant hot spot for C sequestration following disturbance in highly weathered tropical forest soils.

Organic P concentrations were significantly higher throughout the soil profile in response to debris deposition only, highlighting the role of soil organic matter as a mediator of the observed responses on soil C and nutrients. Debris deposition alone led to higher NaOH-organic P concentrations throughout the soil profile a decade after the treatments were applied. The observed increase in NaOH-organic P followed a similar pattern to soil C, resulting in a

significant correlation between C and P. This suggests that transport of organic matter into the soil profile can also enhance nutrient content at depth. Sanford *et al.* (1991) used the CENTURY model to simulate C and P cycling after repeated hurricanes and predicted greater surface soil P in hurricane-affected forests relative to hurricane-free forests. Our results provide empirical evidence of their modeling results and extend the finding to the subsoil. This reveals a potential role of disturbance events in helping to alleviate P limitation, which often limits biological processes in wet tropical forests (Vitousek *et al.*, 2010).

Effects of canopy opening

We hypothesized that canopy opening would decrease soil C and N stocks due to the reduction in litter inputs and the propensity of C and N to be lost during decomposition following disturbance (Vargas and Allen 2012). Contrary to our expectations, there was no significant effect of canopy opening only on soil C and N stocks throughout the soil profile. This is striking given the large decrease in surface litter inputs measured during the first 5-y following the disturbance (Silver *et al.* 2014). Zhang and Zak (1995) found that litter decomposition rates declined in large gaps relative to smaller openings and intact canopies. Our data suggests that changes in environmental conditions associated with canopy opening, separate from debris deposition, are insufficient to deplete soil C and N stocks at a decadal scale of resolution.

We predicted that soil P pools might increase following canopy opening due to a reduction in P uptake by damaged vegetation and the propensity of Fe- and aluminum (Al)-rich soils to retain P. The canopy opening treatment led to an increase in inorganic P concentration at depth (70-90 cm), a response that was not observed in any other treatment. Canopy opening may have induced an increase in aboveground biomass investment in the recovering vegetation, leading to a decrease in C allocation to deep roots and thus lower P uptake at depth. It is possible that at longer time-scales, after aboveground biomass has fully recovered from canopy opening, belowground C investment by vegetation could again allow for root scavenging of inorganic P at depth, causing concentrations to return to pre-disturbance levels. Canopy opening also led to a significant reduction in soil pH in surface soils (0-30 cm). Forest disturbances that affect the canopy have often been found to increase soil acidity by altering soil moisture, nitrate availability, and nitrification rates, although these effects are often most notable at short time-scales (Silver *et al.*, 1996, Silver & Vogt, 1993). The lasting effects of canopy opening on soil acidity in our study suggests that the recovering vegetation is contributing to the maintenance of this effect, perhaps by increases in root exudation rate of organic acids or changes in the species contributing to litterfall (Shiels *et al.*, 2010).

Combined effects of canopy opening and debris deposition

The goals of this study were to disentangle the effects of canopy opening and debris deposition impacts from hurricane disturbance in a wet tropical forest. As discussed above, debris deposition led to a significant increase in soil C, N, and organic P stocks, while canopy opening alone did not significantly affect C and N, and but increased inorganic P at depth. The combined canopy opening and debris deposition treatment resulted in similar responses of soil C and N, albeit not statistically significant, as the debris deposition only treatment. The long-term reduction in aboveground organic inputs (i.e., litterfall) due to canopy opening may have limited the magnitude of this response. Previous results from the CTE and from studies monitoring the recovery of litterfall following hurricanes have shown that aboveground C inputs take at least 5 years to recover to pre-disturbance level (Scatena *et al.*, 1996, Silver *et al.*, 2014). Our results suggest that a one-time pulse of debris deposition without the effects of canopy opening

enhanced C and N pools relative to the control. It is likely that similar processes occurred when debris deposition was coupled with canopy opening, but that reduced litter inputs decreased the amount of C translocated downward. It is interesting that organic P did not show any trend in the canopy opening with debris deposition treatment, suggesting that this fraction could have been exploited by P-limited biota when faced with significant reductions in litterfall nutrient inputs.

Coupled biogeochemical cycles of C, Fe, and P

Our measurements throughout the soil profile and across treatments allowed us to explore relationships between soil C, Fe, and P concentrations, supporting previous work suggesting strong biogeochemical coupling of these elements (Hall *et al.*, 2016, Townsend *et al.*, 2011). The highly weathered soils at our site (i.e., Oxisols) are dominated by Fe and Al oxides, which play a key role in both C and P cycling, especially under fluctuating redox conditions (Chacon *et al.*, 2006). The significant positive correlation between soil C and Fe highlights the role of reactive Fe species in the binding of C to mineral surfaces in the soil—a process that is critical for enhancing rates of soil C sequestration throughout the soil profile (Keiluweit *et al.*, 2016). Moreover, the strong coupling between soil C and Fe was also revealed by the variable responses of soil C to debris deposition across blocks, where the magnitude of the response seemed to be mediated by soil Fe concentrations in each block (i.e., the strongest response of soil C to debris deposition only occurred in the block with the highest soil Fe concentrations). We also found a significant positive correlation between soil C and P, suggesting these elements are bound in soil organic matter whose concentration decreases markedly with depth (as does soil C and P). Although some of these patterns might arise from the vertical distribution of organic matter inputs (i.e., more inputs near the soil surface from litterfall and fine roots), our results highlight the strong biogeochemical coupling of these elements across the landscape and throughout the soil profile.

Implications for disturbance and recovery trajectories

Our results demonstrate that the deposition of organic matter associated with severe storms and hurricanes increased soil C and nutrients over a decade of ecosystem recovery. The increase in soil C and nutrient concentrations at depth (>50 cm) suggest that deep soils are more dynamic than previously believed, and have the potential to serve as sinks of C and nutrients derived from storm-induced pulses of organic matter inputs. However, when coupled with canopy opening, these effects became muted, likely due to the slow recovery of litterfall inputs, enhanced decomposition rates, and resource needs of recovering vegetation. The effects of canopy opening may ultimately limit the amount of C and nutrients transported through the subsoil, decreasing the subsidy, and possibly the resilience of these ecosystems, over the long-term.

References

- Beard KH, Vogt KA, Vogt DJ *et al.* (2005) Structural and functional responses of a subtropical forest to 10 years of hurricanes and drought. *Ecological monographs*, **75**, 345-361.
- Bellingham PJ, Kohyama T, Aiba S-I (1996) The effects of a typhoon on Japanese warm temperate rainforests. *Ecological Research*, **11**, 229-247.
- Boose ER, Foster DR, Fluet M (1994) Hurricane Impacts to Tropical and Temperate Forest Landscapes. *Ecological monographs*, **64**, 370-400.

- Brown S, Lugo A, Silander S (1983) Research history and opportunities in the Luquillo Experimental Forest. General technical report/Southern Forest Experiment Station. Forest Service. USDA (no. SO-44).
- Burslem DFRP, Whitmore TC, Brown GC (2000) Short-term effects of cyclone impact and long-term recovery of tropical rain forest on Kolombangara, Solomon Islands. *Journal of Ecology*, **88**, 1063-1078.
- Chacon N, Silver WL, Dubinsky EA, Cusack DF (2006) Iron Reduction and Soil Phosphorus Solubilization in Humid Tropical Forests Soils: The Roles of Labile Carbon Pools and an Electron Shuttle Compound. *Biogeochemistry*, **78**, 67-84.
- Cotrufo MF, Soong JL, Horton AJ, Campbell EE, Haddix ML, Wall DH, Parton WJ (2015) Formation of soil organic matter via biochemical and physical pathways of litter mass loss. *Nature Geosci*, **8**, 776-779.
- Crausbay SD, Martin PH (2016) Natural disturbance, vegetation patterns and ecological dynamics in tropical montane forests. *Journal of tropical ecology*, **32**, 384-403.
- Dale VH, Joyce LA, McNulty S *et al.* (2001) Climate Change and Forest Disturbances. *BioScience*, **51**, 723-734.
- Ewel JJ, Whitmore JL (1973) The ecological life zones of Puerto Rico and the U.S. Virgin Islands Rio Piedras, Puerto Rico, USDA Forest Service Research Paper ITF-18 ITF-18
- Frangi JL, Lugo AE (1991) Hurricane Damage to a Flood Plain Forest in the Luquillo Mountains of Puerto Rico. *Biotropica*, **23**, 324-335.
- García-Martinó AR, Warner GS, Scatena FN, Civco DL (1996) Rainfall, runoff and elevation relationships in the Luquillo Mountains of Puerto Rico. *Caribbean Journal of Science*, **32**, 413-424.
- González G, Lodge DJ, Richardson BA, Richardson MJ (2014) A canopy trimming experiment in Puerto Rico: The response of litter decomposition and nutrient release to canopy opening and debris deposition in a subtropical wet forest. *Forest Ecology and Management*, **332**, 32-46.
- Hall SJ, Liptzin D, Buss HL, Deangelis K, Silver WL (2016) Drivers and patterns of iron redox cycling from surface to bedrock in a deep tropical forest soil: a new conceptual model. *Biogeochemistry*, **130**, 177-190.
- Hornig F, Yu H, Ma F (1995) Typhoons of 1994 doubled the annual litterfall of the Fu-Shan mixed hardwood forest ecosystem in northeastern Taiwan. *Bulletin of the Taiwan Forestry Research Institute New Series*, **10**, 485-491.
- Keiluweit M, Nico PS, Kleber M, Fendorf S (2016) Are oxygen limitations under recognized regulators of organic carbon turnover in upland soils? *Biogeochemistry*, **127**, 157-171.
- Knutson TR, McBride JL, Chan J *et al.* (2010) Tropical cyclones and climate change. *Nature Geoscience*, **3**, 157-163.
- Leff JW, Wieder WR, Taylor PG, Townsend AR, Nemergut DR, Grandy AS, Cleveland CC (2012) Experimental litterfall manipulation drives large and rapid changes in soil carbon cycling in a wet tropical forest. *Global Change Biology*, **18**, 2969-2979.
- Lin K-C, Hamburg SP, Tang S-L, Hsia Y-J, Lin T-C (2003) Typhoon effects on litterfall in a subtropical forest. *Canadian Journal of Forest Research*, **33**, 2184-2192.
- Lin KC, Chang NH, Wang CP, Liu CP (2002) Green foliage decomposition and its nitrogen dynamics of 4 tree species of the Fushan forest. *Taiwan Journal of Forest Science*, **17**, 75-85.
- Lin T-C, Hamburg SP, Lin K-C *et al.* (2011) Typhoon Disturbance and Forest Dynamics: Lessons from a Northwest Pacific Subtropical Forest. *Ecosystems*, **14**, 127-143.

- Lodge D, Winter D, González G, Clum N (2016) Effects of Hurricane-Felled Tree Trunks on Soil Carbon, Nitrogen, Microbial Biomass, and Root Length in a Wet Tropical Forest. *Forests*, **7**, 264.
- Lodge DJ, Cantrell SA, González G (2014) Effects of canopy opening and debris deposition on fungal connectivity, phosphorus movement between litter cohorts and mass loss. *Forest Ecology and Management*, **332**, 11-21.
- Lodge DJ, McDowell WH, McSwiney CP (1994) The importance of nutrient pulses in tropical forests. *Trends Ecol Evol*, **9**, 384-387.
- Lodge DJ, Scatena FN, Asbury CE, Sanchez MJ (1991) Fine Litterfall and Related Nutrient Inputs Resulting From Hurricane Hugo in Subtropical Wet and Lower Montane Rain Forests of Puerto Rico. *Biotropica*, **23**, 336-342.
- Lugo AE (2000) Effects and outcomes of Caribbean hurricanes in a climate change scenario. *Science of The Total Environment*, **262**, 243-251.
- Lugo AE (2008) Visible and invisible effects of hurricanes on forest ecosystems: an international review. *Austral Ecology*, **33**, 368-398.
- Mage SM, Porder S (2012) Parent Material and Topography Determine Soil Phosphorus Status in the Luquillo Mountains of Puerto Rico. *Ecosystems*, **16**, 284-294.
- Marín-Spiotta E, Swanston CW, Torn MS, Silver WL, Burton SD (2008) Chemical and mineral control of soil carbon turnover in abandoned tropical pastures. *Geoderma*, **143**, 49-62.
- Murphy J, Riley JP (1962) A modified single solution method for the determination of phosphate in natural waters. *Analytica Chimica Acta*, **27**, 31-36.
- Ostertag R, Scatena FN, Silver WL (2003) Forest Floor Decomposition Following Hurricane Litter Inputs in Several Puerto Rican Forests. *Ecosystems*, **6**, 261-273.
- Parrotta JA, Lodge DJ (1991) Fine Root Dynamics in a Subtropical Wet Forest Following Hurricane Disturbance in Puerto Rico. *Biotropica*, **23**, 343-347.
- Rice MD, Lockaby BG, Stanturf JA, Keeland BD (1997) Woody Debris Decomposition in the Atchafalaya River Basin of Louisiana following Hurricane Disturbance. *Soil Science Society of America Journal*, **61**, 1264-1274.
- Sanford RL, Jr., Parton WJ, Ojima DS, Lodge DJ (1991) Hurricane Effects on Soil Organic Matter Dynamics and Forest Production in the Luquillo Experimental Forest, Puerto Rico: Results of Simulation Modeling. *Biotropica*, **23**, 364-372.
- Scatena FN (2013) Relative Scales of Time and Effectiveness of Watershed Processes in a Tropical Montane Rain Forest of Puerto Rico. In: *Natural and Anthropogenic Influences in Fluvial Geomorphology*. pp. 103-111. American Geophysical Union.
- Scatena FN, Moya S, Estrada C, China JD (1996) The First Five Years in the Reorganization of Aboveground Biomass and Nutrient Use Following Hurricane Hugo in the Bisley Experimental Watersheds, Luquillo Experimental Forest, Puerto Rico. *Biotropica*, **28**, 424-440.
- Shaw WB (1983) Tropical cyclones: determinants of pattern and structure in New Zeland's indigenous forests. *Pacific Science*, **37**, 405-414.
- Shiels AB, González G (2014) Understanding the key mechanisms of tropical forest responses to canopy loss and biomass deposition from experimental hurricane effects. *Forest Ecology and Management*, **332**, 1-10.
- Shiels AB, González G, Lodge DJ, Willig MR, Zimmerman JK (2015) Cascading Effects of Canopy Opening and Debris Deposition from a Large-Scale Hurricane Experiment in a Tropical Rain Forest. *BioScience*, **65**, 871-881.

- Shiels AB, Zimmerman JK, García-Montiel DC, Jonckheere I, Holm J, Horton D, Brokaw N (2010) Plant responses to simulated hurricane impacts in a subtropical wet forest, Puerto Rico. *Journal of Ecology*, **98**, 659-673.
- Silver WL, Hall SJ, González G (2014) Differential effects of canopy trimming and litter deposition on litterfall and nutrient dynamics in a wet subtropical forest. *Forest Ecology and Management*, **332**, 47-55.
- Silver WL, Scatena FN, Johnson AH, Siccama TG, Sanchez MJ (1994) Nutrient availability in a montane wet tropical forest: spatial patterns and methodological considerations. *Plant and Soil*, **164**, 129-145.
- Silver WL, Scatena FN, Johnson AH, Siccama TG, Watt F (1996) At what temporal scales does disturbance affect belowground nutrient pools? *Biotropica*, **28**, 441-457.
- Silver WL, Vogt KA (1993) Fine root dynamics following single and multiple disturbances in a subtropical wet forest ecosystem. *Journal of Ecology*, **81**, 729-738.
- Sullivan NH, Bowden WB, McDowell WH (1999) Short-Term Disappearance of Foliar Litter in Three Species before and after a Hurricane. *Biotropica*, **31**, 382-393.
- Tanner EVJ, Kapos V, Healey JR (1991) Hurricane Effects on Forest Ecosystems in the Caribbean. *Biotropica*, **23**, 513-521.
- Tiessen H, Moir J (1993) Characterization of available phosphorus by sequential extraction. In: *Soil Sampling and Methods of Analysis*. (ed Carter M) pp. 75-86. Lewis, Boca Raton, FL, Canadian Society of Soil Science.
- Townsend AR, Cleveland CC, Houlton BZ, Alden CB, White JWC (2011) Multi-element regulation of the tropical forest carbon cycle. *Frontiers in Ecology and the Environment*, **9**, 9-17.
- Turton SM (2008) Landscape-scale impacts of Cyclone Larry on the forests of northeast Australia, including comparisons with previous cyclones impacting the region between 1858 and 2006. *Austral Ecology*, **33**, 409-416.
- Vargas R (2012) How a hurricane disturbance influences extreme CO₂ fluxes and variance in a tropical forest. *Environmental Research Letters*, **7**, 035704.
- Vargas R, Allen MF (2008) Diel patterns of soil respiration in a tropical forest after Hurricane Wilma. *Journal of Geophysical Research*, **113**, G03021.
- Vitousek PM, Porder S, Houlton BZ, Chadwick OA (2010) Terrestrial phosphorus limitation: mechanisms, implications, and nitrogen-phosphorus interactions. *Ecological Applications*, **20**, 5-15.
- Vogel C, Mueller CW, Hoschen C *et al.* (2014) Submicron structures provide preferential spots for carbon and nitrogen sequestration in soils. *Nat Commun*, **5**, 2947.
- Vogt KA, Vogt DJ, Boon P *et al.* (1996) Litter Dynamics Along Stream, Riparian and Upslope Areas Following Hurricane Hugo, Luquillo Experimental Forest, Puerto Rico. *Biotropica*, **28**, 458-470.
- Walsh KJE, McBride JL, Klotzbach PJ *et al.* (2016) Tropical cyclones and climate change. *Wiley Interdisciplinary Reviews: Climate Change*, **7**, 65-89.
- Wang H-C, Lin K-C, Huang C-Y (2016) Temporal and spatial patterns of remotely sensed litterfall in tropical and subtropical forests of Taiwan. *Journal of Geophysical Research: Biogeosciences*, **121**, 509-522.
- Webb LJ (1958) Cyclones as an ecological factor in tropical lowland rain forest, north Queensland. *Australian Journal of Botany*, **6**, 220-228.

- Whigham DF, Olmsted I, Cano EC, Harmon ME (1991) The Impact of Hurricane Gilbert on Trees, Litterfall, and Woody Debris in a Dry Tropical Forest in the Northeastern Yucatan Peninsula. *Biotropica*, **23**, 434-441.
- Wolfgang PJD (1985) The Influence of Cyclones on the Dry Evergreen Forest of Sri Lanka. *Biotropica*, **17**, 1-14.
- Xi W (2015) Synergistic effects of tropical cyclones on forest ecosystems: a global synthesis. *Journal of Forestry Research*, **26**, 1-21.
- Xu X, Hirata E, Shibata H (2004) Effect of typhoon disturbance on fine litterfall and related nutrient input in a subtropical forest on Okinawa Island, Japan. *Basic and Applied Ecology*, **5**, 271-282.
- Zimmerman JK, Pulliam WM, Lodge DJ *et al.* (1995) Nitrogen Immobilization by Decomposing Woody Debris and the Recovery of Tropical Wet Forest from Hurricane Damage. *Oikos*, **72**, 314-322.

Transitional Section

The main conclusions from the first chapter of this dissertation highlight the decadal effects of hurricane disturbances on soil biogeochemistry, in addition to providing a comprehensive description of how soil biogeochemistry varies with depth in a wet tropical forest. These invaluable datasets were critical for constraining and contextualizing the results presented in the second chapter of this dissertation, that studies the long-term (centennial) effects of changes in hurricane frequencies on tropical forest carbon (C) and nutrient cycling. Importantly, being able to combine the results from an field-based experimental study to complement a modeling study represents a unique opportunity and provides added value to these two chapters when considered together. The ability to consider the effects of changing disturbance regimes at different spatial and temporal scales was critical for projecting future changes in form and function of wet tropical forests.

Title: Modeling the effects of increased hurricane frequency on the tropical forest carbon cycle

Key Words: climate change, hurricanes, tropical forest, biomass, soil carbon, Luquillo Experimental Forest

Abstract

Models project that climate change is increasing the frequency of severe storm events such as hurricanes. Hurricanes are an important driver of ecosystem structure and function in tropical coastal and island regions, and thus impact tropical forest carbon cycling. Here we used the DayCent model to explore the effects of increased hurricane frequency on humid tropical forest carbon stocks and fluxes at decadal and centennial time-scales. The model was parameterized with empirical data from the Luquillo Experimental Forest (LEF), Puerto Rico using the historical the 60-year hurricane-return interval, and increasing hurricane frequency to 30 and 10 years. The DayCent model replicated the well-documented cyclical pattern of forest biomass fluctuations in hurricane-impacted forests such as the LEF. At the historical hurricane frequency, the dynamic steady state mean forest biomass was 80.9 ± 0.8 Mg C/ha. Increasing hurricane frequency to 30- and 10-years caused a significant decrease in mean forest biomass to 61.1 ± 0.6 and 33.2 ± 0.2 Mg C/ha, respectively ($p < 0.001$). Increasing hurricane frequency also caused a significant decrease in the leaf area index, which stabilized after approximately 100 years to mean values of 3.5 ± 0.01 m²/m², 3.4 ± 0.01 m²/m², and 3.1 ± 0.004 m²/m² at the 60-, 30- and 10-year frequencies, respectively ($p < 0.001$). Conversely, hurricane events at all intervals had a positive effect on soil C stocks. The fastest rate of change in total soil C, as well as the highest mean values after 500 years, were found at the 10-year hurricane frequency. The passive soil C pool showed the largest positive in response to increasing hurricane frequency, with a significant increase on average of 1.17 ± 0.13 Mg C/ha at the 10-year relative to the 60-year hurricane frequency ($p < 0.001$). The gain in soil C stocks was insufficient to offset the larger losses of aboveground biomass over the time period. The time series of C fluxes reflects how the combined responses of net primary productivity and heterotrophic respiration to changes in hurricane frequency can have major implications for net ecosystem production and limit the potential for this ecosystem to serve as a C sink.

Introduction

Humid tropical forests play an integral role in the global carbon (C) cycle, representing a hotspot of terrestrial C storage in vegetation and soils [Jobbágy and Jackson, 2000; Pan *et al.*, 2013]. The favorable climate conditions that characterize these ecosystems (i.e., warm temperatures, abundant rainfall) promote high rates of ecosystem C fluxes such as heterotrophic respiration and net primary productivity (NPP) [Bond-Lamberty and Thomson, 2010; Cleveland *et al.*, 2015]. These large C stocks and fluxes have been shown to be sensitive to temporal fluctuations in climate and disturbance events, highlighting their vulnerability to climate change [Doughty *et al.*, 2015; Feng *et al.*, 2018; Muller-Landau *et al.*, 2020; Scatena *et al.*, 1996; Vargas, 2012; Waide *et al.*, 1998]. Considering the disproportionate contribution of humid tropical forests to the global C cycle, it is critical to understand the long-term effects of changing climate and disturbance regimes on tropical forest biogeochemistry [Dale *et al.*, 2001; McDowell *et al.*, 2020; Zimmerman *et al.*, 2021].

Natural disturbance regimes play an important role in ecosystem development [Chazdon, 2003; Hogan *et al.*, 2018; Lin *et al.*, 2020; Lodge and McDowell, 1991; Lugo, 2020; Lugo and Waide, 1993]. Across large areas of the humid tropics, the occurrence of periodic extreme events such as hurricanes has been recognized as one of the principal factors in shaping forest structure and function [Lin *et al.*, 2020; Lugo, 2008; Simard *et al.*, 2019; Tanner *et al.*, 1991]. For example, the frequency and intensity of hurricanes can limit the accumulation of live biomass and determine vegetation succession patterns, which help to explain the geographic variation in tropical forest C stocks and fluxes across the hurricane belt [Doyle, 1981; Holm *et al.*, 2017; Lin *et al.*, 2020; Shiels *et al.*, 2015; Uriarte *et al.*, 2009; Weaver, 1998; Weaver, 2002].

Multiple lines of evidence indicate that climate change is affecting hurricane disturbance regimes. For example, the frequency of hurricanes occurring outside of the historical hurricane season has significantly increased in both the Atlantic and Pacific basins from 1900-2019 [Hernández Ayala and Méndez-Tejeda, 2020], and a more recent (1982-2018) landward migration of hurricanes has also been detected [Wang and Toumi, 2021]. There has been a significant increase in the frequency of major hurricanes [Emanuel, 2005; Emanuel, 2013], stimulated by the rapid intensification rates that have been associated with high sea surface temperatures [Bender *et al.*, 2010; Bhatia *et al.*, 2019]. Increasing hurricane frequency related to changing climate may already be impacting forests; the Luquillo Experimental Forest (LEF), Puerto Rico was hit by three major hurricanes within a period of less than 30 y from 1989 to 2017; the historical return interval was 60 y [Zimmerman *et al.*, 2021]. Within this context of changing climate and disturbance regimes, it is important to determine the long-term direction of change in tropical forest C stocks and fluxes such as live biomass, soil C, and NPP.

Hurricanes cause large-scale defoliation and massive reductions in live biomass, as well as the deposition of large masses of organic matter debris on the forest floor [Feng *et al.*, 2020; Hall *et al.*, 2020; Lodge *et al.*, 1991; Scholl *et al.*, 2021; Zimmerman *et al.*, 1995]. The loss of canopy cover across the landscape also causes a transient change in microclimate, with warmer temperatures and increased light availability in the understory [Brokaw and Walker, 1991; Fernandez and Fetcher, 1991; Nicholas and Grear, 1991]. Despite the severity and magnitude of these short-term effects, most tropical forests have been shown to be resilient to the historical hurricane regime, usually recovering to pre-disturbance conditions during the periods between storms [Chazdon, 2003; Everham and Brokaw, 1996; Lugo and Heartsill Scalley, 2014; Silver *et al.*, 1996b; Weaver, 1998; Weaver, 2002; Zimmerman *et al.*, 2021]. The resilience to hurricanes

can be attributed to evolutionary adaptations of the biota to these frequent disturbances [i.e., fast growth of early-successional species, high abundance of decomposers, high resistance to wind damage; *Basnet et al.*, 1993; *Zimmerman et al.*, 2021]. However, there is still considerable uncertainty regarding the long-term (decades to centuries) implications of changes in the hurricane disturbance regime for the tropical forest C cycle [*Holm et al.*, 2017; *Lugo*, 2000].

Ecosystem models represent a useful tool for studying the long-term effects of projected changes in climate and disturbance regime on tropical forest biogeochemistry [*Wieder et al.*, 2015; *Wieder et al.*, 2017]. One of the main ecosystem biogeochemical models that has successfully been applied to study the role of hurricanes on tropical forest structure and function is the Century model and its daily timestep version, the DayCent model [*Parton et al.*, 1994; *Parton et al.*, 1998; *Sanford et al.*, 1991; *Wang and Hall*, 2004]. This modeling approach provides the opportunity to study how changes in the hurricane disturbance regime may affect long-term tropical forest structure and function. Here the DayCent model was parameterized with empirical data from the wet tropical forest at the LEF to study the effects of increasing hurricane frequency on ecosystem C stocks and fluxes at decadal and centennial time-scales. The DayCent model was used to determine the direction and magnitude of the long-term effects of increasing hurricane frequency from the historical 60-year frequency to 30 or 10 years on major tropical forest C stocks, such as live biomass and soil C fractions, as well as major C fluxes, such as heterotrophic respiration and NPP.

Methods

The model was parameterized using long-term climate, soils and vegetation data from the Luquillo Experimental Forest (LEF) in northeast Puerto Rico. This modeling experiment was focused on the subtropical wet forests (locally known as Tabonuco forests), which represent the dominant vegetation type and Holdridge life zone in the lowlands of the LEF (<600 m) and is also a common forest type throughout the Caribbean [*Beard*, 1949; *Ewel and Whitmore*, 1973; *Lugo et al.*, 1981]. The historic return interval in the LEF is approximately 60 years [*Scatena and Larsen*, 1991]. Notably this has increased over the past 30 years to one major hurricane per decade. The role of the hurricane regime in maintaining the structure and function of these forests cannot be overstated, with extensive research projects having described ecological and biogeochemical dynamics driven by hurricanes impacts to the LEF, such as the US-LTER site that has focused on this topic since Hurricane Hugo in 1989 [e.g., *Beard et al.*, 2005; *Lodge and McDowell*, 1991; *Lugo*, 2000; *Scatena et al.*, 1996; *Shiels et al.*, 2015; *Silver et al.*, 1996a; *Stuedler et al.*, 1991].

Long-term temperature and precipitation data collected at the Bisley Experimental Watersheds (termed Bisley) and El Verde Research Area (termed El Verde) within the LEF were used as input for the model [*Scatena*, 1989]. Both sites are classified as lowland wet subtropical forests, with a mean annual precipitation of 3,500 mm and a mean annual temperature of 24 °C [*Harris et al.*, 2012; *Heartsill-Scalley et al.*, 2007]. Soils are classified as clay-rich Oxisols derived from volcanoclastic sandstone and dominated by kaolinite and iron/aluminum hydroxides [*Huffaker*, 2002]. Field-collected data from three soil profiles in Tabonuco forests across the LEF (one each at Bisley and El Verde), including soil bulk density, texture, and pH, also served as initial inputs to the model [*Ping et al.*, 2013].

The damage from category 2 and category 4 hurricanes was scaled based on the empirical data collected from Hurricane Hugo—a category 3 hurricane that impacted the LEF in 1989—

and represent a reasonable range of biomass loss specific to each fraction (Table 5). The percent of biomass from leaves, branches, and large wood transferred to the forest floor as hurricane debris was calculated from before-and-after Hurricane Hugo measurements conducted in the Bisley Experimental Watersheds [Scatena *et al.*, 1993]. Fine-root biomass loss was estimated based on data collected pre- and post-Hurricane Hugo at Bisley and El Verde [Parrotta and Lodge, 1991; Silver and Vogt, 1993]. These hurricane intensities were chosen to represent a range that approximates that of the historical record [Boose *et al.*, 2004], and their proportions were maintained consistent across hurricane frequency treatments.

Table 5. Hurricane-induced percentage loss of each biomass fraction.

Biomass fraction	Category 2 ¹	Category 3 (Hugo) ^{2,3}	Category 4 ¹
Live leaves	50 %	91 %	100 %
Live branches	40 %	54 %	80 %
Live wood	20 %	48 %	60 %
Fine roots	50 %	> 50 %	90 %
Coarse roots	30 %	n/a	60 %

¹These values were scaled from empirical data collected after Hurricane Hugo, a category 3 hurricane that impacted the Luquillo Experimental Forest in 1989.

²[Scatena *et al.*, 1993]

³[Parrotta and Lodge, 1991; Silver and Vogt, 1993]

The model spin-up consisted of a disturbance-free period of 4,000 years in order to reach a stable state, followed by a 1,000 year period with a randomized sequence of category 2 and 4 hurricanes occurring at the historical 60-year frequency. This sequence of spin-ups was designed to begin the experimental treatments on a hurricane-impacted forest and allowed for a pre-treatment comparison of the historical 60-year frequency model output with available empirical data (i.e., biomass, leaf area index, net primary productivity). This comparison revealed that in addition to representing the cyclical patterns of biomass fluctuations, modeled biomass values at the 60-year historical hurricane frequency were within the range of those found in Tabonuco forests at the LEF [Lugo and Heartsill Scalley, 2014; Scatena and Lugo, 1995]. Modeled values of NPP were also comparable with long-term field-based estimates from the LEF, although these values did not include belowground productivity [Weaver and Murphy, 1990]. The model output tended to underestimate maximum LAI levels attained by the forest, which may be related to the limits of the model in representing the upper range of LAI values [Weaver and Murphy, 1990].

The experimental treatment period consisted of the final 500 years of the model runs (beginning in year 3,000) when hurricane frequency was increased from 60-years to 30 and 10 years. Eight replicate model runs for each of the three hurricane frequencies were used to calculate mean time-series for each treatment. Variability within replicate runs was partly due to randomly determining the date of the category 4 hurricane event (one per 60-yr frequency vs. six per 10-yr frequency), and also by allowing for intervals between hurricane events to fluctuate $\pm 2SD$ from the means of 60, 30, and 10 years in each treatment. These sources of variability within each replicate run allowed for a more realistic representation of the irregular intervals between hurricane events. While dates of hurricanes events were determined randomly, at least

one category 2 hurricane occurred between category 4 hurricane events at both the 30- and 10-year frequencies to avoid the compounded impacts of back-to-back category 4 events.

Model output included forest live biomass C, total soil C, active soil C, slow soil C, passive soil C, background litterfall C, and hurricane-induced litterfall C. Model output also included heterotrophic respiration, autotrophic respiration, and net primary productivity (NPP); the above values were used to calculate gross primary productivity (GPP; summation of autotrophic respiration and net primary productivity) and net ecosystem productivity (NEP; difference between net primary productivity and heterotrophic respiration). Model output on leaf area index (LAI) was also considered due to its importance for forest productivity.

All statistical analyses were conducted in R [R Core Team, 2021]. The R package ‘segmented’ was used to identify breakpoints during the simulated treatment period where trends changed in magnitude or direction. Linear models were used to test for significant trends throughout the entire treatment period, as well as over specific time periods identified by the breakpoint analyses. The significance of mean differences between treatments was determined using one-way analyses of variance or Kruskal-Wallis rank sum test, after testing for homogeneity of variance (Levene’s test). Statistical significant was determined as $p < 0.05$ unless otherwise noted. Values reported in the text are means \pm standard errors unless otherwise noted.

Results

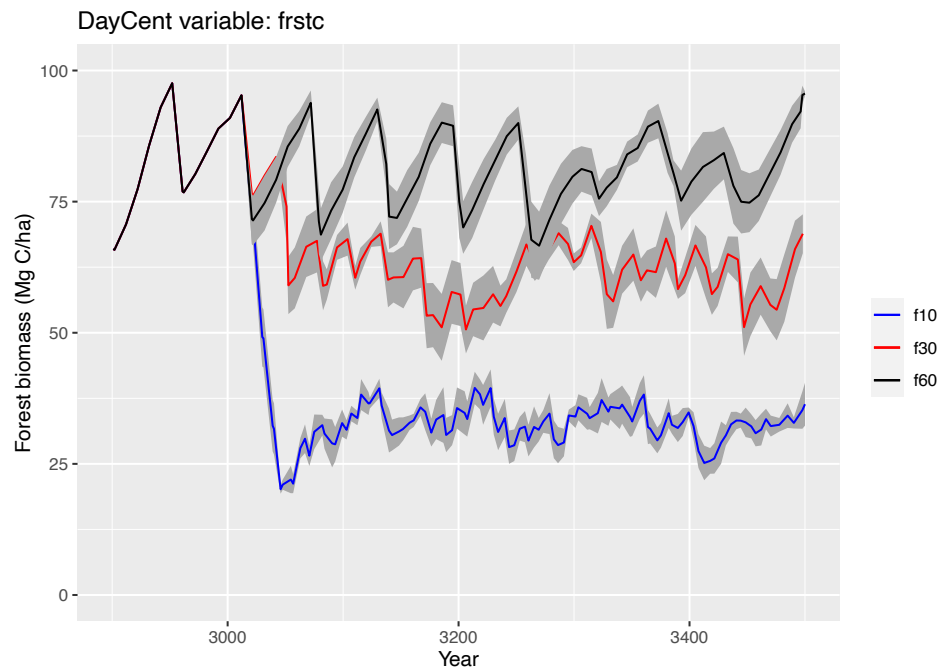


Figure 6. Time-series of live forest biomass C (mean \pm 1 SEM; n=8) by hurricane frequency.

Forest Structure

The model replicated the well-documented cyclical pattern of forest biomass fluctuations in hurricane-impacted forests such as the LEF (Figure 6). After modeling the historical hurricane

frequency of 60 years sustained during a 500-year period, the dynamic steady state mean forest biomass was 80.9 ± 0.8 Mg C/ha compared to the reported value of 71-141 Mg C/ha assuming that aboveground biomass was 75% of the total (Scatena et al. 1993, 1996) (Figure 6; Table 6). Increasing hurricane frequency to 30- and 10-years throughout the same time period caused a significant decrease in mean forest biomass to 61.1 ± 0.6 and 33.2 ± 0.2 Mg C/ha, respectively (Figure 6; Table 6; $p < 0.001$). Increased hurricane frequency was also associated with a decrease in the magnitude of hurricane-induced fluctuations in biomass (Figure 6).

Breakpoint analysis allowed us to calculate the time required for forest biomass to stabilize in response to a change in hurricane frequency. The steepest decline in forest biomass occurred with the 10-year hurricane return interval, and biomass stabilized after approximately 40 years. The magnitude of this decline (biomass loss of 47.7 ± 0.4 Mg C/ha) amounted to a loss of more than 50% of background levels at the historical hurricane frequency (Table 6). A similar pattern was observed for the initial transition period at the 30-year hurricane return interval with a decline in forest biomass of 24% compared to the 60-year hurricane frequency amounting to biomass loss of 19.8 ± 0.3 Mg C/ha (Table 6). This initial reduction in forest biomass at the 30-year frequency took nearly twice as long to stabilize compared to the 10-year frequency (70 vs. 40 years). Following this initial transition period, forest biomass continued to fluctuate in response to individual hurricane events at all frequencies, albeit biomass fluctuations of the greatest magnitude occurred at the 60-year hurricane frequency.

Across all treatments, LAI responded negatively to individual hurricane events, but revealed a strong capacity for resilience in agreement with field observations (Figure 7). Increasing hurricane frequency caused a significant decrease in LAI, which after a transition period of approximately a century, stabilized for the duration of the simulation (400 years) around mean values of 3.5 ± 0.01 m²/m², 3.4 ± 0.01 m²/m², and 3.1 ± 0.004 m²/m² at the 60-, 30- and 10-year frequencies, respectively (Table 7; $p < 0.001$).

Table 6. Forest C stocks and annual aboveground C inputs (mean \pm 1SEM; n=8) for the Luquillo Experimental Forest by hurricane frequency (letters denote significant differences among treatments at $p < 0.05$).

Hurricane frequency	Carbon stocks (Mg C/ha)			Annual carbon inputs (Mg C/ha/yr)	
	Vegetation	Soil	Ratio	Litterfall	Hurricane debris
60 yrs	80.9 ± 0.8^a	76.9 ± 0.06^a	1.1 ± 0.010^a	5.0 ± 0.02^a	0.247 ± 0.001^a
30 yrs	61.1 ± 0.6^b	77.8 ± 0.03^b	0.8 ± 0.008^b	5.1 ± 0.02^b	0.453 ± 0.002^b
10 yrs	33.2 ± 0.2^c	79.0 ± 0.06^c	0.4 ± 0.003^c	5.3 ± 0.01^c	0.894 ± 0.003^c

Table 7. Leaf area index (mean \pm 1SEM; n=8) by hurricane frequency during the last 400 years of the simulations, which excludes the initial transition period (letters denote significant differences among treatments at $p < 0.05$).

Hurricane frequency	Leaf area index (m ² m ⁻²)
60 yrs	3.5 ± 0.01^a
30 yrs	3.4 ± 0.01^{ab}
10 yrs	3.1 ± 0.004^c

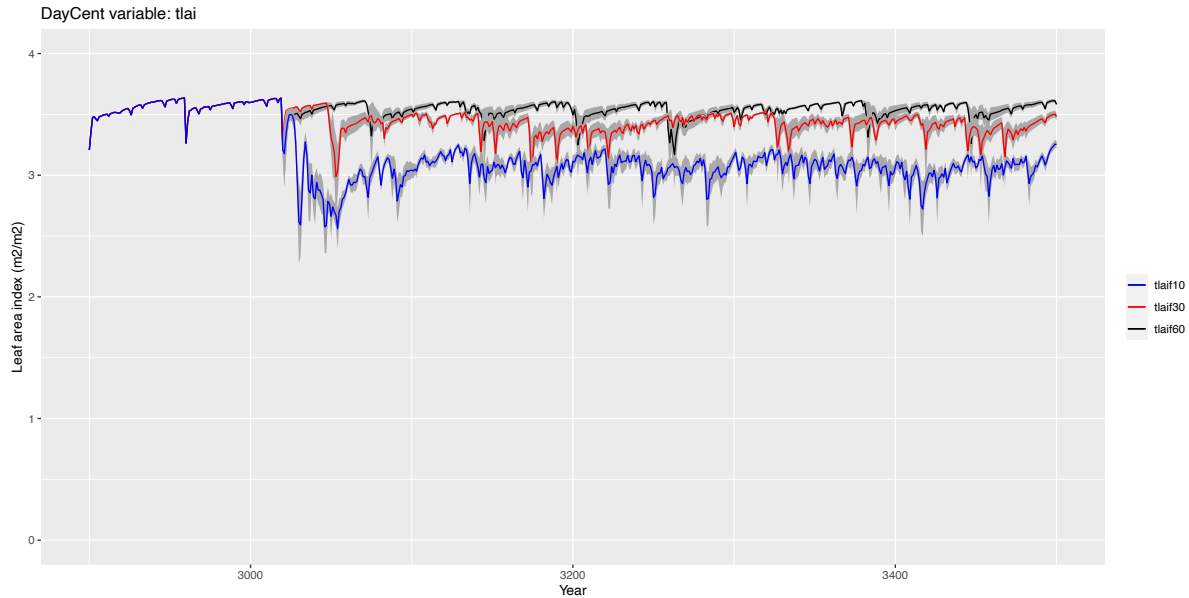


Figure 7. Time-series of leaf area index (mean \pm 1SEM; n=8) by hurricane frequency.

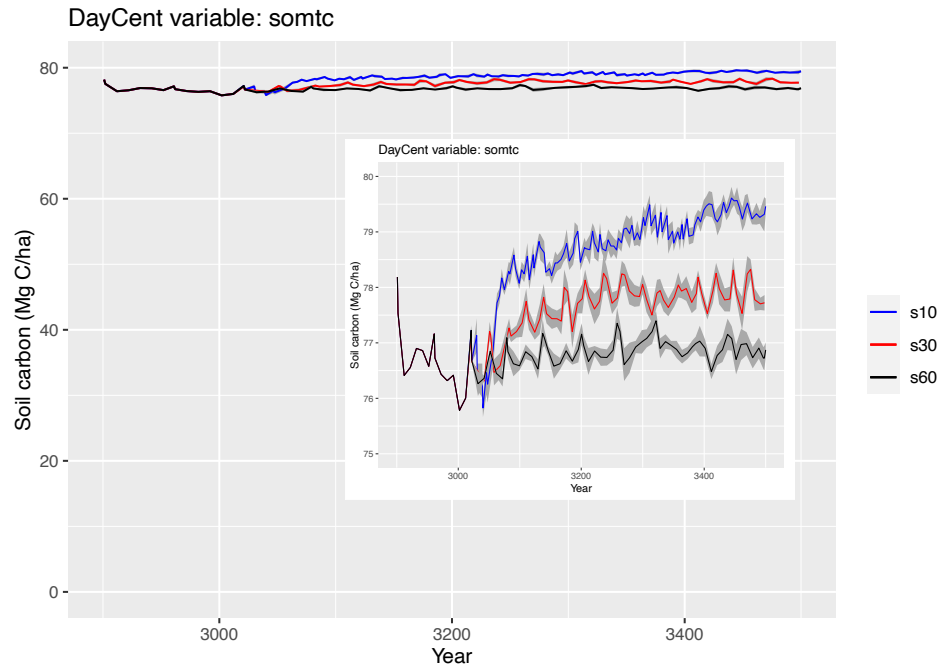


Figure 8. Time-series of total soil C (mean \pm 1SEM; n=8) by hurricane frequency treatment (note inset with shortened y-axis that allows for improved visualization of patterns during treatment period).

Soil Carbon Pools

Modeled total soil C at the historical hurricane frequency revealed a pattern where hurricane-induced debris pulses were followed by a peak in soil C after each event (Figure 8). The accumulation of soil C across the 500 year period resulted in a significant increase in total soil C of approximately 1 to 2 Mg C/ha with increasing hurricane frequency (see inset of Figure 8). Hurricane events had a positive effect on soil C in all treatments, and the fastest rate of

change in total soil C, as well as the highest mean values after 500 year were found at the 10-year hurricane frequency (Figure 8). Breakpoint analysis indicated that the initial transition period lasted approximately 90 years for the 10-year frequency, while it took nearly double the time (approximately 175 years) for the rate of change to stabilize at the 30-year frequency. Following the transition period, soil C continued to increase significantly over time at the 10-year frequency. Notably, after nearly 300 years with a positive trend in the 60-year treatment, a shift occurred towards a negative trend that was not apparent at higher hurricane frequencies.

Excluding the initial transition period (100 years), active soil C fluctuated between 1.90 ± 0.01 Mg C/ha at the 60-year hurricane frequency and 2.01 ± 0.01 Mg C/ha at the 10-year hurricane frequency (Table 8). Increasing hurricane frequency had a positive effect on the active soil C pool, with a significant increase of 0.11 ± 0.05 Mg C/ha at the 10-year hurricane frequency (Table 8; Figure 9a; $p < 0.05$). The second largest modeled soil C pool was slow soil C, which averaged 12.97 ± 0.02 Mg C/ha under the historical 60-year hurricane frequency and showed large fluctuations in response to each hurricane (Table 8; Figure 9b). The effects of increasing hurricane frequency on the slow soil C pool were similar in sign to active soil C but of a larger magnitude increasing on average by 0.48 ± 0.07 Mg C/ha at the 10-year relative to the 60-year hurricane frequency (Table 8). The largest soil C pool was passive soil C, with an average of 59.90 ± 0.07 Mg C/ha under the historical hurricane frequency (Table 8; Figure 9c). The passive soil C pool showed the largest increase in response to increasing hurricane frequency, with a significant increase on average of 1.17 ± 0.13 Mg C/ha at the 10-year relative to the 60-year hurricane frequency (Table 8; Figure 9c; $p < 0.001$). Across all hurricane frequencies, passive soil C was increasing significantly over time, but this temporal trend became stronger as hurricane frequency increased (Figure 9c; $p < 0.001$).

Table 8. Soil C pools (mean \pm 1SEM; n=8) across hurricane frequency treatments (letters denote significant differences among treatments at $p < 0.05$).

Hurricane frequency	Soil Carbon Pools (Mg C/ha)		
	Active	Slow	Passive
60 yrs	1.90 ± 0.01^a	12.97 ± 0.02^a	59.90 ± 0.07^a
30 yrs	1.93 ± 0.01^b	13.14 ± 0.01^b	60.51 ± 0.03^b
10 yrs	2.01 ± 0.01^c	13.45 ± 0.02^c	61.07 ± 0.07^c

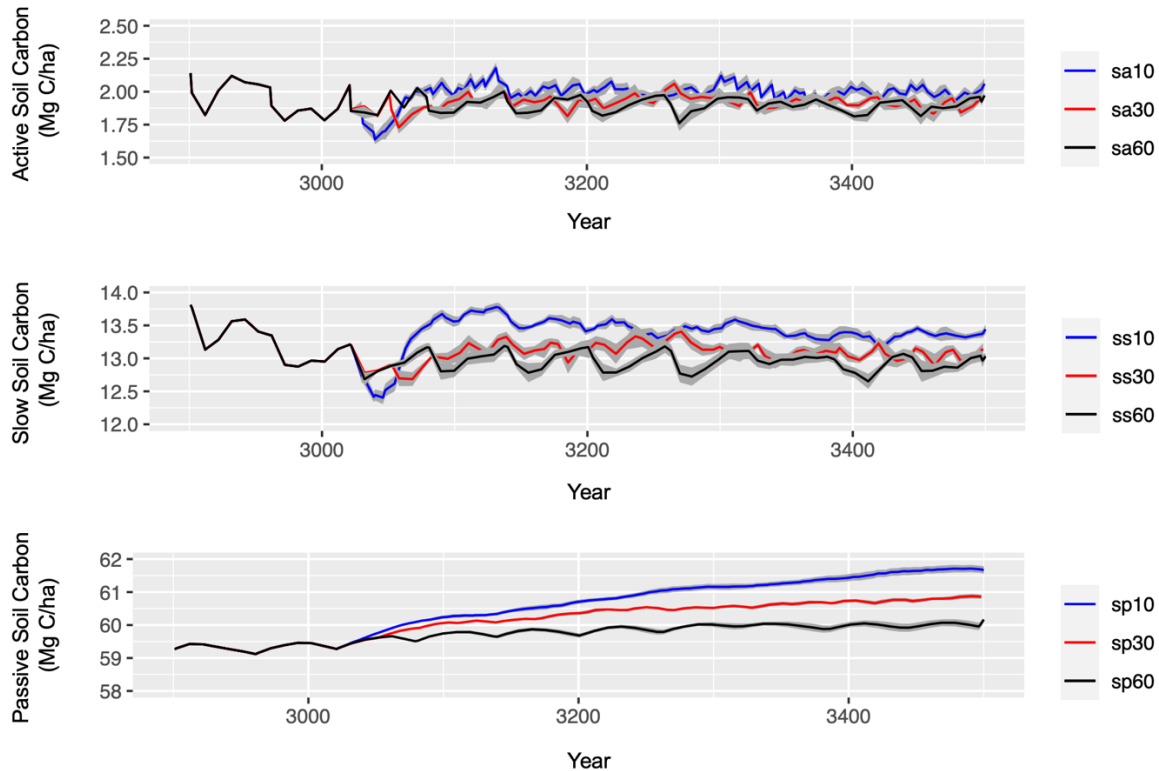


Figure 9. Time-series of soil C fractions (mean \pm 1SEM; n=8) across hurricane frequency treatments: a) active soil C b) slow soil C c) passive soil C (note differences in ranges and increasing magnitudes of y-axes from a-c).

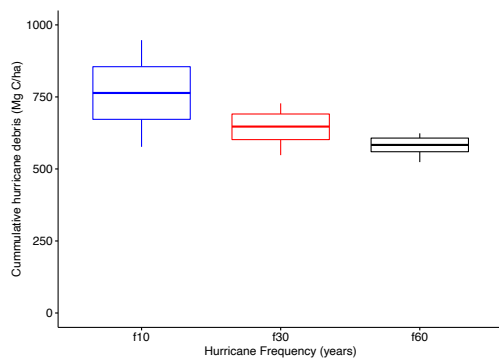


Figure 10. Boxplot of the cumulative hurricane debris inputs showing the significant increase in magnitude at the highest hurricane frequencies ($p < 0.001$).

Changes in the Distribution of Forest Carbon Stocks

The ratio of vegetation C to soil C stocks decreased from 1.1 ± 0.01 at the historical hurricane frequency to 0.4 ± 0.003 at the 10-year hurricane frequency (Table 6; $p < 0.001$) based on the mean values during the last 400 years of the simulation. There was a significant increase in background litterfall with more frequent hurricanes (0.3 ± 0.06 Mg C/ha; Table 6; $p < 0.05$). Moreover, there was a significant positive treatment effect of hurricane frequency on hurricane-induced debris inputs, which doubled the magnitude of background litterfall (0.6 ± 0.02 Mg

C/ha; Table 6; $p < 0.001$). These inputs to the soil surface increased soil C stocks, but the gain in soil C was insufficient to offset the larger losses of aboveground biomass over the time period.

Changes in Carbon Fluxes

Mean annual NPP ranged from 6.2 ± 0.06 Mg C/ha to 6.3 ± 0.04 Mg C/ha and did not differ significantly among treatments (Table 9). Annual heterotrophic respiration under the historical hurricane frequency was 6.4 ± 0.02 Mg C/ha, and there was a significant increase of 0.1 ± 0.06 Mg C/ha to 0.3 ± 0.06 Mg C/ha at 30- and 10-year frequencies, respectively (Table 9; $p < 0.05$). Annual NEP was negative across all treatments (i.e., the forest was a net C source), and decreased significantly from -0.2 ± 0.08 Mg C/ha to -0.4 ± 0.04 Mg C/ha with increasing hurricane frequency (Table 9; $p < 0.001$). Consistent with the large decrease in forest biomass, there was a significant reduction in autotrophic soil respiration as hurricane frequency increased (Table 9; $p < 0.001$). The time series of C fluxes reflects how the combined responses of NPP and heterotrophic respiration to changes in hurricane frequency can have major implications for NEP and limit the potential for this ecosystem to serve as a C sink, as occurs during some periods under the historical hurricane frequency (Figure 11).

Table 9. Annual ecosystem C fluxes (mean \pm 1SEM; n=8) for the Luquillo Experimental Forest across hurricane frequency treatments (negative NEP indicates ecosystem is a C source; letters denote significant differences among treatments at $p < 0.05$).

Hurricane frequency	Annual ecosystem carbon fluxes (Mg C/ha/yr)				
	NPP	Het	Auto	GPP	NEP
60 yrs	6.3 ± 0.03^a	6.4 ± 0.02^a	4.6 ± 0.03^a	10.90 ± 0.04^a	-0.14 ± 0.02^a
30 yrs	6.2 ± 0.03^a	6.5 ± 0.01^a	3.8 ± 0.02^b	10.09 ± 0.04^b	-0.31 ± 0.03^b
10 yrs	6.3 ± 0.03^a	6.7 ± 0.01^b	2.7 ± 0.01^c	9.07 ± 0.04^c	-0.37 ± 0.03^c

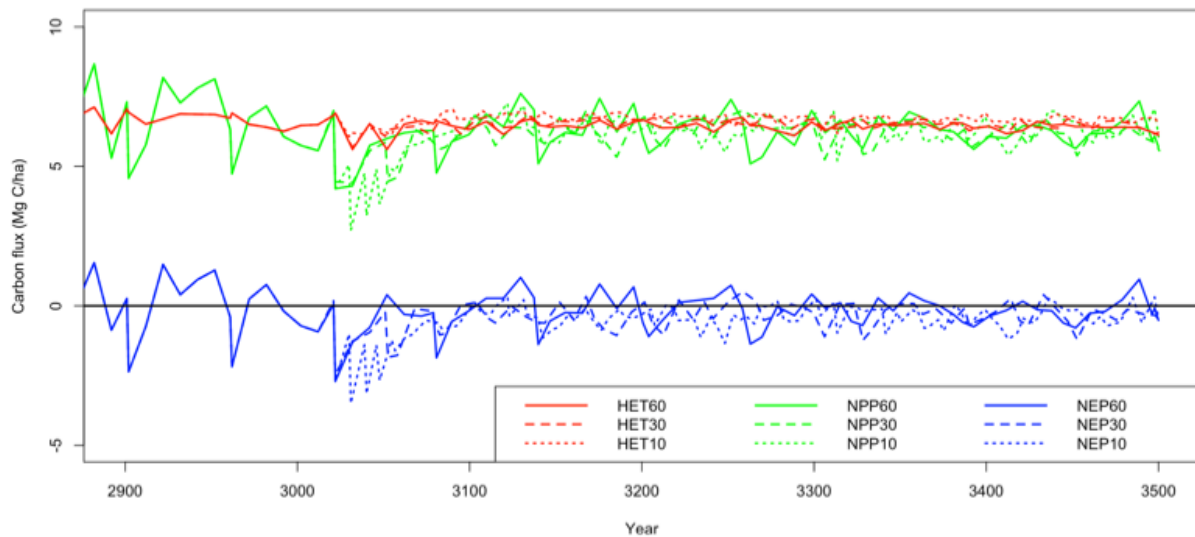


Figure 11. Forest ecosystem C fluxes (Mg C/ha) across hurricane frequency treatments including heterotrophic respiration (HET; red), net primary productivity (NPP; green), and net ecosystem productivity (NEP; blue; calculated as the difference between NPP and HET, such that negative NEP indicates the ecosystem is a C source).

Discussion

Increasing hurricane frequency led to large long-term losses of live forest biomass, highlighting the vulnerability of aboveground C stocks to changes in the disturbance regime. Tropical forests worldwide are facing increasing pressures from intensifying disturbance regimes [Dale *et al.*, 2001; McDowell *et al.*, 2020]. Live forest biomass loss caused by hurricane disturbances has been widely documented in tropical forests, with dramatic reductions (>25-50%) occurring after major storms [i.e., cat. 3-5; Hall *et al.*, 2020; Scatena *et al.*, 1996; Tanner *et al.*, 1991]. If periods of elevated hurricane frequency are sustained over time, shorter periods between hurricanes will strongly limit the ability for live forest biomass to recover to pre-disturbance levels, and effectively reduce the maximum live forest biomass that can be attained [Lin *et al.*, 2020]. Long-term empirical studies documenting the effects of increasing hurricane frequency are lacking, but comparisons across regions suggest that forests that experience more frequent hurricanes tend to have lower canopy height and biomass [Gouvenain and Silander Jr., 2003; Hogan *et al.*, 2018; Ibanez *et al.*, 2019; Lin *et al.*, 2011; Lin *et al.*, 2020; Lugo, 2008; Simard *et al.*, 2019; Xi, 2015].

The duration of the transition period in response to increased hurricane occurrence was determined by the magnitude of the change in frequency, with more frequent hurricanes resulting in a faster transition to a new, dynamic, steady state condition. DayCent does not capture changes in plant community composition. In theory, however, the shorter recovery time between hurricanes could set in motion a gradual shift in species composition favoring early and mid-successional species that could also translate to changes in forest structure in a direction that is consistent with these results [Lin *et al.*, 2020; Xi, 2015]. This process driven by changes in abiotic conditions could result in a disproportionate loss of large trees of late-successional species that represent a significant contribution to tropical forest C stocks, mainly due to the

accumulation of woody biomass [Feng *et al.*, 2018; Sist *et al.*, 2014]. The loss of these late-successional species will feedback to the forest C cycle, as they make up a large proportion of wood C stocks that eventually becomes hurricane debris [Liu *et al.*, 2018; Lodge *et al.*, 1994; Lodge *et al.*, 1991; Zimmerman *et al.*, 1995]. The importance of wood C stocks for explaining the decline in live forest biomass was further supported by the marginal decrease in mean LAI with increasing hurricane frequency. Combined with the lack of a significant treatment effect on NPP, these results suggest that the photosynthetic capacity of the forest is resilient to changes in hurricane frequency. These findings are consistent with shorter-term with observational evidence of the resilience of tropical forest LAI and NPP to hurricane regimes across a range of frequencies [Lin *et al.*, 2011; Lin *et al.*, 2020; Lodge and McDowell, 1991; Scatena *et al.*, 1996; Scatena *et al.*, 1993; Wang and Hall, 2004].

Total soil C stocks increased as hurricanes became more frequent. Soils serve as a reservoir for some of the C lost from plant biomass due to hurricane disturbance [Gutiérrez del Arroyo and Silver, 2018; Sanford *et al.*, 1991; Silver *et al.*, 1996a]. This response was driven by the acceleration of the C flux from live biomass to litterfall, with both background litterfall and hurricane-induced litterfall increasing significantly with hurricane frequency. The importance of disturbance-induced pulses of organic matter as a source of soil C in tropical forests is widely recognized [Gutiérrez del Arroyo and Silver, 2018; Lodge *et al.*, 1994; Sanford *et al.*, 1991], but significant long-term changes have been difficult to detect in field-based studies [Gutiérrez del Arroyo and Silver, 2018; Silver *et al.*, 1996a]. In the model, litterfall represents the principal source of organic matter inputs for the formation of soil C. However, the long-term increase in soil C was only able to account for a small fraction of the losses in biomass C stocks due to increasing hurricane frequency.

Patterns in C fractions that differ in turnover times provides the opportunity to better understand belowground dynamics [Berardi *et al.*, 2020]. Model results suggested that all soil C fractions were enhanced with increasing hurricane frequency. The magnitude of change was proportional to the initial size of the C stock. For example, the largest treatment effects were found for the passive soil C fraction, which was also the fraction with the highest soil C content. By the end of the experimental simulations, the increase in the passive soil C fraction explained most of the total soil C increase, with only a small contribution from the slow-cycling C fraction. The orders of magnitude of soil C fractions were consistent with field studies that have shown the importance of slow-cycling C in tropical forests [Cusack *et al.*, 2010; Gutiérrez del Arroyo and Silver, 2018; Hall *et al.*, 2015; Marín-Spiotta *et al.*, 2008]. There is uncertainty about the long-term stability of the slower cycling C fractions, especially in warm and wet ecosystems such as tropical forests [Hall *et al.*, 2015; Kleber *et al.*, 2015]. However, the results from the current research suggest an increasing importance of the passive C fraction as one of the major C reservoirs in these forests.

One of the greatest concerns about the compounding effects of climate change is that increased disturbance frequency could alter the net C balance of tropical forests and decrease their capacity for serving as C sinks [Brienen *et al.*, 2015; Feng *et al.*, 2018; Lewis, 2006; McDowell *et al.*, 2020; Wood *et al.*, 2012]. The large changes in the distribution of forest C stocks caused by increasing hurricane frequency was accompanied by significant changes in C fluxes. For example, the significant positive relationship between heterotrophic respiration and hurricane frequency was associated with larger soil C pools, which may partly explain the higher rates of litter and soil organic matter decomposition. Given that NPP did not vary significantly by treatment, the forest net C balance became more negative (a larger C source) with increasing

hurricane frequency. The increase in heterotrophic soil respiration resulted in a 2-fold decrease in NEP of these forests. Thus, the forest became a larger C source as hurricane frequency increased and lost the temporary C sink that periodically occurred during the background (60-y) hurricane frequency scenario. The results presented here point to the long-term vulnerability of the tropical forest C sink—in addition to the vulnerability of its biomass C stocks—within the context of increasing hurricane frequency [Feng *et al.*, 2018; Holm *et al.*, 2017].

Comparing the magnitude of the projected declines in biomass to other changes in climate or disturbance regime that have been studied at the LEF (i.e., warming, drought), it is clear that increasing hurricane frequency represents a larger threat for live forest biomass than other climatic pressures [Feng *et al.*, 2018; O'Brien *et al.*, 1992]. Significant declines in biomass with increasing hurricane frequency have also been projected for subtropical dry forests in Puerto Rico, but the magnitude of biomass losses were much lower relative to those reported here due to the lower background biomass of subtropical dry forests [Holm *et al.*, 2017]. The complementary modelling studies of Doyle [1981] and O'Brien *et al.* [1992] applied demographic models to better understand the dynamic relationship between hurricane frequency and forest composition at the LEF, highlighting the potentially catastrophic consequences of high hurricane frequencies. The results from the DayCent model confirm the dramatic changes in forest structure that can be expected at high hurricane frequencies, with cascading long-term effects on both biogeochemical and biotic processes that drive ecosystem function.

Using DayCent to model the long-term effects of increased hurricane frequencies on forest C stocks and fluxes provided insights into how the dynamic relationship between disturbance regimes and forest biogeochemistry might shape tropical forests of the future. This application of the model provided a better understanding on how more frequent hurricane disturbances may affect tropical forest C pools and fluxes, and collectively these results suggest that if hurricanes become more frequent than the 60-year historical average, we can expect a substantial change in the forest structure, as well as C allocation patterns, that will have significant consequences for net ecosystem C fluxes.

References

- Basnet, K., F. N. Scatena, G. E. Likens, and A. E. Lugo (1993), Ecological Consequences of Root Grafting in Tabonuco (*Dacryodes excelsa*) Trees in the Luquillo Experimental Forest, Puerto Rico, *Biotropica*, 25(1), 28-35, doi:10.2307/2388976.
- Beard, J. S. (1949), Natural vegetation of the Windward and Leeward Island, *Oxford Forestry Memoirs*, 21, 1-192.
- Beard, K. H., K. A. Vogt, D. J. Vogt, F. N. Scatena, A. P. Covich, R. Sigurdardottir, T. G. Siccama, and T. A. Crowl (2005), Structural and functional responses of a subtropical forest to 10 years of hurricanes and drought, *Ecological Monographs*, 75(3), 345-361, doi:10.1890/04-1114.
- Bender, M. A., T. R. Knutson, R. E. Tuleya, J. J. Sirutis, G. A. Vecchi, S. T. Garner, and I. M. Held (2010), Modeled Impact of Anthropogenic Warming on the Frequency of Intense Atlantic Hurricanes, *Science*, 327(5964), 454-458, doi:10.1126/science.1180568.
- Berardi, D., E. Brzostek, E. Blanc-Betes, B. Davison, E. H. DeLucia, M. D. Hartman, J. Kent, W. J. Parton, D. Saha, and T. W. Hudiburg (2020), 21st-century biogeochemical modeling: Challenges for Century-based models and where do we go from here?, *GCB Bioenergy*, n/a(n/a), doi:10.1111/gcbb.12730.

- Bhatia, K. T., G. A. Vecchi, T. R. Knutson, H. Murakami, J. Kossin, K. W. Dixon, and C. E. Whitlock (2019), Recent increases in tropical cyclone intensification rates, *Nature communications*, 10(1), 635, doi:10.1038/s41467-019-08471-z.
- Bond-Lamberty, B., and A. Thomson (2010), A global database of soil respiration data, *Biogeosciences*, 7(6), 1915-1926, doi:10.5194/bg-7-1915-2010.
- Boose, E. R., M. I. Serrano, and D. R. Foster (2004), Landscape and regional impacts of hurricanes in Puerto Rico, *Ecological Monographs*, 74(2), 335-352, doi:10.1890/02-4057.
- Brienen, R. J. W., et al. (2015), Long-term decline of the Amazon carbon sink, *Nature*, 519(7543), 344-348, doi:10.1038/nature14283
<http://www.nature.com/nature/journal/v519/n7543/abs/nature14283.html#supplementary-information>.
- Brokaw, N. V. L., and L. R. Walker (1991), Summary of the effects of Caribbean hurricanes on vegetation, *Biotropica*, 23(4a), 442-447.
- Chazdon, R. L. (2003), Tropical forest recovery: legacies of human impact and natural disturbances, *Perspectives in Plant Ecology, Evolution and Systematics*, 6(1), 51-71, doi:<http://dx.doi.org/10.1078/1433-8319-00042>.
- Cleveland, C. C., P. Taylor, K. D. Chadwick, K. Dahlin, C. E. Doughty, Y. Malhi, W. K. Smith, B. W. Sullivan, W. R. Wieder, and A. R. Townsend (2015), A comparison of plot-based, satellite and Earth system model estimates of tropical forest net primary production, *Global Biogeochemical Cycles*, n/a-n/a, doi:10.1002/2014GB005022.
- Cusack, D. F., W. L. Silver, M. S. Torn, and W. H. McDowell (2010), Effects of nitrogen additions on above- and belowground carbon dynamics in two tropical forests, *Biogeochemistry*, 104(1), 203-225, doi:10.1007/s10533-010-9496-4.
- Dale, V. H., et al. (2001), Climate Change and Forest Disturbances, *BioScience*, 51(9), 723-734, doi:10.1641/0006-3568(2001)051[0723:ccafd]2.0.co;2.
- Doughty, C. E., et al. (2015), Drought impact on forest carbon dynamics and fluxes in Amazonia, *Nature*, 519(7541), 78-82, doi:10.1038/nature14213
<http://www.nature.com/nature/journal/v519/n7541/abs/nature14213.html#supplementary-information>.
- Doyle, T. W. (1981), The Role of Disturbance in the Gap Dynamics of a Montane Rain Forest: An Application of a Tropical Forest Succession Model, in *Forest Succession: Concepts and Application*, edited by D. C. West, H. H. Shugart and D. B. Botkin, pp. 56-73, Springer New York, New York, NY, doi:10.1007/978-1-4612-5950-3_6.
- Emanuel, K. (2005), Increasing destructiveness of tropical cyclones over the past 30 years, *Nature*, 436(7051), 686-688, doi:http://www.nature.com/nature/journal/v436/n7051/supinfo/nature03906_S1.html.
- Emanuel, K. A. (2013), Downscaling CMIP5 climate models shows increased tropical cyclone activity over the 21st century, *Proc. Natl. Acad. Sci. U.S.A.*, 110(30), 12219-12224, doi:10.1073/pnas.1301293110.
- Everham, E. M., and N. V. L. Brokaw (1996), Forest damage and recovery from catastrophic wind, *The Botanical Review*, 62(2), 113-185, doi:10.1007/bf02857920.
- Ewel, J. J., and J. L. Whitmore (1973), The ecological life zones of Puerto Rico and the U.S. Virgin Islands *Rep. ITF-18*, Institute of Tropical Forestry, Rio Piedras, Puerto Rico.
- Fassig, O. L. (1930), On the frequency of hurricanes in the vicinity of Porto Rico, *Monthly Weather Review*, 58(8), 326-327, doi:10.1175/1520-0493(1930)58<326:Otfohi>2.0.Co;2.

- Feng, X., M. Uriarte, G. González, S. Reed, J. Thompson, J. K. Zimmerman, and L. Murphy (2018), Improving predictions of tropical forest response to climate change through integration of field studies and ecosystem modeling, *Global Change Biology*, 24(1), e213-e232, doi:10.1111/gcb.13863.
- Feng, Y., R. I. Negrón-Juárez, and J. Q. Chambers (2020), Remote sensing and statistical analysis of the effects of hurricane María on the forests of Puerto Rico, *Remote Sensing of Environment*, 247, 111940, doi:<https://doi.org/10.1016/j.rse.2020.111940>.
- Fernandez, D. S., and N. Fetcher (1991), Changes in Light Availability Following Hurricane Hugo in a Subtropical Montane Forest in Puerto Rico, *Biotropica*, 23(4), 393-399, doi:10.2307/2388257.
- Gouvenain, R. C. d., and J. A. Silander Jr. (2003), Do Tropical Storm Regimes Influence the Structure of Tropical Lowland Rain Forests?, *Biotropica*, 35(2), 166-180, doi:<https://doi.org/10.1111/j.1744-7429.2003.tb00276.x>.
- Gutiérrez del Arroyo, O., and W. L. Silver (2018), Disentangling the long-term effects of disturbance on soil biogeochemistry in a wet tropical forest ecosystem, *Global Change Biology*, n/a-n/a, doi:10.1111/gcb.14027.
- Hall, J., R. Muscarella, A. Quebbeman, G. Arellano, J. Thompson, J. K. Zimmerman, and M. Uriarte (2020), Hurricane-Induced Rainfall is a Stronger Predictor of Tropical Forest Damage in Puerto Rico Than Maximum Wind Speeds, *Scientific reports*, 10(1), 4318, doi:10.1038/s41598-020-61164-2.
- Hall, S. J., G. McNicol, T. Nataka, and W. L. Silver (2015), Large fluxes and rapid turnover of mineral-associated carbon across topographic gradients in a humid tropical forest: insights from paired ¹⁴C analysis, *Biogeosciences Discussions*, 12(2), 891-932, doi:10.5194/bgd-12-891-2015.
- Harris, N. L., A. E. Lugo, S. Brown, and T. Heartsill-Scalley (2012), Luquillo Experimental Forest: Research History and Opportunities *Rep.*, 152 pp, USDA Forest Service, Washington, D.C.
- Heartsill-Scalley, T., F. N. Scatena, C. Estrada, W. H. McDowell, and A. E. Lugo (2007), Disturbance and long-term patterns of rainfall and throughfall nutrient fluxes in a subtropical wet forest in Puerto Rico, *Journal of Hydrology*, 333(2-4), 472-485, doi:<http://dx.doi.org/10.1016/j.jhydrol.2006.09.019>.
- Hernández Ayala, J. J., and R. Méndez-Tejeda (2020), Increasing frequency in off-season tropical cyclones and its relation to climate variability and change, *Weather Clim. Dynam.*, 1(2), 745-757, doi:10.5194/wcd-1-745-2020.
- Hogan, J. A., et al. (2018), The Frequency of Cyclonic Wind Storms Shapes Tropical Forest Dynamism and Functional Trait Dispersion, *Forests*, 9(7), 404.
- Holm, J. A., S. J. Van Bloem, G. R. Larocque, and H. H. Shugart (2017), Shifts in biomass and productivity for a subtropical dry forest in response to simulated elevated hurricane disturbances, *Environmental Research Letters*, 12(2), 025007.
- Huffaker, L. (2002), Soil survey of Caribbean National Forest and Luquillo Experimental Forest, Commonwealth of Puerto Rico, edited, U.S. Gov. Print. Office, Washington, D.C.
- Ibanez, T., G. Keppel, C. Menkes, T. W. Gillespie, M. Lengaigne, M. Mangeas, G. Rivas-Torres, and P. Birnbaum (2019), Globally consistent impact of tropical cyclones on the structure of tropical and subtropical forests, *Journal of Ecology*, 107(1), 279-292, doi:<https://doi.org/10.1111/1365-2745.13039>.

- Jobbágy, E. G., and R. B. Jackson (2000), The vertical distribution of soil organic carbon and its relation to climate and vegetation, *Ecological applications*, 10(2), 423-436.
- Kleber, M., K. Eusterhues, M. Keiluweit, C. Mikutta, R. Mikutta, and P. S. Nico (2015), Mineral–Organic Associations: Formation, Properties, and Relevance in Soil Environments, in *Advances in Agronomy*, edited by L. S. Donald, pp. 1-140, Academic Press, doi:<http://dx.doi.org/10.1016/bs.agron.2014.10.005>.
- Lewis, S. L. (2006), Tropical forests and the changing earth system, *Philosophical transactions of the Royal Society of London. Series B, Biological sciences*, 361(1465), 195-210, doi:10.1098/rstb.2005.1711.
- Lin, T.-C., S. P. Hamburg, K.-C. Lin, L.-J. Wang, C.-T. Chang, Y.-J. Hsia, M. A. Vadeboncoeur, C. M. Mabry McMullen, and C.-P. Liu (2011), Typhoon Disturbance and Forest Dynamics: Lessons from a Northwest Pacific Subtropical Forest, *Ecosystems*, 14(1), 127-143, doi:10.1007/s10021-010-9399-1.
- Lin, T.-C., J. A. Hogan, and C.-T. Chang (2020), Tropical Cyclone Ecology: A Scale-Link Perspective, *Trends Ecol. Evol.*, 35(7), 594-604, doi:<https://doi.org/10.1016/j.tree.2020.02.012>.
- Liu, X., X. Zeng, X. Zou, G. González, C. Wang, and S. Yang (2018), Litterfall Production Prior to and during Hurricanes Irma and Maria in Four Puerto Rican Forests, *Forests*, 9(6), 367.
- Lodge, D. J., and W. H. McDowell (1991), Summary of Ecosystem-Level Effects of Caribbean Hurricanes, *Biotropica*, 23(4), 373-378, doi:10.2307/2388254.
- Lodge, D. J., W. H. McDowell, and C. P. McSwiney (1994), The importance of nutrient pulses in tropical forests, *Trends Ecol. Evol.*, 9(10), 384-387.
- Lodge, D. J., F. N. Scatena, C. E. Asbury, and M. J. Sanchez (1991), Fine Litterfall and Related Nutrient Inputs Resulting From Hurricane Hugo in Subtropical Wet and Lower Montane Rain Forests of Puerto Rico, *Biotropica*, 23(4), 336-342, doi:10.2307/2388249.
- Lugo, A. E. (2000), Effects and outcomes of Caribbean hurricanes in a climate change scenario, *Science of The Total Environment*, 262(3), 243-251, doi:[http://dx.doi.org/10.1016/S0048-9697\(00\)00526-X](http://dx.doi.org/10.1016/S0048-9697(00)00526-X).
- Lugo, A. E. (2008), Visible and invisible effects of hurricanes on forest ecosystems: an international review, *Austral Ecology*, 33(4), 368-398, doi:10.1111/j.1442-9993.2008.01894.x.
- Lugo, A. E. (2020), Effects of Extreme Disturbance Events: From Ecesis to Social–Ecological–Technological Systems, *Ecosystems*, doi:10.1007/s10021-020-00491-x.
- Lugo, A. E., and T. Heartsill Scalley (2014), Research in the Luquillo Experimental Forest Has Advanced Understanding of Tropical Forests and Resolved Management Issues, in *USDA Forest Service Experimental Forests and Ranges: Research for the Long Term*, edited by D. C. Hayes, S. L. Stout, R. H. Crawford and A. P. Hoover, pp. 435-461, Springer, New York.
- Lugo, A. E., R. Schmidt, and S. Brown (1981), Tropical forests in the Caribbean, *Ambio*, 318-324.
- Lugo, A. E., and R. B. Waide (1993), Catastrophic and background disturbance of tropical ecosystems at the Luquillo Experimental Forest, *Journal of Biosciences*, 18(4), 475-481, doi:10.1007/bf02703080.
- Marín-Spiotta, E., C. W. Swanston, M. S. Torn, W. L. Silver, and S. D. Burton (2008), Chemical and mineral control of soil carbon turnover in abandoned tropical pastures, *Geoderma*, 143(1–2), 49-62, doi:<http://dx.doi.org/10.1016/j.geoderma.2007.10.001>.

- McDowell, N. G., et al. (2020), Pervasive shifts in forest dynamics in a changing world, *Science*, 368(6494), eaaz9463, doi:10.1126/science.aaz9463.
- Muller-Landau, H. C., K. C. Cushman, E. E. Arroyo, I. Martinez Cano, K. J. Anderson-Teixeira, and B. Backiel (2020), Patterns and mechanisms of spatial variation in tropical forest productivity, woody residence time, and biomass, *New Phytologist*, n/a(n/a), doi:<https://doi.org/10.1111/nph.17084>.
- Nicholas, V. L. B., and J. S. Grear (1991), Forest Structure Before and After Hurricane Hugo at Three Elevations in the Luquillo Mountains, Puerto Rico, *Biotropica*, 23(4), 386-392, doi:10.2307/2388256.
- O'Brien, S. T., B. P. Hayden, and H. H. Shugart (1992), Global climatic change, hurricanes, and a tropical forest, *Climatic Change*, 22(3), 175-190, doi:10.1007/BF00143026.
- Pan, Y., R. A. Birdsey, O. L. Phillips, and R. B. Jackson (2013), The Structure, Distribution, and Biomass of the World's Forests, *Annual Review of Ecology, Evolution, and Systematics*, 44(1), 593-622, doi:doi:10.1146/annurev-ecolsys-110512-135914.
- Parrotta, J. A., and D. J. Lodge (1991), Fine Root Dynamics in a Subtropical Wet Forest Following Hurricane Disturbance in Puerto Rico, *Biotropica*, 23(4), 343-347, doi:10.2307/2388250.
- Parton, W., P. L. Woomer, and A. Martin (1994), Modelling soil organic matter dynamics and plant productivity in tropical ecosystems, in *The biological management of tropical soil fertility* edited by P. L. Woomer and M. J. Swift, pp. 171-188, Wiley.
- Parton, W. J., M. Hartman, D. Ojima, and D. Schimel (1998), DAYCENT and its land surface submodel: description and testing, *Global and Planetary Change*, 19(1-4), 35-48, doi:[http://dx.doi.org/10.1016/S0921-8181\(98\)00040-X](http://dx.doi.org/10.1016/S0921-8181(98)00040-X).
- Ping, C.-L., G. J. Michaelson, C. A. Stiles, and G. González (2013), Soil characteristics, carbon stores, and nutrient distribution in eight forest types along an elevation gradient, eastern Puerto Rico, *Ecological Bulletins*, 54, 67-86.
- R Core Team (2021), R: A language and environment for statistical computing, edited, R Foundation for Statistical Computing, Vienna, Austria.
- Sanford, R. L., Jr., W. J. Parton, D. S. Ojima, and D. J. Lodge (1991), Hurricane Effects on Soil Organic Matter Dynamics and Forest Production in the Luquillo Experimental Forest, Puerto Rico: Results of Simulation Modeling, *Biotropica*, 23(4), 364-372, doi:10.2307/2388253.
- Scatena, F. N. (1989), An Introduction to the Physiography and History of the Bisley Experimental Watersheds in the Luquillo Mountains of Puerto Rico *Rep.*, Southern Forest Experiment Station, USDA Forest Service, New Orleans, Louisiana, General Technical Report SO-72.
- Scatena, F. N., and M. C. Larsen (1991), Physical Aspects of Hurricane Hugo in Puerto Rico, *Biotropica*, 23(4), 317-323, doi:10.2307/2388247.
- Scatena, F. N., and A. E. Lugo (1995), Geomorphology, disturbance, and the soil and vegetation of two subtropical wet steepland watersheds of Puerto Rico, *Geomorphology*, 13(1-4), 199-213, doi:[http://dx.doi.org/10.1016/0169-555X\(95\)00021-V](http://dx.doi.org/10.1016/0169-555X(95)00021-V).
- Scatena, F. N., S. Moya, C. Estrada, and J. D. China (1996), The First Five Years in the Reorganization of Aboveground Biomass and Nutrient Use Following Hurricane Hugo in the Bisley Experimental Watersheds, Luquillo Experimental Forest, Puerto Rico, *Biotropica*, 28(4), 424-440, doi:10.2307/2389086.
- Scatena, F. N., W. Silver, T. Siccama, A. Johnson, and M. J. Sanchez (1993), Biomass and Nutrient Content of the Bisley Experimental Watersheds, Luquillo Experimental Forest,

- Puerto Rico, Before and After Hurricane Hugo, 1989, *Biotropica*, 25(1), 15-27, doi:10.2307/2388975.
- Scholl, M. A., M. Bassiouni, and A. J. Torres-Sánchez (2021), Drought stress and hurricane defoliation influence mountain clouds and moisture recycling in a tropical forest, *Proc. Natl. Acad. Sci. U.S.A.*, 118(7), e2021646118, doi:10.1073/pnas.2021646118.
- Shiels, A. B., G. González, D. J. Lodge, M. R. Willig, and J. K. Zimmerman (2015), Cascading Effects of Canopy Opening and Debris Deposition from a Large-Scale Hurricane Experiment in a Tropical Rain Forest, *BioScience*, 65(9), 871-881, doi:10.1093/biosci/biv111.
- Silver, W. L., F. N. Scatena, A. H. Johnson, T. G. Siccama, and F. Watt (1996a), At what temporal scales does disturbance affect belowground nutrient pools?, *Biotropica*, 28(4a), 441-457.
- Silver, W. L., F. N. Scatena, A. H. Johnson, T. G. Siccama, and F. Watt (1996b), At what temporal scales does disturbance affect belowground nutrient pools?, *Biotropica*, 441-457.
- Silver, W. L., and K. A. Vogt (1993), Fine root dynamics following single and multiple disturbances in a subtropical wet forest ecosystem, *Journal of Ecology*, 81(4), 729-738.
- Simard, M., L. Fatoyinbo, C. Smetanka, V. H. Rivera-Monroy, E. Castañeda-Moya, N. Thomas, and T. Van der Stocken (2019), Mangrove canopy height globally related to precipitation, temperature and cyclone frequency, *Nature Geoscience*, 12(1), 40-45, doi:10.1038/s41561-018-0279-1.
- Sist, P., L. Mazzei, L. Blanc, and E. Rutishauser (2014), Large trees as key elements of carbon storage and dynamics after selective logging in the Eastern Amazon, *Forest Ecology and Management*, 318, 103-109, doi:<https://doi.org/10.1016/j.foreco.2014.01.005>.
- Stuedler, P. A., J. M. Melillo, R. D. Bowden, M. S. Castro, and A. E. Lugo (1991), The Effects of Natural and Human Disturbances on Soil Nitrogen Dynamics and Trace Gas Fluxes in a Puerto Rican Wet Forest, *Biotropica*, 23(4), 356-363, doi:10.2307/2388252.
- Tanner, E. V. J., V. Kapos, and J. R. Healey (1991), Hurricane Effects on Forest Ecosystems in the Caribbean, *Biotropica*, 23(4), 513-521, doi:10.2307/2388274.
- Uriarte, M., C. D. Canham, J. Thompson, J. K. Zimmerman, L. Murphy, A. M. Sabat, N. Fetcher, and B. L. Haines (2009), Natural disturbance and human land use as determinants of tropical forest dynamics: results from a forest simulator, *Ecological Monographs*, 79(3), 423-443, doi:10.1890/08-0707.1.
- Vargas, R. (2012), How a hurricane disturbance influences extreme CO₂ fluxes and variance in a tropical forest, *Environmental Research Letters*, 7(3), 035704, doi:10.1088/1748-9326/7/3/035704.
- Wadsworth, F. H. (1951), Forest management in the Luquillo Mountains. I. The setting, *Caribbean Forester*, 12, 93-114.
- Waide, R. B., J. K. Zimmerman, and F. N. Scatena (1998), Controls of primary productivity: lessons from the Luquillo Mountains in Puerto Rico *Ecology*, 79(1), 31-37, doi:10.1890/0012-9658(1998)079[0031:COPPLF]2.0.CO;2.
- Wang, H., and C. A. S. Hall (2004), Modeling the effects of Hurricane Hugo on spatial and temporal variation in primary productivity and soil carbon and nitrogen in the Luquillo Experimental Forest, Puerto Rico, *Plant and Soil*, 263(1), 69-84, doi:10.1023/B:PLSO.0000047719.44971.dd.
- Wang, S., and R. Toumi (2021), Recent migration of tropical cyclones toward coasts, *Science*, 371(6528), 514-517, doi:10.1126/science.abb9038.

- Weaver, P. L. (1998), Hurricane effects and long-term recovery in a subtropical rain forest, edited, pp. 249-270, Parthenon Publishing Group, Carnforth.
- Weaver, P. L. (2002), A chronology of hurricane induced changes in puerto rico's lower montane rain forest, *Interciencia*, 27, 252-258.
- Weaver, P. L., and P. G. Murphy (1990), Forest Structure and Productivity in Puerto Rico's Luquillo Mountains, *Biotropica*, 22(1), 69-82, doi:10.2307/2388721.
- Wieder, W. R., C. C. Cleveland, W. K. Smith, and K. Todd-Brown (2015), Future productivity and carbon storage limited by terrestrial nutrient availability, *Nature Geosci*, advance online publication, doi:10.1038/ngeo2413
<http://www.nature.com/ngeo/journal/vaop/ncurrent/abs/ngeo2413.html#supplementary-information>.
- Wieder, W. R., M. D. Hartman, B. N. Sulman, Y.-P. Wang, C. D. Koven, and G. B. Bonan (2017), Carbon cycle confidence and uncertainty: Exploring variation among soil biogeochemical models, *Global Change Biology*, n/a-n/a, doi:10.1111/gcb.13979.
- Wood, T. E., M. A. Cavaleri, and S. C. Reed (2012), Tropical forest carbon balance in a warmer world: a critical review spanning microbial-to ecosystem-scale processes, *Biological Reviews*, 87(4), 912-927.
- Xi, W. (2015), Synergistic effects of tropical cyclones on forest ecosystems: a global synthesis, *Journal of Forestry Research*, 26(1), 1-21, doi:10.1007/s11676-015-0018-z.
- Zimmerman, J. K., W. M. Pulliam, D. J. Lodge, V. Quiñones-Orfila, N. Fetcher, S. Guzmán-Grajales, J. A. Parrotta, C. E. Asbury, L. R. Walker, and R. B. Waide (1995), Nitrogen Immobilization by Decomposing Woody Debris and the Recovery of Tropical Wet Forest from Hurricane Damage, *Oikos*, 72(3), 314-322, doi:10.2307/3546116.
- Zimmerman, J. K., T. E. Wood, G. González, A. Ramirez, W. L. Silver, M. Uriarte, M. R. Willig, R. B. Waide, and A. E. Lugo (2021), Disturbance and resilience in the Luquillo Experimental Forest, *Biological Conservation*, 253, 108891, doi:<https://doi.org/10.1016/j.biocon.2020.108891>.

Title: Soil biogeochemical responses to throughfall exclusion in a wet tropical forest in Puerto Rico

Keywords: drought, tropical forests, throughfall exclusion, soil biogeochemistry, soil greenhouse gas fluxes, soil carbon, nitrogen, phosphorus

Abstract

Climate change is driving altered precipitation patterns across the tropics, with projections of intensifying drought and changing rainfall seasonality in large areas of wet tropical forests such as the Amazon and the Caribbean. Near constant warm, wet conditions in wet tropical forests tend to promote rapid soil carbon and nutrient cycling, but these may slow significantly during extended periods of low soil water availability associated with increasing droughts in the future. In this context, studying the ecological consequences of drought as a major disturbance in these ecosystems is critical, especially due to their important role within the global climate system. To study the response of soil biogeochemistry to drought in a wet tropical forest, I established the Luquillo Throughfall Exclusion Experiment in the Luquillo Experimental Forest, Puerto Rico. Following a pre-treatment period, throughfall exclusion began in 03/2017 and continued until 11/2018, with the post-treatment period lasting until 01/2019. During this time, I monitored hourly temperature, volumetric moisture, and oxygen concentrations at three depths, conducted quarterly soil samplings for key biogeochemical variables, and measured soil greenhouse gas (GHG) fluxes with manual static flux chambers. Throughfall exclusion significantly reduced volumetric moisture from ~ 0.5 to $\sim 0.3 \text{ m}^3 \text{ m}^{-3}$ at 0-15 cm, and increased oxygen concentrations. Throughfall exclusion was effective in reducing the redox fluctuations that characterize these soils, maintaining surface soil oxygen concentrations between ~ 18 - 21% , in contrast to control soils which experienced mean daily values as low as $\sim 12\%$. The treatment effect on moisture and oxygen was stronger at the soil surface (0-15 cm), while responses at depth were buffered due to multiple factors. The observed changes in soil microclimate in the upper soil profile affected redox-sensitive biogeochemical processes. Specifically, we found that drought plots had significantly lower concentrations of labile P at 0-15 cm, and a decrease of almost 30% in soil CO_2 efflux (3.41 vs. 2.45 $\text{g C/m}^2/\text{day}$). Soil CH_4 fluxes also responded significantly to the treatment, which enhanced CH_4 uptake causing the soil to shift from net source to net sink. Collectively, these results suggest that in wet tropical forests drought disturbances have the potential to significantly alter microclimate conditions in the upper soil profile, with major implications for soil nutrient availability and the magnitude and direction of soil GHG fluxes.

Introduction

Intensifying disturbance regimes in forest ecosystems globally is likely to feed back on ecosystem-scale carbon (C) and nutrient cycling [McDowell *et al.*, 2020]. In the humid tropics, where the highest biomass levels and rates of C and nutrient fluxes co-occur [Malhi *et al.*, 1999; Pan *et al.*, 2013; Raich and Schlesinger, 1992], the importance of disturbance regimes for driving the short- and long-term trajectories of ecosystem processes has been widely recognized [Beard *et al.*, 2005; Lin *et al.*, 2020a; Meir and Grace, 2005; Scatena and Lugo, 1995; Teh *et al.*, 2009]. The historical emphasis of disturbance ecology in the humid tropical has been the study of large-scale atmospheric disturbances such as hurricanes and typhoons, or land-use changes related to local, regional, and global socio-economic dynamics [Asner *et al.*, 2009; Chazdon *et al.*, 2016; Grau *et al.*, 2003; Lin *et al.*, 2011; Lugo and Waide, 1993; Zimmerman *et al.*, 2021]. However, ongoing and projected climate change is demonstrating that the humid tropics will also be facing more frequent periods of hydrological stress due to decreasing precipitation levels and changes in the seasonality of water availability [Asner and Alencar, 2010; Henareh Khalyani *et al.*, 2016; Lewis *et al.*, 2011; Meir and Ian Woodward, 2010; O'Connell *et al.*, 2018; Phillips *et al.*, 2009; Ramseyer *et al.*, 2019]. Within this context, the wide-ranging ecological impacts of drought on wet tropical forests are still widely understudied, especially belowground biogeochemical processes that drive ecosystem C and nutrient dynamics [Billings and Phillips, 2011; Meir *et al.*, 2015; Schlesinger *et al.*, 2015].

The nature of drought in tropical forests can vary widely, with a marked seasonal dry period occurring in some regions of the humid tropics, while others experience extended dry periods only rarely due to atmospheric phenomena such as Saharan dust intrusion or strong ENSO events [Bonal *et al.*, 2015; Ferreira dos Santos *et al.*, 2018; Miller *et al.*, 2021]. One important characteristic that defines any drought is its temporal duration. The initial and long-term effects of drought are not necessarily consistent over time due to the independent timescales of response among different ecosystem components [i.e., autotrophic vs. heterotrophic respiration; Cattânio *et al.*, 2002; Davidson *et al.*, 2008; Rowland *et al.*, 2015; van Straaten *et al.*, 2011]. Although short-term (e.g., 3-month) drought manipulations have been shown to have significant effects on ecosystem processes [Wood and Silver, 2012], drought intensity usually increases with the duration of the event [Beard *et al.*, 2005; van Straaten *et al.*, 2011]. Drought sensitivity of vegetation varies largely as a result of the rooting depth and hydraulic safety margins of the prevailing vegetation types [Santiago *et al.*, 2016]. For microbial communities, drought impacts have been shown to result from different physiological moisture constraints, such as higher drought sensitivity of bacteria vs fungi [Manzoni *et al.*, 2011; Stark and Firestone, 1995]. There can also be strong legacy effects of short drought periods on soil microbial communities [Bouskill *et al.*, 2016a; Bouskill *et al.*, 2016b; Bouskill *et al.*, 2013] leading to longer-term (months to year) impacts of drought even in humid ecosystems such as wet tropical forests.

The effects of drought on soil redox conditions and substrate availability are likely to be important biogeochemical determinants of ecosystem drought response [Schuur and Matson, 2001; Vasconcelos *et al.*, 2004]. High rainfall in humid tropical forests often leads to saturated soils and periods of soil anoxia that limit the activity of microbial heterotrophs [Silver *et al.*, 1999]. Low redox events can also release available phosphorus (P) associated with iron (Fe) reduction [Chacon *et al.*, 2006; but see Lin *et al.*, 2020b]. Decreased soil moisture can improve

soil aeration [Cleveland *et al.*, 2010], which could stimulating biological activity of heterotrophs and increase rates of soil C loss. Enhanced aeration can also drive Fe oxidation and an associated decrease in soil P availability [Yang and Liptzin, 2015].

An important consideration when studying drought responses of soil biogeochemistry are the confounded effects of other disturbances that may have preceded the drought or simultaneously impact the ecosystem, such as deforestation, storms, or insect outbreaks [McDowell *et al.*, 2020; Zimmerman *et al.*, 2021]. Wet tropical forests in the Atlantic and Pacific basins can have a high exposure to hurricanes and typhoons, respectively [Lin *et al.*, 2020a], and these events sometimes coincide with drought events affecting patterns of ecosystem recovery [i.e., soil moisture and nutrient availability, litterfall; Beard *et al.*, 2005; Parrotta and Lodge, 1991]. The projections of increasing frequency of major storms [Bender *et al.*, 2010; Walsh *et al.*, 2016], coupled with a reduction in rainfall for large areas of the tropics [Bhardwaj *et al.*, 2018; Chadwick *et al.*, 2016; Henareh Khalyani *et al.*, 2016], require an improved understanding of the potential short- and long-term consequences of the interactive effects of these changes in disturbance regime for ecosystem C and nutrient cycling in wet tropical forests. One way to attain this goal would be to continue promoting field-based experimental manipulations that can capture the natural variability that ecosystems experience (i.e., such as extreme disturbance events), providing the rare opportunity to study the interactive effects of multiple disturbances.

I used a throughfall exclusion experiment to study the effects of drought on soil biogeochemical cycling in the Luquillo Experimental Forest in Puerto Rico. The Luquillo Throughfall Exclusion Experiment began in late 2016 and lasted through early 2019. Hurricanes Irma and María impacted the forest in September 2017. Thus, the experiment was able to consider both the independent and interactive effects of two major ecological disturbances on soil biogeochemical cycling in this wet tropical forest. I hypothesized that throughfall exclusion would reduce moisture and improve the soil aeration status, decreasing biological activity in the soil and reducing soil nutrient availability. I also hypothesized that the effects of the hurricanes would be of opposite direction and of larger magnitude than the effects of throughfall exclusion on soil biogeochemistry.

Materials and Methods

The experiment was conducted in El Verde Research Area (18°20'N, 65°49'W), part of the NSF-sponsored Luquillo Long-Term Ecological Research program and Critical Zone Observatory located within the Luquillo Experimental Forest (LEF) in northeastern Puerto Rico. The site is classified as a subtropical wet forest based on the Holdridge life zone system [Ewel and Whitmore, 1973], with a mean annual precipitation of 3,500 mm and a mean annual temperature of 24 °C with little intra-annual variation [Harris *et al.*, 2012]. The study site was located at approximately 350 m.a.s.l. within the Tabonuco forest type that contains more than 150 tree species [Little, 1970; Weaver, 2010]. Soils are deep, highly weathered Oxisols and Ultisols rich in clays and iron [Huffaker, 2002]. Plot location was restricted to the upper topographic zone, which is well drained and has high P sorption rates [Lin *et al.*, 2020b; Ping *et al.*, 2013; Silver *et al.*, 1999].

In late 2016, a total of ten plots (2.4 x 4.8 meters) were established in areas between tree stems (to allow for shelter placement) with five plots randomly assigned to the throughfall exclusion treatment and five to an untreated control. The treatment consisted of excluding 100% of throughfall (incoming precipitation minus canopy interception) using transparent plastic

shelters constructed with PVC frames and installed 0.5 m high and parallel to the ground surface, following the design of a previous drought experiment at the site that used smaller shelters [Wood *et al.*, 2013; Wood and Silver, 2012]. After the three-month pre-treatment period, shelters were installed on five plots in March 2017 and maintained in place until November 2018, which marked the beginning of the three month post-treatment period. Importantly, the back-to-back passing of category 4 hurricanes Irma and María in September 2017 disturbed the forest canopy. Shelters were secured in place prior to the storms, but there was inevitable damage caused by the winds and falling debris, so all damaged shelters were replaced by October 2017 (~1 month post-hurricanes). Litterfall accumulated on the shelter tops was manually deposited on the plots weekly.

The goal of the throughfall exclusion treatment was to significantly reduce soil moisture inputs relative to control plots, rather than exclude all water entering our plots which would be unrealistic in this high humidity environment. Subsurface lateral drainage and surface flow were not excluded as this would have created confounding effects due to soil disturbance and removal of water flow pathways. Even during a severe natural drought, some rain occurred, and soils received and retained some moisture in this wet ecosystem [O'Connell *et al.*, 2018].

We continuously monitored volumetric soil moisture (VSM), soil temperature, and soil oxygen (O₂) concentrations in the middle of each plot at 0-15 cm, 15-30 cm, and 30-45 cm depths from December 2016 (start of pre-treatment period) until January 2019 (end of post-treatment period). Hourly sensor measurements were recorded with dataloggers (Model: CR1000X, Campbell Scientific, Inc.) that were kept energized using deep-cycle marine batteries charged with a portable gasoline generator.

In addition to high frequency sensor measurements, we also conducted bi-weekly to monthly measurements of soil greenhouse gas fluxes (carbon dioxide, CO₂; methane, CH₄; nitrous oxide, N₂O) using static flux chambers throughout the duration of our experiment. Gas samples (30 mL) were collected with plastic syringes from static flux chambers (installed to 3 cm depth and removed between measurements) and stored in pre-evacuated 20 mL glass Wheaton vials and thick Geo-Microbial septa (GMT, Ochelata, Oklahoma, USA) to be shipped overnight from Puerto Rico to California. Gas concentrations were measured at the Silver Lab in UC Berkeley using a gas chromatograph (Shimadzu, Columbia, Maryland) equipped with a flame ionization detector, thermal conductivity detector, and electron capture detector for CH₄, CO₂, and N₂O, respectively. Significant fluxes for each gas were calculated in R [R Core Team, 2021] based on the significance of a linear model fitted to the time-series of concentration change during the measurement period (due to the soil-atmosphere concentration gradients CO₂ always has positive fluxes, while CH₄ and N₂O can have positive or negative fluxes).

Soils were sampled six times between January 2017 and January 2019. During each soil sampling campaign, soils were collected from the 0-15 cm, 15-30 cm, and 30-45 cm depths using three replicate 5 cm diameter cores from each plot. We measured soil pH in a 1:1 soil to water slurry (citation), as well as gravimetric soil moisture by oven-drying subsamples at 105°C to a constant weight. Total soil C and N content were measured on a CE Instruments NC 2100 Elemental Analyzer (Rodano, Milano, Italy) on soils that were air-dried and ground. To measure labile (i.e., soluble phosphate) and recalcitrant (i.e., bound to Fe or Al) phosphorus (P) pools, we used sequential NaHCO₃ and NaOH extractions, respectively [Tiessen and Moir, 1993]. Briefly, we first extracted approximately 1.5 g fresh soil with 0.5 M NaHCO₃ followed by 0.1 M NaOH. Both extracts were analyzed colorimetrically for inorganic P and total P after digestion with acid ammonium persulfate. Organic P was calculated as the difference between total and inorganic P

[Murphy and Riley, 1962]. We measured Fe species as these have been shown to be an important predictor of both C and P cycling in this ecosystem [Chacon *et al.*, 2006; Hall and Silver, 2015]. Concentrations of reduced and oxidized iron (Fe(II) + Fe(III)) were measured with a 0.5 M HCl extraction and analyzed colorimetrically. Soils were extracted with 0.2 M sodium citrate/0.05 M sodium ascorbate solution and analyzed on an inductively coupled plasma atomic emission spectrometer (Perkin-Elmer, USA) for poorly crystalline Fe.

We used linear mixed effects models to test for the effects of treatment, depth, and sampling date on variables measured during the six soil sampling dates, using the plot as a random factor [R Core Team, 2021]. We tested for significant correlations between mean soil GHG fluxes and mean daily soil microclimate (VSM, soil O₂, soil temperature) using the ‘corrplot’ and ‘Hmisc’ R packages [R Core Team, 2021]. We also used the Wilcoxon-test to test for treatment differences within soil microclimate variables and soil GHG fluxes during the different time periods of the experiment (i.e., pre-treatment, treatment, post-treatment).

Results

Volumetric soil moisture, soil oxygen, and soil temperature

Background volumetric soil moisture (VSM) at 0-15 cm in control plots had periods of continuous soil saturation contrasting with extended periods of fluctuating VSM due to frequent dry and rewetting cycles (Figure 12a). While temporal fluctuations of VSM were comparable between the treatment and control plots during the pre-treatment period, on average there was a small but significant difference between treatments at 0-15 cm ($p < 0.001$, Control: $0.462 \pm 0.005 \text{ m}^3 \text{ m}^{-3}$ vs. Drought: $0.445 \pm 0.005 \text{ m}^3 \text{ m}^{-3}$), with lower VSM in pre-treatment drought plots (Table 10). Once throughfall exclusion began in March 2017, a larger significant difference developed between treatments ($p < 0.001$, Control: $0.463 \pm 0.002 \text{ m}^3 \text{ m}^{-3}$ vs. Drought: $0.291 \pm 0.002 \text{ m}^3 \text{ m}^{-3}$), with VSM in control plots remaining near pre-treatment values, while drought plots decreased to $< 0.3 \text{ m}^3 \text{ m}^{-3}$ by June 2017, when the second soil sampling occurred (Figure 12a). The effects of Hurricane María on VSM in control plots were limited to returning soils to saturation following a two-week period of no rainfall between Hurricanes Irma and María (Figure 12a). Significant differences in mean VSM were maintained for the duration of the treatment period ($p < 0.05$; Table 10). After shelters were removed in November 2018, VSM began to recover in drought plots, with values approaching those of the control plots by April 2019 (Figure 12a). However, the difference in mean VSM between treatments was still significant during the post-treatment period in the surface soils ($p < 0.05$; Table 10).

There was a notable reduction in the magnitude of VSM fluctuations below 15 cm, as well as in the variability within treatments, with values in control plots remaining $> 0.4 \text{ m}^3 \text{ m}^{-3}$ throughout the entire experiment at both 15-30 and 30-45 cm (Figure 12b-c). Similar to surface soils, there were periods of continuous soil saturation in control plots, but the signal from dry-rewetting cycles was muted, reflecting the decreasing influence of individual rainfall events on VSM with increasing depth. As occurred at 0-15 cm, differences between control and pre-treatment plots in mean VSM at 15-30 cm and 30-45 cm were also significant ($p < 0.05$), but of small magnitude (at 15-30 cm, Control: $0.483 \pm 0.002 \text{ m}^3 \text{ m}^{-3}$ vs. Drought: $0.478 \pm 0.001 \text{ m}^3 \text{ m}^{-3}$; at 30-45 cm, Control: $0.478 \pm 0.001 \text{ m}^3 \text{ m}^{-3}$ vs. Drought: $0.474 \pm 0.001 \text{ m}^3 \text{ m}^{-3}$). The effects of throughfall exclusion on VSM at depth were also significant throughout treatment period ($p < 0.05$), with almost an order of magnitude increase in the mean difference between treatments (at 15-30 cm, Control: $0.490 \pm 0.001 \text{ m}^3 \text{ m}^{-3}$ vs. Drought $0.453 \pm 0.001 \text{ m}^3 \text{ m}^{-3}$; at 30-45 cm,

Control: $0.490 \pm 0.001 \text{ m}^3 \text{ m}^{-3}$ vs. Drought: $0.457 \pm 0.001 \text{ m}^3 \text{ m}^{-3}$). The recovery of VSM at depth during the post-treatment period was slow, especially at 30-45 cm where there were still significant differences between treatments six months after shelters were removed ($p < 0.001$, Control: $0.486 \pm 0.001 \text{ m}^3 \text{ m}^{-3}$ vs. Drought $0.466 \pm 0.001 \text{ m}^3 \text{ m}^{-3}$). Differences between treatments in VSM also remained significant during the post-treatment period at 15-30 cm ($p < 0.001$, Control: $0.478 \pm 0.002 \text{ m}^3 \text{ m}^{-3}$ vs. Drought: $0.459 \pm 0.002 \text{ m}^3 \text{ m}^{-3}$).

Table 10. Mean daily volumetric soil moisture, soil oxygen concentration, and soil temperature (\pm SE) at 0-15 cm by treatment and time-period. Different capital letters denote significance between treatments for each variable at $p < 0.05$.

Time Period (n=days)	Volumetric soil moisture ($\text{m}^3 \text{ m}^{-3}$)		Soil oxygen concentration (%)		Soil temperature ($^{\circ}\text{C}$)	
	Control	Drought	Control	Drought	Control	Drought
Pre (n=117)	0.462 $\pm 0.005^{\text{A}}$	0.445 $\pm 0.005^{\text{B}}$	17.7 $\pm 0.2^{\text{A}}$	18.5 $\pm 0.1^{\text{B}}$	21.04 $\pm 0.08^{\text{A}}$	21.08 $\pm 0.08^{\text{A}}$
Treatment (n=580)	0.463 $\pm 0.002^{\text{A}}$	0.291 $\pm 0.002^{\text{B}}$	15.2 $\pm 0.1^{\text{A}}$	18.3 $\pm 0.1^{\text{B}}$	23.32 $\pm 0.05^{\text{A}}$	23.58 $\pm 0.05^{\text{B}}$
Post (n=175)	0.380 $\pm 0.005^{\text{A}}$	0.350 $\pm 0.004^{\text{B}}$	17.7 $\pm 0.1^{\text{A}}$	17.6 $\pm 0.1^{\text{A}}$	22.24 $\pm 0.10^{\text{A}}$	22.50 $\pm 0.10^{\text{B}}$

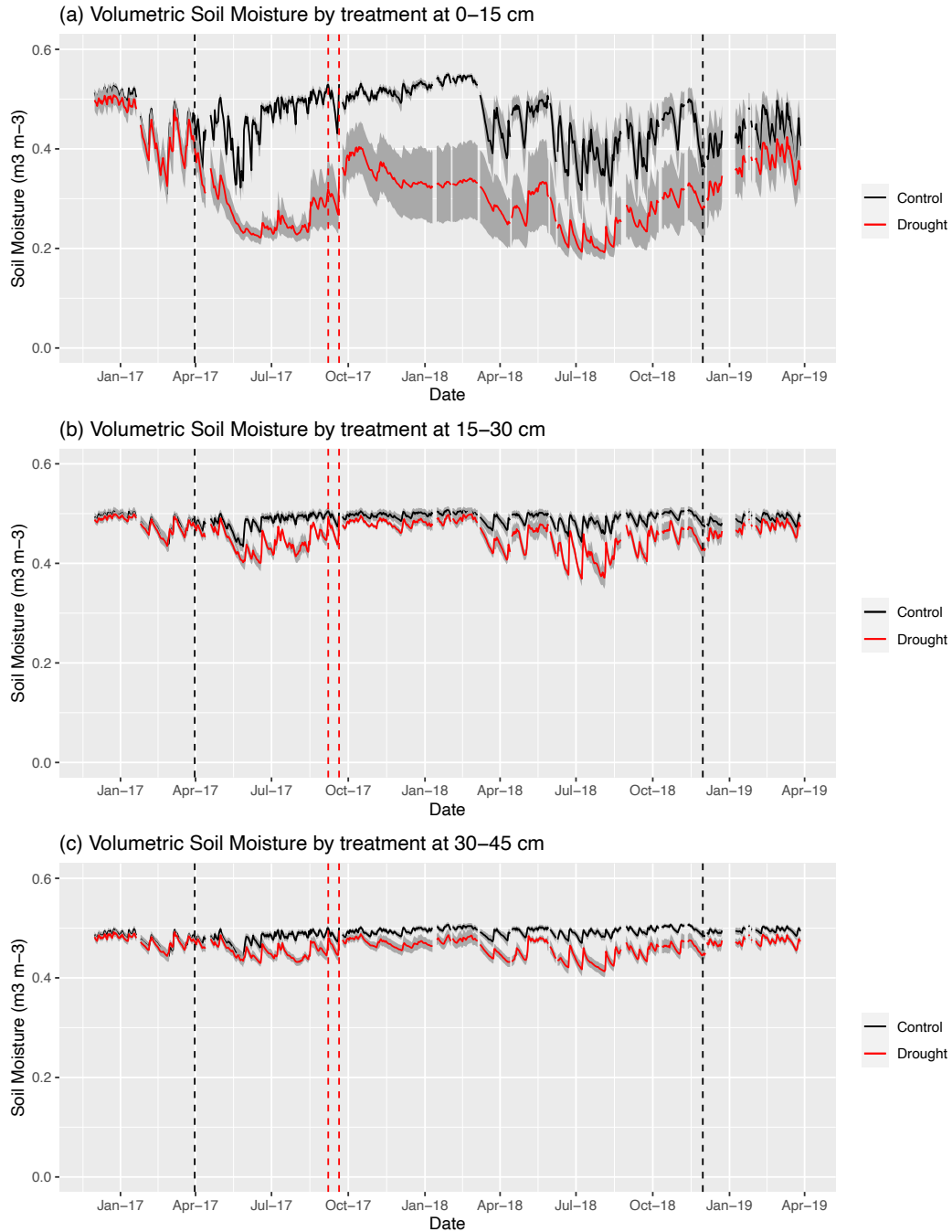


Figure 12a-c. Mean daily volumetric soil moisture (\pm SE, $n = 5$) by treatment for a) 0-15 cm, b) 15-30 cm, c) 30-45 cm. Black vertical dashed lines indicate start/end of throughfall exclusion period (March 2017 and November 2018, respectively), and red vertical dashed lines indicate Hurricanes Irma and María in September 2017.

Soil oxygen (O₂) concentrations in control plots were highly variable over time across all depths (Figure 13a-c). Throughout the entire experiment, there was a trend in control plots of decreasing soil O₂ concentrations with depth ($p < 0.05$) and synchronized temporal fluctuations of similar magnitude in response to rainfall events ($p < 0.05$). About midway into the pre-treatment period increased levels of soil aeration occurred over a one-week period at the end of January 2017, lasting towards the start of throughfall exclusion in March 2017. As with VSM, there was a small (0.8%) but significant difference in soil O₂ concentration at 0-15 cm between pretreatment and control plots ($p < 0.001$, Table 10).

Throughfall exclusion treatments increased soil aeration at all depths, with near atmospheric O₂ concentrations (~20%) at 0-15 cm depth prior to the hurricanes and during the final months of the treatment period (Figure 13a). The large excursions of decreasing soil O₂ in control plots observed at all depths during periods of high rainfall were absent in drought plots during much of the treatment period. Mean soil O₂ concentrations during the treatment period at 0-15 cm were 18.3 ± 0.1 % and 15.2 ± 0.1 % in control and drought plots, respectively ($p < 0.0001$; Table 10). There was also a significant treatment effect on soil O₂ concentration at depth ($p < 0.0001$), with mean treatment differences ranging between 2 and 2.7 % at 15-30 cm (Control: 14.7 ± 0.1 % vs. Drought: 16.7 ± 0.1 %) and 30-45 cm (Control: 14.5 ± 0.1 % vs. Drought: 17.2 ± 0.1 %), respectively. During the post-treatment period, mean soil O₂ concentrations were comparable between treatments and controls with differences less than 0.5 % at all depths (Table 10).

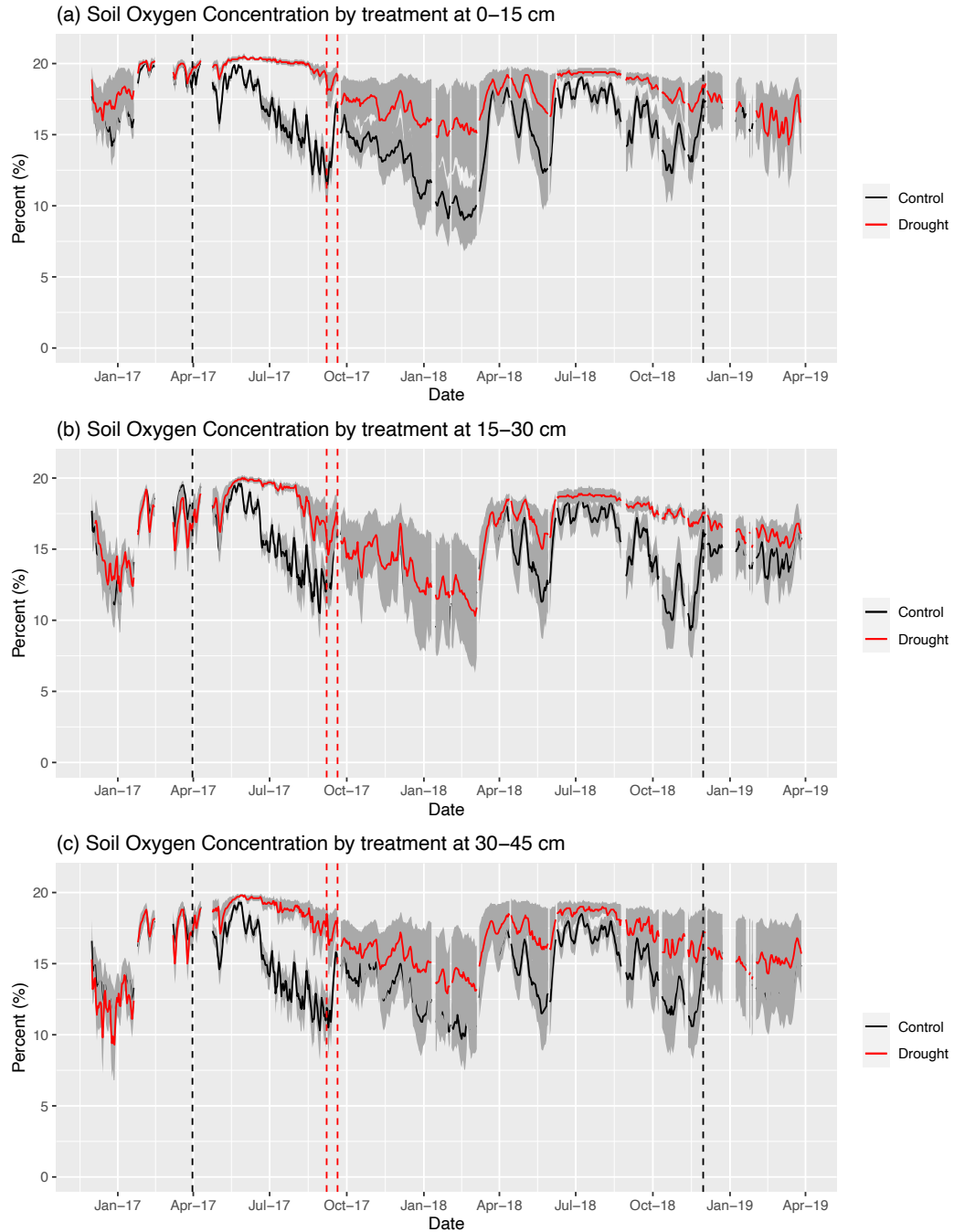


Figure 13a-c. Mean daily soil oxygen concentrations (\pm SE, $n = 5$ per depth) by treatment for a) 0-15 cm, b) 15-30 cm, c) 30-45 cm. Black vertical dashed lines indicate start/end of throughfall exclusion period (March 2017 and November 2018, respectively), and red vertical dashed lines indicate Hurricanes Irma and María in September 2017.

Soil temperature followed a seasonal pattern at all depths, with values ranging between a minimum of approximately 20 °C in February/March and a maximum of 25 °C in August/September (Figure 14a-c). Both seasonal and short-term fluctuations in temperature became slightly attenuated with depth, with surface soils (0-15 cm) showing the largest day-to-day variability (Figure 14a). There were no significant differences between pretreatment and control plots for soil temperature at any depth (Table 10).

There was no significant treatment effect of throughfall exclusion on soil temperature during the first six months of the experiment (Figure 14a). However, following the hurricanes, soil temperatures in drought plots were significantly higher at 0-15 cm ($p < 0.05$; Table 10). Post-hurricane differences in soil temperature between treatment and control plots were observed from October to March and became negligible from April to September (Figure 14a-c). A significant temperature effect was observed post-treatment in the drought plots, especially at depths below 15 cm, where soil temperature was elevated by approximately 0.3 °C ($p < 0.001$; at 15-30 cm, Control: 22.48 ± 0.09 °C vs. Drought: 22.79 ± 0.09 °C; at 30-45 cm, Control: 22.58 ± 0.09 °C vs. Drought: 22.88 ± 0.08 °C).

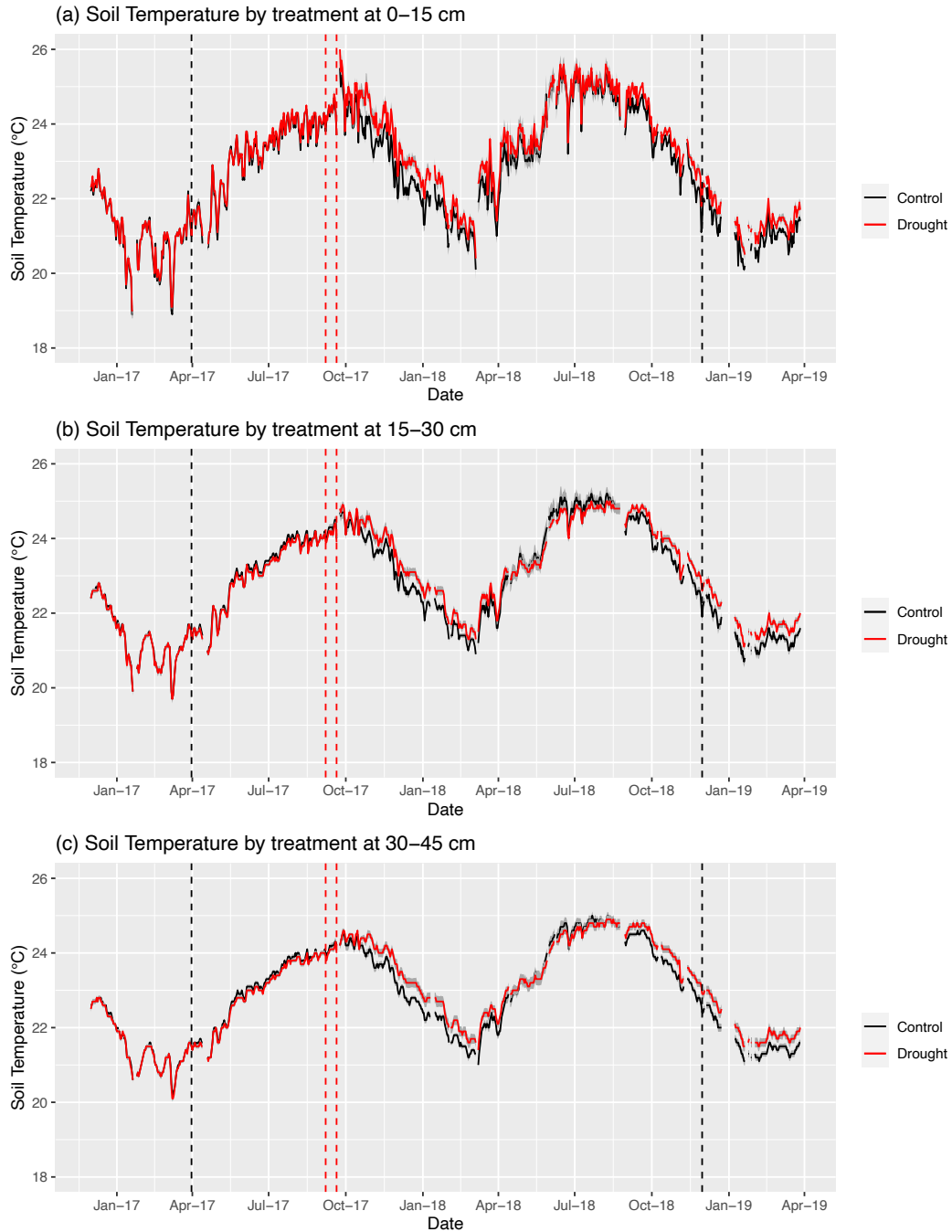


Figure 14a-c. Mean daily soil temperature (\pm SE, $n = 5$) by treatment for a) 0-15 cm, b) 15-30 cm, and c) 30-45 cm. Black vertical dashed lines indicate start/end of throughfall exclusion period (March 2017 and November 2018, respectively), and red vertical dashed lines indicate Hurricanes Irma and María in September 2017.

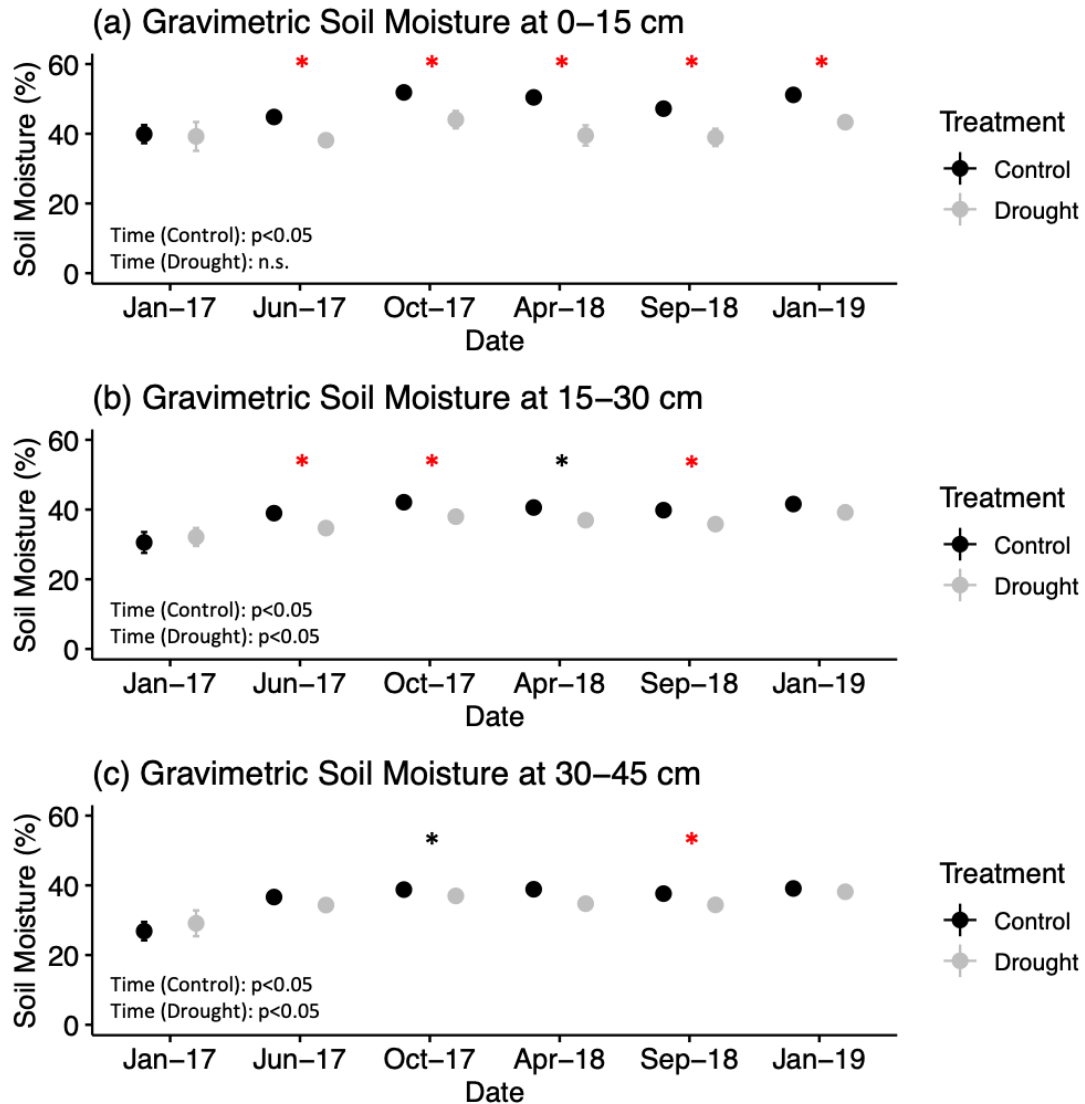


Figure 15a-c. Mean gravimetric soil moisture (\pm SE, $n = 5$) by treatment at a) 0-15 cm, b) 15-30 cm, and c) 30-45 cm. Sampling dates are arranged chronologically and include the pre-treatment and post-treatment samplings (Jan-17 and Jan-19, respectively), and the post-hurricane sampling (Oct-17). Other three samplings (Jun-17, Apr-18, Sep-18) occurred with throughfall exclusion. Red and black asterisks denote significance at $p < 0.05$ and $p < 0.1$, respectively.

Gravimetric soil moisture and Soil pH

Gravimetric soil moisture (GSM) decreased significantly with depth for all sampling dates and for both treatments ($p < 0.05$). Soil GSM was significantly higher in Oct. 2017 for all treatments and depths ($p < 0.05$), except in surface soils of drought plots (0-15 cm). The lowest GSM values in the control plots were measured during the pre-treatment sampling, while significantly higher values near saturation ($> 50\%$) were observed at the surface during most of the other sampling dates ($p < 0.05$).

No significant differences in GSM were observed between treatment and control plots at any depth in the pre-treatment sampling. Throughfall exclusion significantly decreased GSM at 0-15 cm for the other five sampling dates, including in the post-treatment sampling ($p < 0.05$).

Mean GSM at 0-15 cm during the treatment period was $49 \pm 2\%$ and $40 \pm 1\%$ in control and drought plots, respectively. In drought plots at 0-15 cm, GSM showed no significant change over time (Figure 15a). Smaller but significant declines in GSM at 15-30 cm and 30-45 cm occurred during at least two sampling dates within the treatment period ($p < 0.05$); GSM increased rapidly at depth in the post-treatment sampling period.

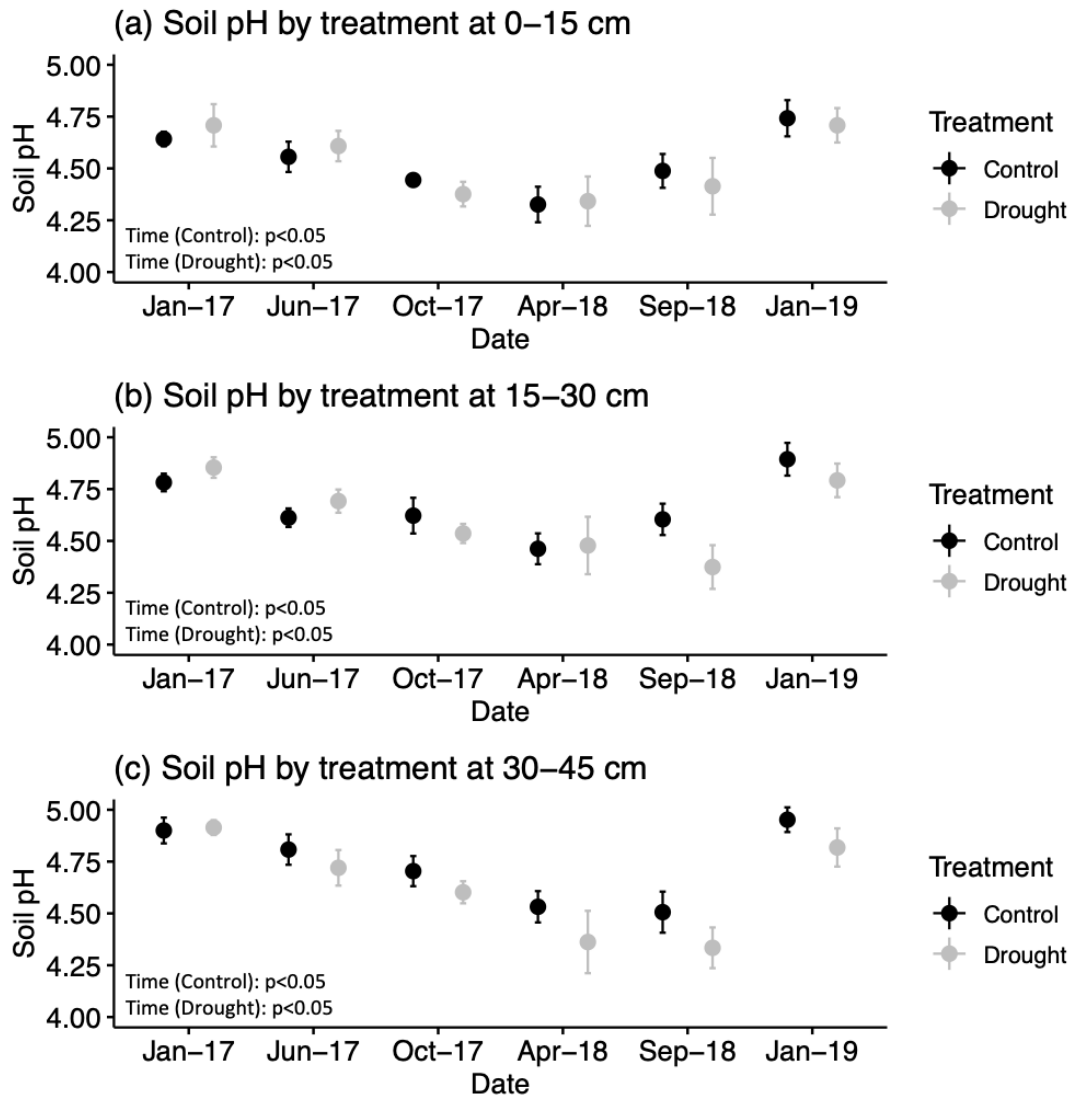


Figure 16a-c. Mean soil pH (\pm SE, $n = 5$) by treatment at a) 0-15 cm, b) 15-30 cm, and c) 30-45 cm. Sampling dates are arranged chronologically and include the pre-treatment and post-treatment samplings (Jan-17 and Jan-19, respectively), and the post-hurricane sampling (Oct-17). Other three samplings (Jun-17, Apr-18, Sep-18) occurred with throughfall exclusion.

Mean soil pH ranged between 4 and 5, with a significant depth effect ($p < 0.05$) with the lowest values found at the surface. There was no significant treatment effect of throughfall exclusion at any sampling date or depth. However, there was a significant yet transient decrease

in soil pH over time in both treatments ($p < 0.05$). Soil pH at 30-45 cm decreased between April and September 2018, while surface soils (0-15 cm and 15-30 cm) increased during this period.

HCl-extractable Fe^{2+} and Fe^{3+} and Citrate ascorbate-extractable Fe

Mean HCl-extractable soil Fe^{2+} concentrations remained low throughout the experiment in both treatment and control plots (< 0.5 mg Fe/g dry soil) and showed a significant decrease with depth during the first four sampling dates ($p < 0.05$). There was a significant increase in reduced iron over time below 15 cm in both treatment and control plots, and especially at 30-45 cm (Supplementary Figure 1b-c). There was a three-fold increase in soil Fe^{2+} at 30-45 cm in control plots between the pre-treatment and post-treatment sampling dates (0.042 vs. 0.152 mg Fe/g dry soil, respectively). Soil Fe^{2+} at 0-15 cm was variable over time (although only significantly in drought plots).

Mean HCl-extractable total Fe concentrations (Fe^{2+} and Fe^{3+}) were at least an order of magnitude higher than soil Fe^{2+} and showed a significant depth gradient during the two pre-hurricane sampling dates with the highest values at 0-15 cm ($p < 0.05$). There was no significant treatment effect on total HCl-extractable soil Fe at any sampling date or depth, and concentrations increased following the hurricanes at a similar magnitude in both treatments and at all depths (Supplementary Figure 2a-c). Total HCl-extractable soil Fe increased by an order of magnitude to >4 mg Fe/g dry soil throughout the entire soil profile between the June 2017 and October 2017 sampling dates. At 15-30 cm and 30-45 cm, total HCl-extractable soil Fe peaked first in October 2017, and values at 0-15 cm continued increasing for an additional sampling date reaching a maximum in April 2018. HCl-extractable Fe in surface soils declined quickly thereafter, while soils below 15 cm remained high until the end of the experiment.

Mean citrate ascorbate-extractable soil Fe was comparable between treatments at all depths and sampling dates, showing a significant depth gradient throughout the experiment ($p < 0.05$). Values at the surface were nearly double those at depth during the two pre-hurricane sampling dates. Citrate ascorbate-extractable soil Fe peaked at all depths during the post-hurricane sampling in October 2017. Citrate ascorbate-extractable soil Fe values declined thereafter throughout the soil profile during the April and September 2018 samplings and were still elevated at all depths in the post-treatment sampling date relative to the start of the experiment.

Soil phosphorus, nitrogen, and carbon concentrations

The $NaHCO_3$ -extractable P fraction was low across the soil profile, with mean values below 5 ug P/g dry soil throughout the experiment (Supplementary Figure 4a-c). Drought plots in two out of four sampling dates within the treatment period had significantly lower labile soil P at 0-15 cm ($p < 0.05$), while no significant treatment effect was detected at depth (Figure 17). At all depths and for both treatments, there was significant variation in $NaHCO_3$ -extractable P soil P over time ($p < 0.01$), with lowest concentrations measured in October 2017 and January 2019 (~ 1 to 3 ug P/g dry soil).

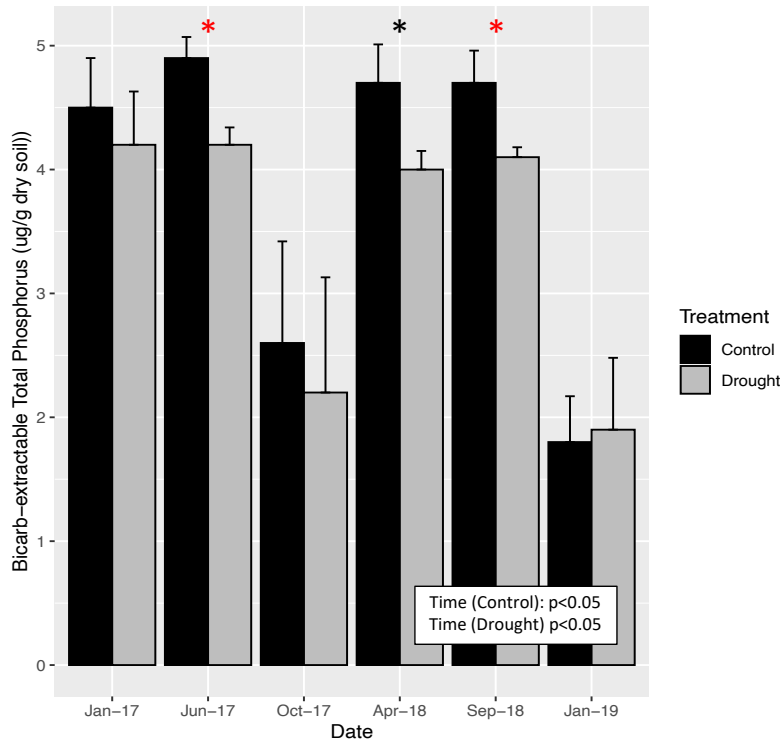


Figure 17. Mean NaHCO_3 -extractable total soil phosphorus (+ SE, $n = 5$) at 0-15 cm by treatment. Red and black asterisk indicate significance at $p < 0.05$ or $p < 0.1$, respectively.

There was no significant treatment effect of throughfall exclusion on NaOH-extractable inorganic, organic, or total P at any depth or sampling date, but there was a significant increase in NaOH-extractable inorganic soil P over time ($p < 0.05$). While this significant response was observed for both treatments and at all depths, it was most evident below 15 cm where inorganic soil P concentrations tended to be significantly lower than at the surface ($p < 0.05$, Supplementary Figure 16a-c). On the final sampling date, mean NaOH-extractable inorganic soil P concentration remained significantly higher than pre-treatment values in both control and drought plots, with mean values >20 ug P/g dry soil throughout the entire soil profile ($p < 0.05$; more than 2x pre-treatment values at 15-30 cm and 30-45 cm).

Contrary to the response of inorganic soil P, NaOH-extractable organic and total soil P did not change over time at 0-15 cm (Supplementary Figures 6a and 7a). Significant variation in organic and total soil P was observed over time in the control or drought treatments at some depths ($p < 0.05$), but there was no trend below 15 cm, with comparable values in the pre- and post-treatment sampling dates for both treatments (Supplementary Figures 6b-c and 7b-c).

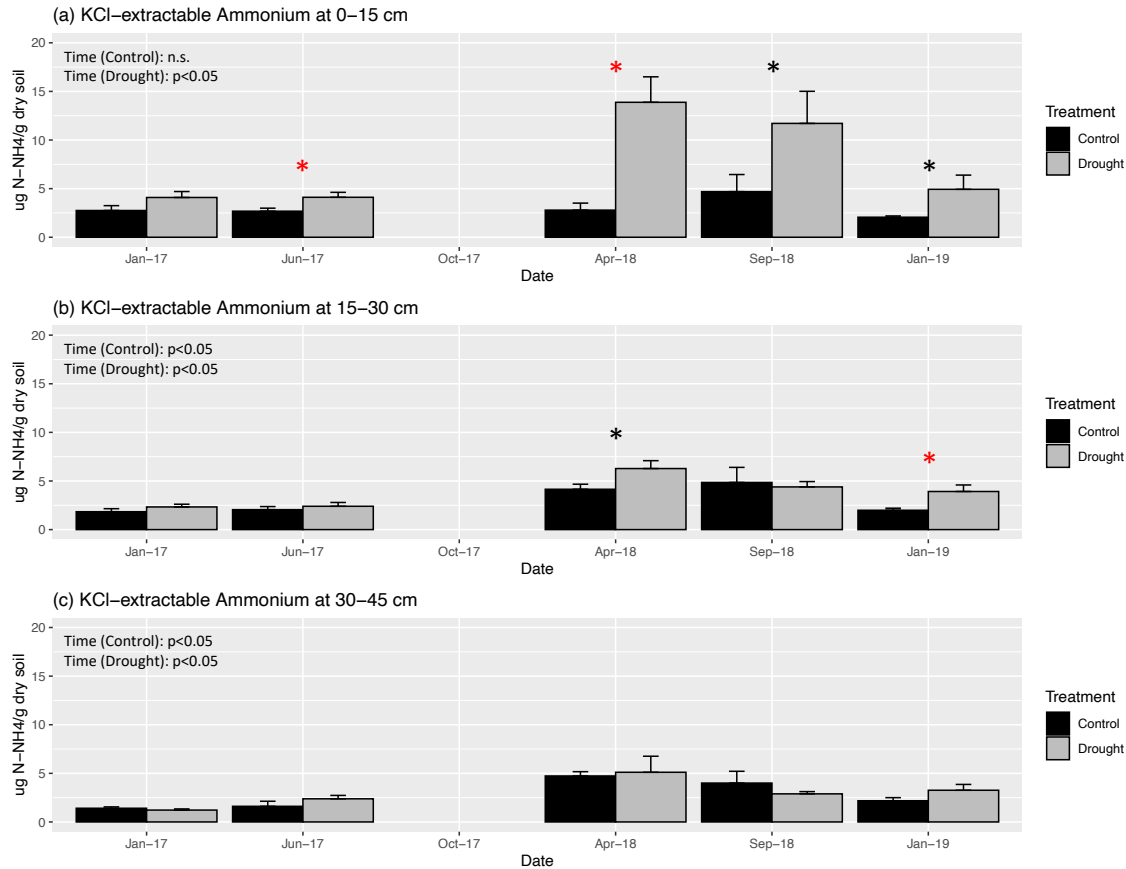


Figure 18a-c. Mean KCl-extractable soil ammonium (+ SE, n = 5) by treatment at a) 0-15 cm, b) 15-30 cm, and c) 30-45 cm. Red and black asterisk indicate significance at $p < 0.05$ or $p < 0.1$, respectively.

Soil ammonium (NH₄) concentrations at 0-15 cm were 2.99 ± 0.44 ug N-NH₄/g dry soil in control plots, with no significant variation over time (Figure 18a). Soil NH₄ was significantly higher in the treatment relative to the control by the second sampling date ($p < 0.05$) and remained elevated throughout the rest of the experiment. Soil NH₄ concentrations tended to be lower at depth than at the surface, especially at 30-45 cm, where the pre-treatment mean was 1.41 ± 0.14 ug N-NH₄/g dry soil and 1.22 ± 0.12 ug N-NH₄/g dry soil in control and drought plots, respectively (Figure 18c). There was a significant increase in soil NH₄ across all treatments at 15-30 cm and 30-45 cm between the June and April sampling dates ($p < 0.05$). The only significant treatment effects on soil NH₄ concentration at depth occurred three months after shelters were removed in the post-treatment sampling, with a significant difference between treatments at 15-30 cm (Control: 1.99 ± 0.21 ug N-NH₄/g dry soil; Drought: 3.92 ± 0.67 ug N-NH₄/g dry soil).

Mean KCl-extractable soil nitrate (NO₃) concentrations were an order of magnitude lower than soil NH₄; at depth; soil NO₃ concentrations were below the detection limit of the analytical instrumentation for many of the samples. Pre-treatment soil NO₃ concentrations in control and drought plots ranged from 0.02 to 0.13 ug N-NO₃/g dry soil, with significantly higher values at 0-15 cm ($p < 0.05$). No significant treatment effects were detected. There was a significant increase in soil NO₃ on the April 2018 sampling date that was observed in both

control and drought plots at all depths ($p < 0.05$). The magnitude of the increase was largest at 0-15 cm, where concentrations increased for both treatments from 0.1 to >3 $\mu\text{g N-NO}_3/\text{g}$ dry soil. The responses at depth were also significant, peaking at values between 0.5 and 1.5 $\mu\text{g N-NO}_3/\text{g}$ dry soil (Supplementary Figure 8a-c). Soil NO_3 concentrations gradually decreased over time after the April sampling date.

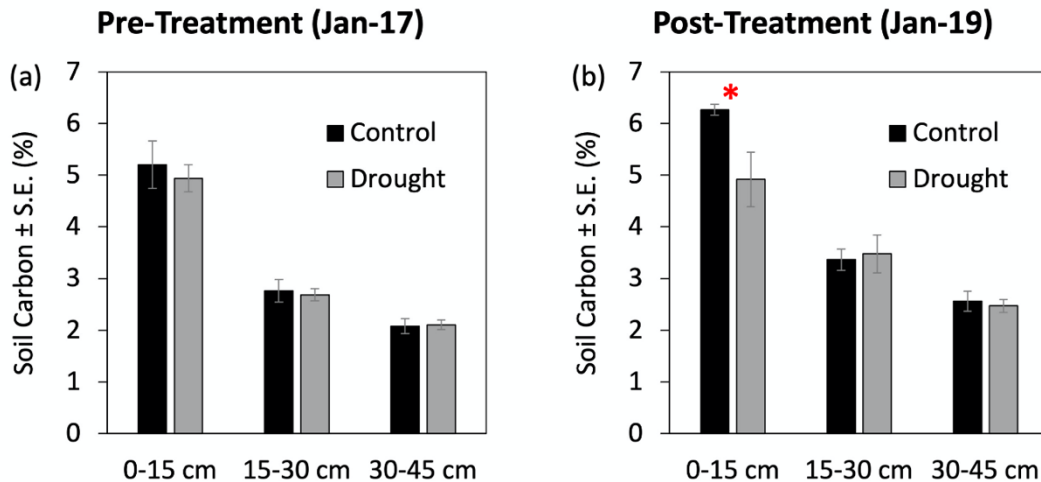


Figure 19a-b. Mean total soil carbon (\pm SE, $n = 5$) by treatment and depth at the a) pre-treatment sampling in January 2017 and b) post-treatment sampling in January 2019. Red asterisk indicates significance at $p < 0.05$.

There was no significant difference between treatment and controls in soil organic C during the pre-treatment period, with comparable values in control and drought plots at all depths (Figure 19a). Mean values in control and drought plots at 0-15 cm were 5.2 ± 0.5 % and 4.9 ± 0.3 %, respectively. Soil organic C decreased significantly with increasing depth at both sampling dates ($p < 0.05$). Soil organic C in the post-treatment sampling revealed a significant negative legacy effect of throughfall exclusion at 0-15 cm ($p < 0.05$), while there were no significant treatment effects at depth (Figure 19b). Again, for both treatment and control there was a significant depth gradient of soil C in the post-treatment sampling that became somewhat steeper in the control plots relative to the pre-treatment sampling ($p < 0.05$).

In control plots, there was a trend of higher soil organic C in the post-treatment sampling in January 2019 that was marginally significant at all depths (Figure 20a; $p < 0.1$). At 0-15 cm, mean soil organic C in control plots increased from 5.2 ± 0.5 % in January 2017 to 6.3 ± 0.1 % in January 2019. A similar trend was observed in drought plots below 15 cm, with a significant positive effect of time on total soil C at 30-45 cm (Figure 20b; $p < 0.05$). Conversely, at 0-15 cm in drought plots, soil organic C remained unchanged throughout the experiment with pre- and post-treatment mean values of 4.9 ± 0.3 % and 4.9 ± 0.5 %, respectively.

Correlations: gravimetric soil moisture, pH, iron, nitrogen, and phosphorus concentrations

Across the six soil sampling dates, gravimetric soil moisture (GSM) in control plots was strongly positively correlated with citrate ascorbate-extractable Fe at both 0-15 cm ($p < 0.01$, $r^2 = 0.89$) and 15-30 cm ($p < 0.05$, $r^2 = 0.61$). In drought plots, there was a significant negative correlation between GSM and NaHCO_3 -extractable total P at 0-15 cm ($p < 0.01$, $r^2 = 0.93$). At 0-15 cm for both treatments, there was a significant positive correlation between HCl-extractable

total Fe and KCl-extractable NO_3 ($p < 0.05$, Control $r^2 = 0.70$ vs. Drought $r^2 = 0.71$). At 15-30 cm for both treatments, and at 30-45 cm in control plots, there was a significant positive correlation between HCl-extractable total Fe and citrate ascorbate-extractable Fe (for 15-30 cm Control: $p < 0.01$, $r^2 = 0.91$; Drought: $p < 0.05$, $r^2 = 0.75$, for 30-45 cm Control: $p < 0.05$, $r^2 = 0.67$). In drought plots at 15-30 cm, there was a significant positive correlation between KCl-extractable NH_4 and HCl-extractable total Fe ($p < 0.05$, $r^2 = 0.88$), citrate ascorbate-extractable Fe ($p < 0.05$, $r^2 = 0.76$), and NaOH-extractable inorganic P ($p < 0.01$, $r^2 = 0.92$). In these same plots/depth, KCl-extractable NO_3^- had a significant positive correlation with NaOH-extractable inorganic P ($p < 0.05$, $r^2 = 0.89$) and KCl-extractable NH_4 ($p < 0.05$, $r^2 = 0.87$).

There was a significant positive correlation between NaOH-extractable organic P and NaOH-extractable total P ($p < 0.05$) at all three depths in control plots ($r^2 = 0.80-0.88$), but only at 0-15 cm in drought plots ($r^2 = 0.68$). In drought plots at 0-15 cm, there was a significant negative correlation between soil pH and KCl-extractable NO_3 ($p < 0.05$, $r^2 = 0.76$) and NH_4 ($p < 0.01$, $r^2 = 0.89$), and a significant positive correlation between KCl-extractable NO_3 and NH_4 ($p < 0.05$, $r^2 = 0.86$). In drought plots at 30-45 cm, KCl-extractable NO_3 was significantly correlated with soil pH ($p < 0.05$, $r^2 = 0.81$) and HCl-extractable total Fe ($p < 0.05$, $r^2 = 0.82$), while KCl-extractable NH_4 was significantly correlated with citrate ascorbate-extractable Fe ($p < 0.01$, $r^2 = 0.95$). In these same plots/depth, there was also a significant positive correlation between citrate ascorbate-extractable Fe and NaOH-extractable inorganic P ($p < 0.05$, $r^2 = 0.65$).

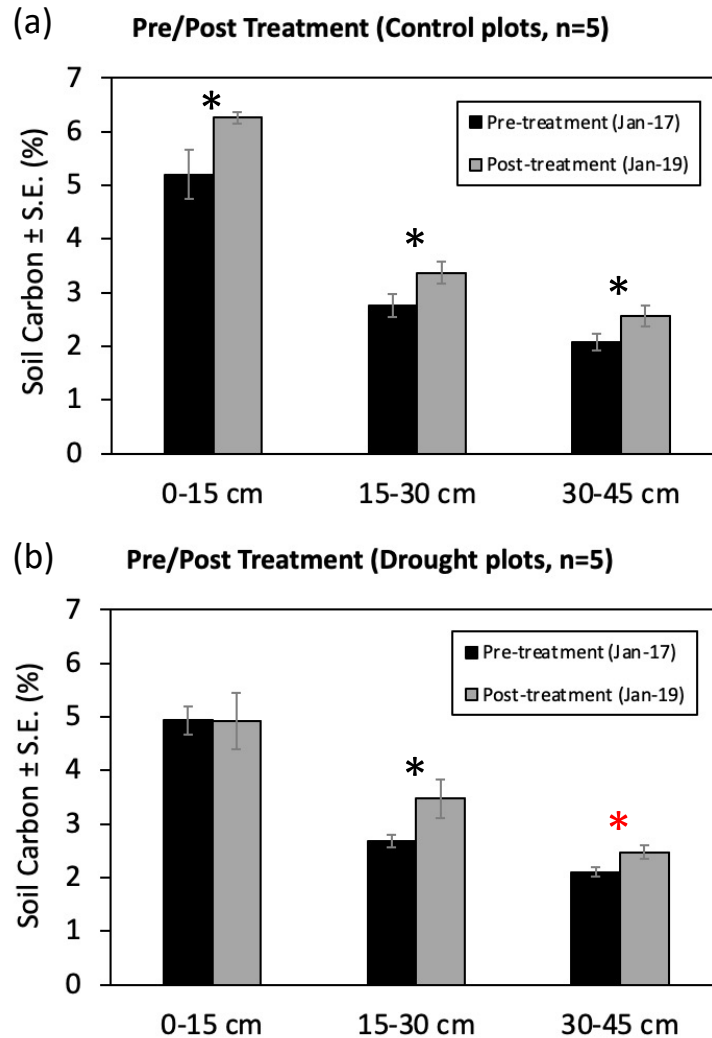


Figure 20a-b. Mean total soil carbon (\pm SE, $n = 5$) by sampling date and depth in the a) control plots and b) drought plots. Red and black asterisks indicate significance at $p < 0.05$ and $p < 0.1$, respectively.

Soil greenhouse gas fluxes: CO_2 , CH_4 , N_2O

During the pre-treatment period, soils in both control and drought plots were significant sources of CO_2 and N_2O , and sinks of CH_4 , with the magnitude of fluxes being similar between pretreatment and control plot (Table 11). Throughfall exclusion significantly reduced soil CO_2 fluxes in drought plots (Figure 21 and Figure 23a; $p < 0.05$), with a larger range of values in control relative to drought plots during the treatment period (range of 4.9 vs. 1.9 g C- CO_2 m² day⁻¹ in control and drought plots, respectively). Across all 28 sampling dates with throughfall exclusion, mean soil CO_2 fluxes were significantly lower in drought than in control plots ($p < 0.05$; Control: 3.4 ± 0.2 g C- CO_2 m² day⁻¹ vs. Drought: 2.5 ± 0.1 g C- CO_2 m² day⁻¹) with significant differences between treatments ($p < 0.05$) in three sampling dates when hot moments of soil respiration observed in control plots did not occur in drought plots (Figure 21). The recovery of soil CO_2 fluxes was rapid, with similar mean values in control and drought plots during four post-treatment sampling dates (Table 11). However, treatment effects were reversed

on the final sampling date in January 2019, when mean soil CO₂ fluxes were significantly higher in drought plots relative to control plots (Figure 21; $p < 0.05$).

Table 11. Mean soil greenhouse gas fluxes (\pm SE) for different periods during the experiment. Letters indicate significance at $p < 0.05$ between treatments within each period for each gas.

Time Period	Soil CO ₂ Efflux (g C-CO ₂ m ² day ⁻¹)		Soil CH ₄ Flux (g C-CH ₄ ha day ⁻¹)		Soil N ₂ O Flux (g N-N ₂ O ha day ⁻¹)	
	Control	Drought	Control	Drought	Control	Drought
Pre-treatment (n=3)	4.3 $\pm 0.7^A$	3.7 $\pm 0.3^A$	-2.8 $\pm 3.9^A$	-3.7 $\pm 1.2^A$	0.2 $\pm 0.1^A$	1.1 $\pm 0.6^A$
Throughfall exclusion (n=28)	3.4 $\pm 0.2^A$	2.5 $\pm 0.1^B$	0.9 $\pm 1.4^A$	-3.2 $\pm 1.2^B$	3.7 $\pm 2.6^A$	1.3 $\pm 1.1^A$
Post-treatment (n=4)	2.6 $\pm 0.4^A$	3.0 $\pm 0.2^A$	6.0 $\pm 2.1^A$	-3.4 $\pm 3.8^A$	1.5 $\pm 0.7^A$	-2.0 $\pm 2.8^A$

Mean soil CH₄ effluxes were negative in both control and drought plots during the pre-treatment period, with no significant differences in magnitude (Table 11). Soils of both treatment and controls fluctuated as sinks and sources of CH₄ over time (net zero fluxes were slightly more common in control plots). There was a significant treatment effect of throughfall exclusion on mean soil CH₄ efflux ($p < 0.05$), with control plots becoming net sources, while soils in drought plots remained net sinks during the treatment period (Figure 23b). Accordingly, the largest positive mean soil CH₄ flux was measured in control plots (33 ± 21 g C-CH₄ ha day⁻¹), while the largest negative mean soil CH₄ efflux was measured in drought plots (-26 ± 15 g C-CH₄ ha day⁻¹), both in early 2018 (Figure 22a). Post-treatment CH₄ effluxes were highly variable with no significant treatment effect.

Mean soil N₂O flux was highly variable, with both negative and positive values, and no significant treatment differences observed (Table 11, Figure 23c). Throughout most of the experiment, soil N₂O flux was near zero, but there was a hot moment in March and April 2018 that was observed in both treatment and control plots, with a higher peak in control plots (Figure 22b).

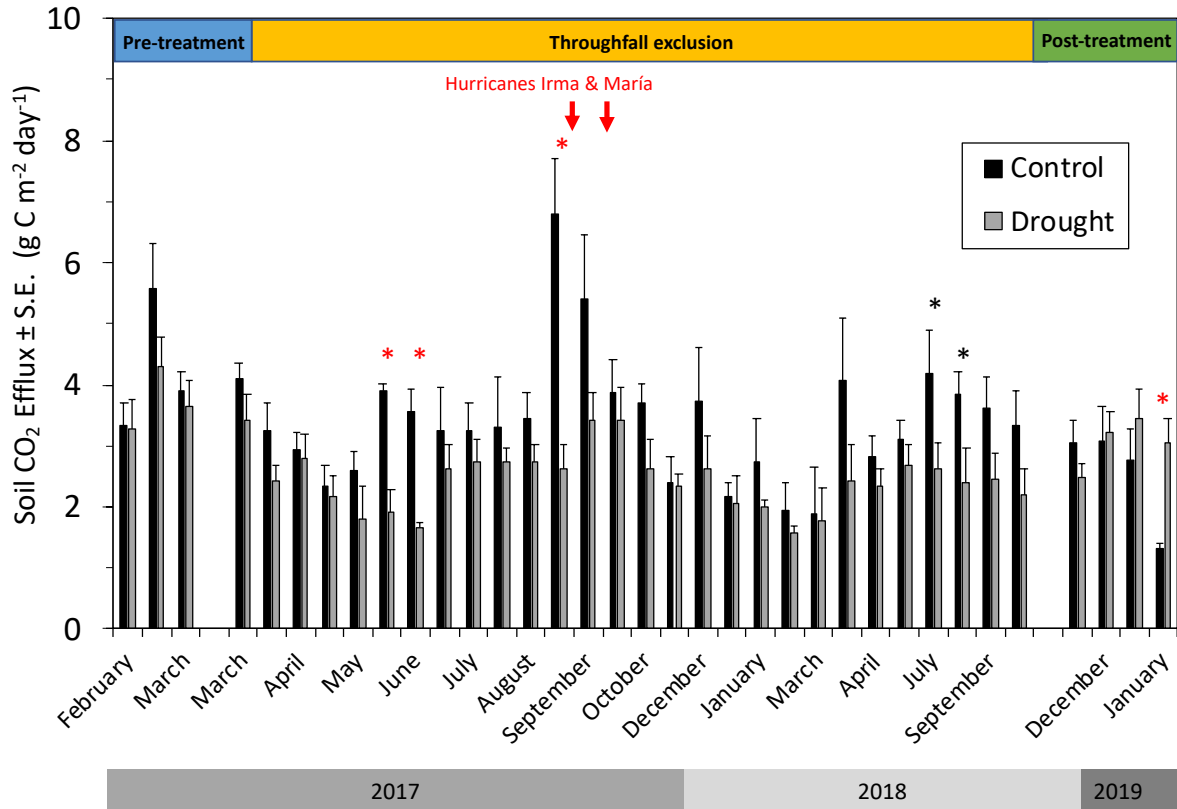


Figure 21. Mean surface soil CO₂ efflux (\pm SE, $n = 5$) by treatment and sampling date. Red and black asterisks indicate significance at $p < 0.05$ and $p < 0.1$, respectively.

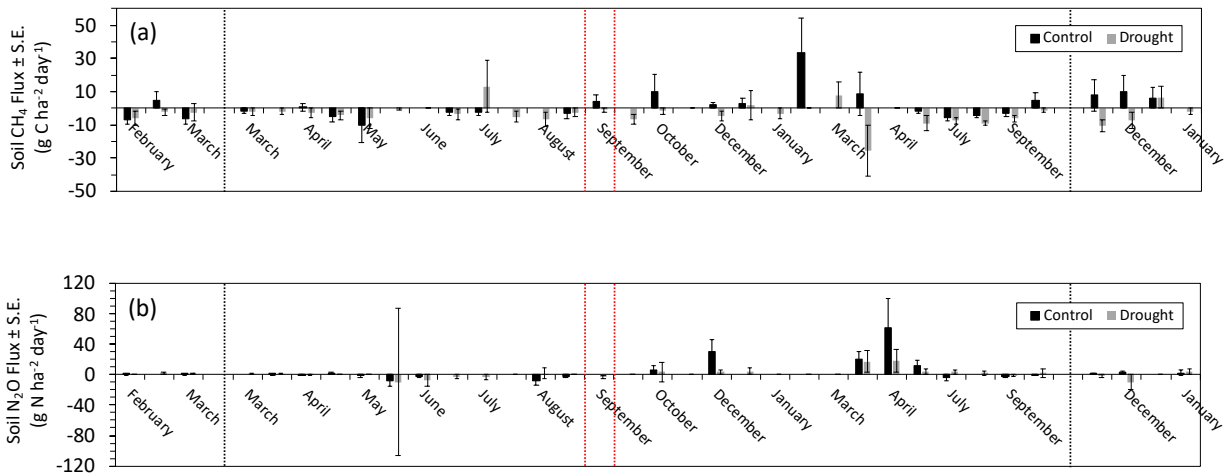


Figure 22a-b. Mean surface a) soil CH₄ and b) soil N₂O fluxes (\pm SE, $n = 5$) by treatment and sampling date. Black dashed lines indicate start/end of throughfall exclusion treatments and red dashed lines indicate Hurricanes Irma and María in September 2017.

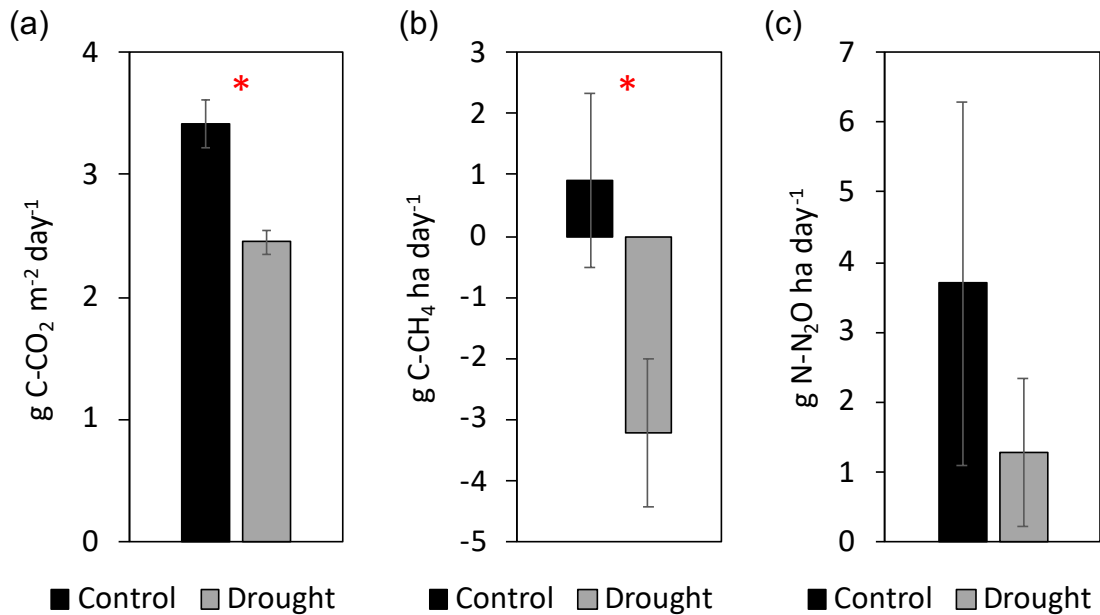


Figure 23a-c. Mean surface soil greenhouse gas fluxes (\pm SE, $n = 28$) of a) CO_2 , b) CH_4 , and c) N_2O during the throughfall exclusion period from March 2017 to November 2018. Red asterisk indicates significance at $p < 0.05$.

Across the soil GHG sampling dates, there was a significant negative correlation between mean daily VSM and soil O_2 concentrations at 0-15 cm ($p < 0.05$), that was much stronger in control relative to drought plots (Control $r^2 = 0.60$, Drought $r^2 = 0.16$). In the drought plots, there was also a significant negative correlation between mean daily VSM and soil temperature at 0-15 cm ($p < 0.001$, $r^2 = 0.28$). Aside from these effects of VSM on soil oxygen and temperature, mean daily VSM at 0-15 cm showed a significant positive correlation with mean soil CO_2 efflux for the throughfall exclusion treatment only ($p < 0.05$, $r^2 = 0.21$). In the control plots, mean soil CH_4 flux showed a significant positive correlation with mean daily VSM ($p < 0.01$, $r^2 = 0.19$), and a significant negative correlation with mean daily soil oxygen concentrations ($p < 0.001$, $r^2 = 0.29$), both at 0-15 cm.

Discussion

The throughfall exclusion manipulation was effective in replicating soil microclimate conditions experienced during actual drought periods in this forest [O'Connell *et al.*, 2018], and the lowest VSM attained was comparable with those of other drought experiments in wet tropical forests [Sotta *et al.*, 2007; van Straaten *et al.*, 2011; Wood and Silver, 2012]. Significant reductions of VSM occurred at all depths with throughfall exclusion and were coupled with an increase in soil O_2 concentration likely due to increased diffusion rates in drier soils. The positive response of soil aeration to throughfall exclusion was similar in magnitude across depths, despite the large differences of the treatment effects on VSM with depth, demonstrating that small changes in VSM can have large effects on soil redox conditions especially below 15 cm. There was a significant negative correlation between mean daily VSM and soil O_2 concentration at 0-15 cm suggesting surface soil moisture was tightly coupled with soil O_2 availability. However, the stronger relationship between VSM and soil O_2 found in control plots highlights the

importance of high VSM for driving periods with low redox that became less frequent with throughfall exclusion.

The importance of VSM as a driver of soil temperature was also revealed in the drought plots, where there was a significant negative correlation between VSM and soil temperature at 0-15 cm. Drier soils can be more sensitive to temperature fluctuations due to their reduced capacity for heat conductance [Mount and Paetzold, 2002], thus representing an additional stress on soil biota with potential consequences for soil biogeochemical processes [Wood *et al.*, 2012]. Collectively, the responses of soil microclimate to throughfall exclusion indicate that drought could exacerbate the effects of climate change because of the coupling of VSM, soil O₂, and soil temperature. It is critical to consider not only the moisture stress caused by drought, but also the significant implications of decreasing VSM for soil redox conditions and thermal conductivity throughout the soil profile.

Throughfall exclusion had no effect on soil temperature during the first six months of the experiment in which the forest canopy was closed. However, the large structural changes caused by the canopy disturbance from Hurricane María in September 2017 [Feng *et al.*, 2020; Reed *et al.*, 2020; Scholl *et al.*, 2021] induced a peak in soil temperature that was evident for both treatment and control plots at all depths. After the hurricane, soil temperatures tracked the regular seasonal pattern in both treatments, but drought plots remained significantly warmer than the controls. The changes in magnitude of the treatment difference of soil temperature throughout the year suggest that throughfall exclusion shelters were not driving the observed warming in drought plots, which became apparent only during the period from October to April in both 2017 and 2018. Given the intermittent nature of these treatment differences, it is also unlikely that continuously lower VSM in drought plots could explain all the post-hurricane treatment differences in soil temperature that were significant even at 30-45 cm. It is possible that the short-term re-wetting during the hurricane and subsequent re-drying could have altered temperature conductivity in the drought plots [Mount and Paetzold, 2002]. Despite a recovering trend of VSM after shelters were removed, post-treatment soil temperature remained warmer in droughted relative to control plots. Based on these results, and the significant negative correlation between soil temperature and VSM in drought plots, there is evidence for an increasing importance of VSM for regulating the thermal balance of soils under future climate regimes, especially following canopy disturbance.

Three months after throughfall exclusion began (June 2017), there were already significant changes in soil nutrients evident in surface soils of the drought plots. Decreasing soil moisture and increasing aeration likely contributed to the decrease in NaHCO₃-extractable soil P observed in the drought treatment, effectively contributing the potential for P-limitation in this forest. Reduced moisture may have decreased rates of labile P solubilization [Wood *et al.*, 2015], but it is also important to consider the high potential for P sorption of these Fe-rich soils, which likely increased in the drought plots as soils become aerated [Brenner *et al.*, 2018; Lin *et al.*, 2018; Lin *et al.*, 2020b; Lin *et al.*, 2021]. Soil NH₄ concentrations at 0-15 cm increased slightly but significantly after three months of throughfall exclusion. The initial accumulation of soil NH₄ in surface soils of drought plots may have resulted from enhanced soil N mineralization due to improved redox conditions for microbial heterotrophs in drier soils, combined with a reduction of soil N uptake by fine roots and microbes limited by low moisture availability [Billings and Phillips, 2011; Templer *et al.*, 2008; Wood and Silver, 2012]. The rapid drought sensitivity of these N and P, and the opposite direction of their response, demonstrates that drought can have both significant positive and negative effects on nutrient availability.

A large increase in NH_4 concentrations was observed in the surface soils in April 2018 in drought plots. This may be due to both the physical effects of soil drought (e.g., reduced connectivity within the soil matrix and reduced leaching intensity), as well as physiological stress of microbial communities [Manzoni *et al.*, 2011; Stark and Firestone, 1995]. Additionally, there was a potential legacy effect of drought on soil NH_4 at depth, with values remaining significantly higher in drought plots at 15-30 cm on the post-treatment sampling. In contrast to soil NH_4 , the peak of soil NO_3 (also in April 2018), was of similar magnitude between treatments suggesting that soil NO_3 was unaffected by throughfall exclusion. Disturbance-induced responses of soil N have been previously linked to fine-root mortality in this forest [Silver *et al.*, 1996; Silver and Vogt, 1993], but these results highlight the importance of considering the role of soil drought for determining the response of soil NH_4 . The changes of soil pH over time coupled with inorganic N suggest that these soils may have experienced a pulse of acidification after the hurricanes caused by dissolved organic acids, organic C and nutrients, inorganic nutrients derived from the decomposing organic matter that accumulated on the forest floor and soil matrix [Binkley and Richter, 1987; Lodge *et al.*, 1994; Lodge *et al.*, 1991; Silver and Vogt, 1993].

Initial drought responses of soil nutrients were maintained during the subsequent sampling dates and in some cases became stronger over time. There was a significant increase in HCl-extractable Fe(III), citrate ascorbate Fe, KCl-extractable NO_3 , and NaOH-extractable inorganic P after the hurricane (October 2017) in both treatment and control plots throughout the entire soil profile. The large deposition of organic matter likely drove changes in Fe pools and the wet conditions after the storms may have led to increased N and P mineralization or release of P from Fe surfaces [Chacon *et al.*, 2006; Lodge *et al.*, 1994].

Measuring disturbance-induced changes of soil organic C in forest soils over time has been complicated by the high spatial heterogeneity of background soil properties and of disturbance effects themselves [Gutiérrez del Arroyo and Silver, 2018; Reed *et al.*, 2020; Silver *et al.*, 1996; Zhou *et al.*, 2016]. Most drought studies conducted in tropical forests have focused on the effects on soil C fluxes rather than soil C pools [i.e., soil respiration, plant-atmosphere fluxes; Bonal *et al.*, 2015; Brando *et al.*, 2008; Cleveland *et al.*, 2010; Doughty *et al.*, 2015], but a global meta-analysis found a small net positive effect of soil drought on the soil C pool [Zhou *et al.*, 2016]. The effect of drought on soil C will ultimately be determined by the net change of C inputs to and outputs from the soil, which can sometimes be independently affected by drought [i.e., litterfall rates; Beard *et al.*, 2005]. While soil organic C concentrations were initially comparable between treatment and control plots, there was a significant negative effect of drought at 0-15 cm in the post-treatment sampling. Throughfall exclusion may have limited the process of soil organic C formation at the surface, but not below 15 cm where significant differences over time were detected. The differential effects of throughfall exclusion on soil organic C concentrations with depth suggest that processes at the surface were predominantly affected by the drought conditions (i.e., debris fragmentation, formation of particulate C). The mobility of dissolved soil organic C into the deeper soil layers where mineral-C associations dominate was apparently sufficient for increasing soil C at depth in drought plots, although we did not measure soil C fractions so we can only speculate about the relative contributions of different fractions to the significant changes in soil C over time [Cotrufo *et al.*, 2015]. In these C-rich ecosystems, it is very likely that throughfall exclusion effectively increased the concentration of the soil solution (i.e., DOM) despite reducing the volume of water moving

through the soil column, as has been found to occur in a comparable wet tropical forest in Costa Rica [Cleveland *et al.*, 2010].

Tropical forest soils have the highest rates of soil respiration globally, and those on the wetter end of the climate gradient (such as this site) can also represent a significant net source of CH₄ to the atmosphere [Bond-Lamberty *et al.*, 2020; Teh *et al.*, 2005]. Across wet tropical forests, drought can have both positive and negative effects on soil respiration, as both water stress and low redox, especially in clayey soils, can inhibit microbial and root activity [Cleveland *et al.*, 2010; Meir *et al.*, 2015; O'Connell *et al.*, 2018]. For the entirety of the treatment period of this experiment, throughfall exclusion significantly decreased soil respiration by approximately 25%, demonstrating that biological activity in these soils likely experienced drought stress, with significant implications for the tropical forest C cycle due to the large contribution of soil respiration to ecosystem respiration [Chambers *et al.*, 2004; Doughty *et al.*, 2015]. Maximum treatment differences were observed during hot moments of soil respiration in control plots that were not evident in drought plots, highlighting the disproportionate importance of these few large fluxes on soil C loss [Barcellos *et al.*, 2018; Kuzyakov and Blagodatskaya, 2015]. Treatment differences in soil respiration were likely caused by a combination of substrate limitation and moisture stress that reduces CO₂ production from litter and soil microbes, as well as fine roots [Sotta *et al.*, 2007; van Straaten *et al.*, 2011; Vasconcelos *et al.*, 2004; Wood and Silver, 2012]. These results suggest that soil biota in humid tropical forests are unlikely to benefit from the increased soil aeration or changes in soil chemistry caused by severe drought conditions.

Soil drying shifted CH₄ fluxes from a net source to a net sink. Previous work has shown both positive and negative drought responses of soil CH₄ fluxes [Cattânio *et al.*, 2002; Davidson *et al.*, 2004; Davidson *et al.*, 2008; Wood and Silver, 2012], but the dominant response in upland soils has been an increase in net CH₄ uptake, likely due to the combination of decreased production and the stimulation of methanotrophy [Billings and Phillips, 2011]. Like CO₂ fluxes, the high variability of soil CH₄ fluxes was characterized by the occurrence of hot spots and hot moments, with a dominance of soil CH₄ consumption events in drought plots and CH₄ production events in control plots. The coupling between soil aeration and soil CH₄ fluxes was evident in drought plots where soil O₂ concentration and CH₄ fluxes were significantly negatively correlated. Ongoing and projected climate change is already affecting the magnitude of the soil CH₄ sink in some tropical and temperate forests [Ni and Groffman, 2018; O'Connell *et al.*, 2018; Zhao *et al.*, 2019], and these results point to an increasing potential for soil CH₄ uptake as drought frequency increases in wet tropical forests. While moisture appears to be the main control on soil respiration, it is clear that soil redox conditions is critical for driving soil CH₄ fluxes in these soils [Teh *et al.*, 2005], highlighting the importance of measuring both VSM and soil O₂ concentration across the soil profile. Overall, the results of soil GHG fluxes indicate that under a future climate with drier and more aerated soils it is likely that there will be a significant reduction in soil C loss, both as CO₂ and CH₄.

Wet tropical forest soils have been found to be net sources of N₂O [Keller *et al.*, 1986; Keller and Reiners, 1994; Keller *et al.*, 2000], with some studies finding a stimulation of net fluxes with throughfall exclusion [Wieder *et al.*, 2011], while others find an enhancement of the soil N₂O sink potential [Davidson *et al.*, 2004; Davidson *et al.*, 2008; Wood and Silver, 2012]. The low magnitude and large variability of soil N₂O fluxes observed in this forest precluded any significant differences between treatments, but confirmed the potential for hot moments of net positive fluxes, as mean values in both treatments was positive. Similar to soil CH₄, soil N₂O

fluxes were highly sporadic and most often there were no net fluxes measured. However, there was a significant peak of soil N₂O production in April 2018 that was evident in both treatments, and coincided with the peak in soil NO₃ concentration. Although these datasets were collected at different time scales, they strongly suggest there was a pulse of soil N cycling at the end of the dry season in 2018 that was unaffected by the throughfall exclusion treatment.

The significant effects of throughfall exclusion on soil microclimate supported our initial hypothesis about the importance of the relationship between soil moisture and soil aeration for driving biological activity in the soil during drought. Soil drying and the associated increased aeration resulted in lower soil respiration and increased soil CH₄ uptake, while also reducing the availability of labile P and soil organic C in surface soils. However, contrary to our hypothesis, soil NH₄ actually accumulated significantly in drought plots, indicating that some of the effect of drought may be positive for at least some nutrients. Our second hypothesis was not supported by the results, as the effects of the hurricane on soil biogeochemistry were less pervasive and were most significant for soil Fe pools, which increased significantly post-hurricane. The maintenance of treatment differences in soil GHG fluxes and soil N and P availability even after the hurricane disturbance, which deposited a large pulse of organic matter on the forest floor, suggest that water limitation as a result of our experimental manipulation was more important than substrate availability for soil biological activity in this post-disturbance context.

References

- Asner, G. P., and A. Alencar (2010), Drought impacts on the Amazon forest: the remote sensing perspective, *New Phytologist*, 187(3), 569-578, doi:10.1111/j.1469-8137.2010.03310.x.
- Asner, G. P., T. K. Rudel, T. M. Aide, R. Defries, and R. Emerson (2009), A contemporary assessment of change in humid tropical forests, *Conservation Biology*, 23(6), 1386-1395, doi:10.1111/j.1523-1739.2009.01333.x.
- Barcellos, D., C. S. O'Connell, W. Silver, C. Meile, and A. Thompson (2018), Hot Spots and Hot Moments of Soil Moisture Explain Fluctuations in Iron and Carbon Cycling in a Humid Tropical Forest Soil, *Soil Systems*, 2(4), 59.
- Beard, K. H., K. A. Vogt, D. J. Vogt, F. N. Scatena, A. P. Covich, R. Sigurdardottir, T. G. Siccama, and T. A. Crowl (2005), Structural and functional responses of a subtropical forest to 10 years of hurricanes and drought, *Ecological Monographs*, 75(3), 345-361, doi:10.1890/04-1114.
- Bender, M. A., T. R. Knutson, R. E. Tuleya, J. J. Sirutis, G. A. Vecchi, S. T. Garner, and I. M. Held (2010), Modeled Impact of Anthropogenic Warming on the Frequency of Intense Atlantic Hurricanes, *Science*, 327(5964), 454-458, doi:10.1126/science.1180568.
- Bhardwaj, A., V. Misra, A. Mishra, A. Wootten, R. Boyles, J. H. Bowden, and A. J. Terando (2018), Downscaling future climate change projections over Puerto Rico using a non-hydrostatic atmospheric model, *Climatic Change*, doi:10.1007/s10584-017-2130-x.
- Billings, S. A., and N. Phillips (2011), Forest Biogeochemistry and Drought, in *Forest Hydrology and Biogeochemistry: Synthesis of Past Research and Future Directions*, edited by F. D. Levia, D. Carlyle-Moses and T. Tanaka, pp. 581-597, Springer Netherlands, Dordrecht, doi:10.1007/978-94-007-1363-5_29.
- Binkley, D., and D. Richter (1987), Nutrient Cycles and H⁺ Budgets of Forest Ecosystems, in *Advances in Ecological Research*, edited by A. Macfadyen and E. D. Ford, pp. 1-51, Academic Press, doi:[http://dx.doi.org/10.1016/S0065-2504\(08\)60086-0](http://dx.doi.org/10.1016/S0065-2504(08)60086-0).

- Bonal, D., B. Burban, C. Stahl, F. Wagner, and B. Hérault (2015), The response of tropical rainforests to drought—lessons from recent research and future prospects, *Annals of Forest Science*, 1-18, doi:10.1007/s13595-015-0522-5.
- Bond-Lamberty, B., et al. (2020), COSORE: A community database for continuous soil respiration and other soil-atmosphere greenhouse gas flux data, *Global Change Biology*, 26(12), 7268-7283, doi:<https://doi.org/10.1111/gcb.15353>.
- Bouskill, N., et al. (2016a), Belowground response to drought in a tropical forest soil. II. Change in microbial function impacts carbon composition, *Frontiers in microbiology*, 7, doi:10.3389/fmicb.2016.00323.
- Bouskill, N., et al. (2016b), Belowground response to drought in a tropical forest soil. I. Changes in microbial functional potential and metabolism, *Frontiers in microbiology*, 7, doi:10.3389/fmicb.2016.00525.
- Bouskill, N. J., H. C. Lim, S. Borglin, R. Salve, T. E. Wood, W. L. Silver, and E. L. Brodie (2013), Pre-exposure to drought increases the resistance of tropical forest soil bacterial communities to extended drought, *The ISME journal*, 7(2), 384-394, doi:<http://www.nature.com/ismej/journal/v7/n2/supinfo/ismej2012113s1.html>.
- Brando, P. M., D. C. Nepstad, E. A. Davidson, S. E. Trumbore, D. Ray, and P. Camargo (2008), Drought effects on litterfall, wood production and belowground carbon cycling in an Amazon forest: results of a throughfall reduction experiment, *Philosophical transactions of the Royal Society of London. Series B, Biological sciences*, 363(1498), 1839-1848, doi:10.1098/rstb.2007.0031.
- Brenner, J., W. Porter, J. R. Phillips, J. Childs, X. Yang, and M. A. Mayes (2018), Phosphorus sorption on tropical soils with relevance to Earth system model needs, *Soil Research*, -, doi:<https://doi.org/10.1071/SR18197>.
- Cattânio, J. H., E. A. Davidson, D. C. Nepstad, L. V. Verchot, and I. L. Ackerman (2002), Unexpected results of a pilot throughfall exclusion experiment on soil emissions of CO₂, CH₄, N₂O, and NO in eastern Amazonia, *Biol Fertil Soils*, 36(2), 102-108, doi:10.1007/s00374-002-0517-x.
- Chacon, N., W. L. Silver, E. A. Dubinsky, and D. F. Cusack (2006), Iron Reduction and Soil Phosphorus Solubilization in Humid Tropical Forests Soils: The Roles of Labile Carbon Pools and an Electron Shuttle Compound, *Biogeochemistry*, 78(1), 67-84, doi:10.1007/s10533-005-2343-3.
- Chadwick, R., P. Good, G. Martin, and D. P. Rowell (2016), Large rainfall changes consistently projected over substantial areas of tropical land, *Nature Clim. Change*, 6(2), 177-181, doi:10.1038/nclimate2805.
- Chambers, J. Q., E. S. Tribuzy, L. C. Toledo, B. F. Crispim, N. Higuchi, J. d. Santos, A. C. Araújo, B. Kruijt, A. D. Nobre, and S. E. Trumbore (2004), Respiration from a tropical forest ecosystem: partitioning of sources and low carbon use efficiency *Ecological Applications*, 14(sp4), 72-88, doi:10.1890/01-6012.
- Chazdon, R. L., et al. (2016), Carbon sequestration potential of second-growth forest regeneration in the Latin American tropics, *Science Advances*, 2(5), doi:10.1126/sciadv.1501639.
- Cleveland, C. C., W. R. Wieder, S. C. Reed, and A. R. Townsend (2010), Experimental drought in a tropical rain forest increases soil carbon dioxide losses to the atmosphere, *Ecology*, 91(8), 2313-2323.

- Cotrufo, M. F., J. L. Soong, A. J. Horton, E. E. Campbell, M. L. Haddix, D. H. Wall, and W. J. Parton (2015), Formation of soil organic matter via biochemical and physical pathways of litter mass loss, *Nature Geosci*, 8(10), 776-779, doi:10.1038/ngeo2520.
- Davidson, E. A., F. Y. Ishida, and D. C. Nepstad (2004), Effects of an experimental drought on soil emissions of carbon dioxide, methane, nitrous oxide, and nitric oxide in a moist tropical forest, *Global Change Biology*, 10(5), 718-730.
- Davidson, E. A., D. C. Nepstad, F. Y. Ishida, and P. M. Brando (2008), Effects of an experimental drought and recovery on soil emissions of carbon dioxide, methane, nitrous oxide, and nitric oxide in a moist tropical forest, *Global Change Biology*, 14(11), 2582-2590, doi:10.1111/j.1365-2486.2008.01694.x.
- Doughty, C. E., et al. (2015), Drought impact on forest carbon dynamics and fluxes in Amazonia, *Nature*, 519(7541), 78-82, doi:10.1038/nature14213.
- Ewel, J. J., and J. L. Whitmore (1973), The ecological life zones of Puerto Rico and the U.S. Virgin Islands *Rep. ITF-18*, Institute of Tropical Forestry, Rio Piedras, Puerto Rico.
- Feng, Y., R. I. Negrón-Juárez, and J. Q. Chambers (2020), Remote sensing and statistical analysis of the effects of hurricane María on the forests of Puerto Rico, *Remote Sensing of Environment*, 247, 111940, doi:<https://doi.org/10.1016/j.rse.2020.111940>.
- Ferreira dos Santos, V. A. H., M. J. Ferreira, J. V. F. Cardoso Rodrigues, M. Neves Garcia, J. V. Barbosa Ceron, B. W. Nelson, and S. R. Saleska (2018), Causes of reduced leaf-level photosynthesis during strong El Niño drought in a Central Amazon forest, *Global Change Biology*, 0(ja), doi:doi:10.1111/gcb.14293.
- Grau, H. R., T. M. Aide, J. K. Zimmerman, J. R. Thomlinson, E. Helmer, and X. Zou (2003), The ecological consequences of socioeconomic and land-use changes in postagriculture Puerto Rico, *BioScience*, 53(12), 1159-1168.
- Gutiérrez del Arroyo, O., and W. L. Silver (2018), Disentangling the long-term effects of disturbance on soil biogeochemistry in a wet tropical forest ecosystem, *Global Change Biology*, n/a-n/a, doi:10.1111/gcb.14027.
- Hall, S. J., and W. L. Silver (2015), Reducing conditions, reactive metals, and their interactions can explain spatial patterns of surface soil carbon in a humid tropical forest, *Biogeochemistry*, 1-17, doi:10.1007/s10533-015-0120-5.
- Harris, N. L., A. E. Lugo, S. Brown, and T. Heartsill-Scalley (2012), Luquillo Experimental Forest: Research History and Opportunities *Rep.*, 152 pp, USDA Forest Service, Washington, D.C.
- Henareh Khalyani, A., W. A. Gould, E. Harmsen, A. Terando, M. Quinones, and J. A. Collazo (2016), Climate change implications for tropical islands: Interpolating and interpreting statistically downscaled GCM projections for management and planning, *Journal of Applied Meteorology and Climatology*, doi:10.1175/JAMC-D-15-0182.1.
- Huffaker, L. (2002), Soil survey of Caribbean National Forest and Luquillo Experimental Forest, Commonwealth of Puerto Rico, edited, U.S. Gov. Print. Office, Washington, D.C.
- Keller, M., W. A. Kaplan, and S. C. Wofsy (1986), Emissions of N₂O, CH₄ and CO₂ from tropical forest soils, *Journal of Geophysical Research: Atmospheres*, 91(D11), 11791-11802, doi:10.1029/JD091iD11p11791.
- Keller, M., and W. A. Reiners (1994), Soil-atmosphere exchange of nitrous oxide, nitric oxide, and methane under secondary succession of pasture to forest in the Atlantic lowlands of Costa Rica, *Global Biogeochemical Cycles*, 8(4), 399-409, doi:10.1029/94GB01660.

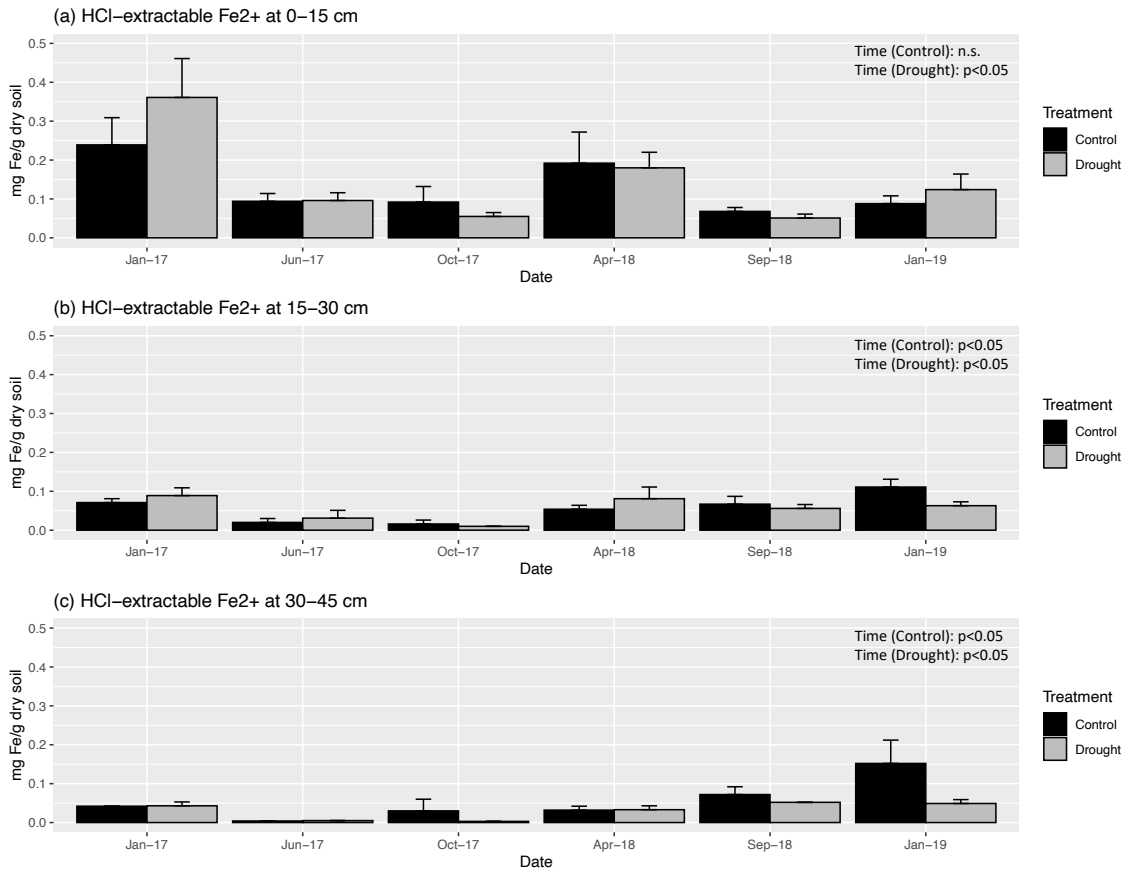
- Keller, M., A. M. Weitz, B. Bryan, M. M. Rivera, and W. L. Silver (2000), Soil-atmosphere nitrogen oxide fluxes: Effects of root disturbance, *Journal of Geophysical Research: Atmospheres*, 105(D14), 17693-17698, doi:10.1029/2000JD900068.
- Kuzyakov, Y., and E. Blagodatskaya (2015), Microbial hotspots and hot moments in soil: Concept & review, *Soil Biology and Biochemistry*, 83, 184-199, doi:<http://dx.doi.org/10.1016/j.soilbio.2015.01.025>.
- Lewis, S. L., P. M. Brando, O. L. Phillips, G. M. F. van der Heijden, and D. Nepstad (2011), The 2010 Amazon Drought, *Science*, 331(6017), 554-554, doi:10.1126/science.1200807.
- Lin, T.-C., S. P. Hamburg, K.-C. Lin, L.-J. Wang, C.-T. Chang, Y.-J. Hsia, M. A. Vadeboncoeur, C. M. Mabry McMullen, and C.-P. Liu (2011), Typhoon Disturbance and Forest Dynamics: Lessons from a Northwest Pacific Subtropical Forest, *Ecosystems*, 14(1), 127-143, doi:10.1007/s10021-010-9399-1.
- Lin, T.-C., J. A. Hogan, and C.-T. Chang (2020a), Tropical Cyclone Ecology: A Scale-Link Perspective, *Trends Ecol. Evol.*, 35(7), 594-604, doi:<https://doi.org/10.1016/j.tree.2020.02.012>.
- Lin, Y., A. Bhattacharyya, A. N. Campbell, P. S. Nico, J. Pett-Ridge, and W. L. Silver (2018), Phosphorus Fractionation Responds to Dynamic Redox Conditions in a Humid Tropical Forest Soil, *Journal of Geophysical Research: Biogeosciences*, 123(9), 3016-3027, doi:10.1029/2018jg004420.
- Lin, Y., A. Gross, C. S. O'Connell, and W. L. Silver (2020b), Anoxic conditions maintained high phosphorus sorption in humid tropical forest soils, *Biogeosciences*, 17(1), 89-101, doi:10.5194/bg-17-89-2020.
- Lin, Y., A. Gross, and W. L. Silver (2021), Low Redox Decreases Potential Phosphorus Limitation on Soil Biogeochemical Cycling Along a Tropical Rainfall Gradient, *Ecosystems*, doi:10.1007/s10021-021-00662-4.
- Little, E. L. (1970), Relationships of trees of the Luquillo Experimental Forest, in *A Tropical Rain Forest: a study of irradiation and ecology at El Verde, Puerto Rico*, edited by H. T. Odum and R. F. Pigeon, U.S. Atomic Energy Commission, Oak Ridge, Tennessee.
- Lodge, D. J., W. H. McDowell, and C. P. McSwiney (1994), The importance of nutrient pulses in tropical forests, *Trends Ecol. Evol.*, 9(10), 384-387.
- Lodge, D. J., F. N. Scatena, C. E. Asbury, and M. J. Sanchez (1991), Fine Litterfall and Related Nutrient Inputs Resulting From Hurricane Hugo in Subtropical Wet and Lower Montane Rain Forests of Puerto Rico, *Biotropica*, 23(4), 336-342, doi:10.2307/2388249.
- Lugo, A. E., and R. B. Waide (1993), Catastrophic and background disturbance of tropical ecosystems at the Luquillo Experimental Forest, *Journal of Biosciences*, 18(4), 475-481, doi:10.1007/bf02703080.
- Malhi, Y., D. Baldocchi, and P. Jarvis (1999), The carbon balance of tropical, temperate and boreal forests, *Plant, Cell & Environment*, 22(6), 715-740.
- Manzoni, S., J. P. Schimel, and A. Porporato (2011), Responses of soil microbial communities to water stress: results from a meta-analysis, *Ecology*, 93(4), 930-938, doi:10.1890/11-0026.1.
- McDowell, N. G., et al. (2020), Pervasive shifts in forest dynamics in a changing world, *Science*, 368(6494), eaaz9463, doi:10.1126/science.aaz9463.
- Meir, P., and J. Grace (2005), The effects of drought on tropical forest ecosystems, in *Tropical Forests and Global Atmospheric Change*, edited by Y. Malhi and O. L. Phillips, Oxford University Press.

- Meir, P., and F. Ian Woodward (2010), Amazonian rain forests and drought: response and vulnerability, *New Phytologist*, 187(3), 553-557, doi:10.1111/j.1469-8137.2010.03390.x.
- Meir, P., T. E. Wood, D. R. Galbraith, P. M. Brando, A. C. L. Da Costa, L. Rowland, and L. V. Ferreira (2015), Threshold Responses to Soil Moisture Deficit by Trees and Soil in Tropical Rain Forests: Insights from Field Experiments, *BioScience*, 65(9), 882-892, doi:10.1093/biosci/biv107.
- Miller, P. W., M. Williams, and T. Mote (2021), Modeled Atmospheric Optical and Thermodynamic Responses to an Exceptional Trans-Atlantic Dust Outbreak, *Journal of Geophysical Research: Atmospheres*, n/a(n/a), e2020JD032909, doi:<https://doi.org/10.1029/2020JD032909>.
- Mount, H. R., and R. F. Paetzold (2002), The temperature regime for selected soils in the United States *Rep. Soil Survey Investigation Report No. 48*, United States Department of Agriculture, National Resources Conservation Service, National Soil Survey Center, Lincoln, Nebraska.
- Murphy, J., and J. P. Riley (1962), A modified single solution method for the determination of phosphate in natural waters, *Analytica Chimica Acta*, 27(0), 31-36, doi:[http://dx.doi.org/10.1016/S0003-2670\(00\)88444-5](http://dx.doi.org/10.1016/S0003-2670(00)88444-5).
- Ni, X., and P. M. Groffman (2018), Declines in methane uptake in forest soils, *Proc. Natl. Acad. Sci. U.S.A.*, 115(34), 8587-8590, doi:10.1073/pnas.1807377115.
- O'Connell, C. S., L. Ruan, and W. L. Silver (2018), Drought drives rapid shifts in tropical rainforest soil biogeochemistry and greenhouse gas emissions, *Nature communications*, 9(1), 1348, doi:10.1038/s41467-018-03352-3.
- Pan, Y., R. A. Birdsey, O. L. Phillips, and R. B. Jackson (2013), The Structure, Distribution, and Biomass of the World's Forests, *Annual Review of Ecology, Evolution, and Systematics*, 44(1), 593-622, doi:doi:10.1146/annurev-ecolsys-110512-135914.
- Parrotta, J. A., and D. J. Lodge (1991), Fine Root Dynamics in a Subtropical Wet Forest Following Hurricane Disturbance in Puerto Rico, *Biotropica*, 23(4), 343-347, doi:10.2307/2388250.
- Phillips, O. L., et al. (2009), Drought sensitivity of the Amazon rainforest, *Science*, 323(5919), 1344-1347, doi:10.1126/science.1164033.
- Ping, C.-L., G. J. Michaelson, C. A. Stiles, and G. González (2013), Soil characteristics, carbon stores, and nutrient distribution in eight forest types along an elevation gradient, eastern Puerto Rico, *Ecological Bulletins*, 54, 67-86.
- R Core Team (2021), R: A language and environment for statistical computing, edited, R Foundation for Statistical Computing, Vienna, Austria.
- Raich, J. W., and W. H. Schlesinger (1992), The global carbon dioxide flux in soil respiration and its relationship to vegetation and climate, *Tellus B*, 44(2), 81-99.
- Ramseyer, C. A., P. W. Miller, and T. L. Mote (2019), Future precipitation variability during the early rainfall season in the El Yunque National Forest, *Science of The Total Environment*, 661, doi:<https://doi.org/10.1016/j.scitotenv.2019.01.167>.
- Reed, S. C., R. Reibold, M. A. Cavaleri, A. M. Alonso-Rodríguez, M. E. Berberich, and T. E. Wood (2020), Soil biogeochemical responses of a tropical forest to warming and hurricane disturbance, in *Advances in Ecological Research*, edited, Academic Press, doi:<https://doi.org/10.1016/bs.aecr.2020.01.007>.

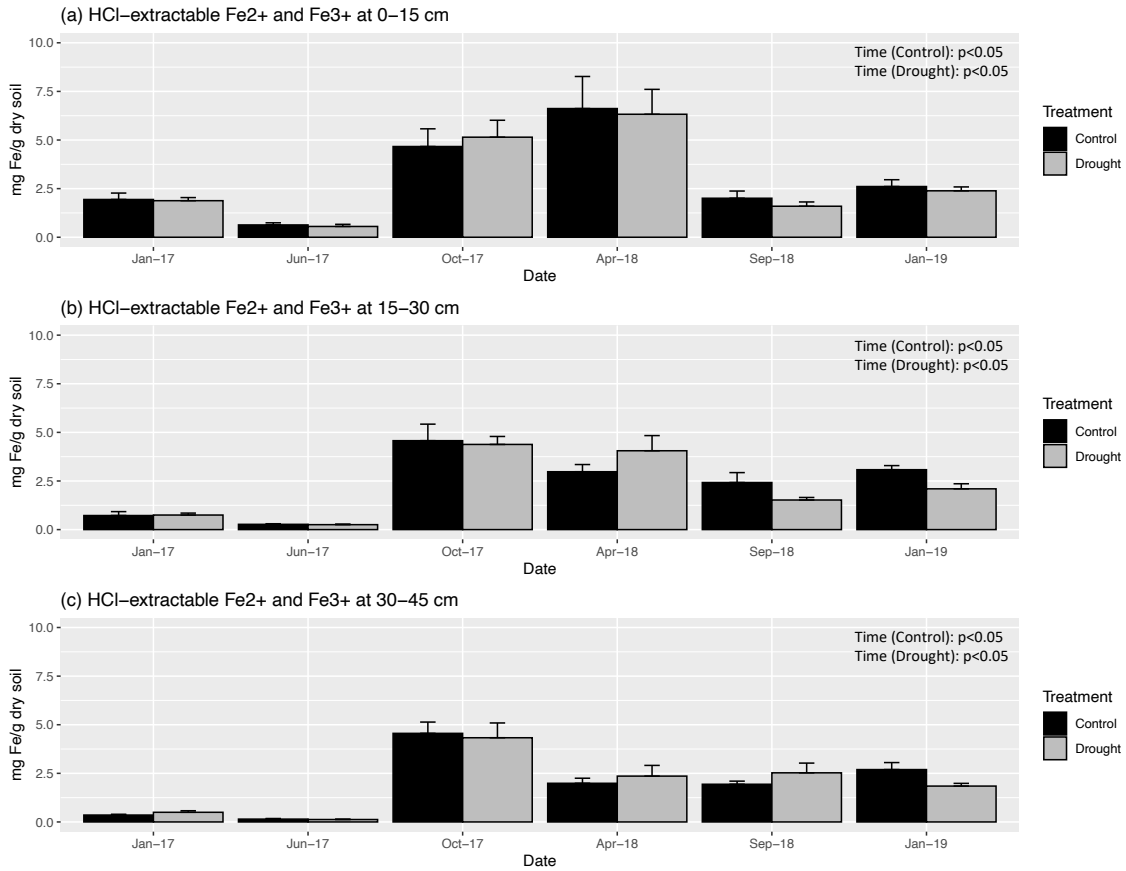
- Rowland, L., et al. (2015), After more than a decade of soil moisture deficit, tropical rainforest trees maintain photosynthetic capacity, despite increased leaf respiration, *Global Change Biology*, 21(12), 4662-4672, doi:10.1111/gcb.13035.
- Santiago, L. S., D. Bonal, M. E. Guzman, and E. Ávila-Lovera (2016), Drought Survival Strategies of Tropical Trees, in *Tropical Tree Physiology: Adaptations and Responses in a Changing Environment*, edited by G. Goldstein and S. L. Santiago, pp. 243-258, Springer International Publishing, Cham, doi:10.1007/978-3-319-27422-5_11.
- Scatena, F. N., and A. E. Lugo (1995), Geomorphology, disturbance, and the soil and vegetation of two subtropical wet steepland watersheds of Puerto Rico, *Geomorphology*, 13(1-4), 199-213, doi:[http://dx.doi.org/10.1016/0169-555X\(95\)00021-V](http://dx.doi.org/10.1016/0169-555X(95)00021-V).
- Schlesinger, W. H., M. C. Dietze, R. B. Jackson, R. P. Phillips, C. C. Rhoades, L. E. Rustad, and J. M. Vose (2015), Forest Biogeochemistry in Response to Drought, *Global Change Biology*, n/a-n/a, doi:10.1111/gcb.13105.
- Scholl, M. A., M. Bassiouni, and A. J. Torres-Sánchez (2021), Drought stress and hurricane defoliation influence mountain clouds and moisture recycling in a tropical forest, *Proc. Natl. Acad. Sci. U.S.A.*, 118(7), e2021646118, doi:10.1073/pnas.2021646118.
- Schuur, E. A., and P. A. Matson (2001), Net primary productivity and nutrient cycling across a mesic to wet precipitation gradient in Hawaiian montane forest, *Oecologia*, 128(3), 431-442, doi:10.1007/s004420100671.
- Silver, W. L., A. Lugo, and M. Keller (1999), Soil oxygen availability and biogeochemistry along rainfall and topographic gradients in upland wet tropical forest soils, *Biogeochemistry*, 44(3), 301-328.
- Silver, W. L., F. N. Scatena, A. H. Johnson, T. G. Siccama, and F. Watt (1996), At what temporal scales does disturbance affect belowground nutrient pools?, *Biotropica*, 28(4a), 441-457.
- Silver, W. L., and K. A. Vogt (1993), Fine root dynamics following single and multiple disturbances in a subtropical wet forest ecosystem, *Journal of Ecology*, 81(4), 729-738.
- Sotta, E. D., E. Veldkamp, L. Schwendenmann, B. R. Guimarães, R. K. Paixão, M. d. L. P. Ruivo, A. C. Lola da Costa, and P. Meir (2007), Effects of an induced drought on soil carbon dioxide (CO₂) efflux and soil CO₂ production in an Eastern Amazonian rainforest, Brazil, *Global Change Biology*, 13(10), 2218-2229, doi:10.1111/j.1365-2486.2007.01416.x.
- Stark, J. M., and M. K. Firestone (1995), Mechanisms for soil moisture effects on activity of nitrifying bacteria, *Applied and environmental microbiology*, 61(1), 218-221.
- Teh, Y. A., W. L. Silver, and M. E. Conrad (2005), Oxygen effects on methane production and oxidation in humid tropical forest soils, *Global Change Biology*, 11(8), 1283-1297, doi:10.1111/j.1365-2486.2005.00983.x.
- Teh, Y. A., W. L. Silver, and F. N. Scatena (2009), A decade of belowground reorganization following multiple disturbances in a subtropical wet forest, *Plant and Soil*, 323(1-2), 197-212, doi:10.1007/s11104-009-9926-z.
- Templer, P. H., W. L. Silver, J. Pett-Ridge, K. M. DeAngelis, and M. K. Firestone (2008), Plant and microbial controls on nitrogen retention and loss in a humid tropical forest, *Ecology*, 89(11), 3030-3040, doi:10.1890/07-1631.1.
- Tiessen, H., and J. Moir (1993), Characterization of available phosphorus by sequential extraction, in *Soil Sampling and Methods of Analysis*, edited by M. Carter, pp. 75-86, Canadian Society of Soil Science, Lewis, Boca Raton, FL.

- van Straaten, O., E. Veldkamp, and M. D. Corre (2011), Simulated drought reduces soil CO₂ efflux and production in a tropical forest in Sulawesi, Indonesia, *Ecosphere*, 2(10), art119, doi:10.1890/ES11-00079.1.
- Vasconcelos, S. S., et al. (2004), Moisture and substrate availability constrain soil trace gas fluxes in an eastern Amazonian regrowth forest, *Global Biogeochemical Cycles*, 18(2), n/a-n/a, doi:10.1029/2003gb002210.
- Walsh, K. J. E., et al. (2016), Tropical cyclones and climate change, *Wiley Interdisciplinary Reviews: Climate Change*, 7(1), 65-89, doi:10.1002/wcc.371.
- Weaver, P. L. (2010), Forest structure and composition in the lower montane rain forest of the Luquillo Mountains, Puerto Rico, *Interciencia*, 35(9), 640-646.
- Wieder, W. R., C. C. Cleveland, and A. R. Townsend (2011), Throughfall exclusion and leaf litter addition drive higher rates of soil nitrous oxide emissions from a lowland wet tropical forest, *Global Change Biology*, 17(10), 3195-3207, doi:10.1111/j.1365-2486.2011.02426.x.
- Wood, T. E., M. A. Cavaleri, and S. C. Reed (2012), Tropical forest carbon balance in a warmer world: a critical review spanning microbial-to ecosystem-scale processes, *Biological Reviews*, 87(4), 912-927.
- Wood, T. E., M. Detto, and W. L. Silver (2013), Sensitivity of soil respiration to variability in soil moisture and temperature in a humid tropical forest, *PloS one*, 8(12), e80965, doi:10.1371/journal.pone.0080965.
- Wood, T. E., D. Matthews, K. Vandecar, and D. Lawrence (2015), Short-term variability in labile soil phosphorus is positively related to soil moisture in a humid tropical forest in Puerto Rico, *Biogeochemistry*, 127(1), 35-43, doi:10.1007/s10533-015-0150-z.
- Wood, T. E., and W. L. Silver (2012), Strong spatial variability in trace gas dynamics following experimental drought in a humid tropical forest, *Global Biogeochemical Cycles*, 26(3), GB3005, doi:10.1029/2010gb004014.
- Yang, W. H., and D. Liptzin (2015), High potential for iron reduction in upland soils, *Ecology*, 96(7), 2015-2020, doi:10.1890/14-2097.1.
- Zhao, J.-F., et al. (2019), Tropical forest soils serve as substantial and persistent methane sinks, *Scientific reports*, 9(1), 16799, doi:10.1038/s41598-019-51515-z.
- Zhou, X., L. Zhou, Y. Nie, Y. Fu, Z. Du, J. Shao, Z. Zheng, and X. Wang (2016), Similar responses of soil carbon storage to drought and irrigation in terrestrial ecosystems but with contrasting mechanisms: A meta-analysis, *Agriculture, Ecosystems & Environment*, 228, 70-81, doi:<http://dx.doi.org/10.1016/j.agee.2016.04.030>.
- Zimmerman, J. K., T. E. Wood, G. González, A. Ramirez, W. L. Silver, M. Uriarte, M. R. Willig, R. B. Waide, and A. E. Lugo (2021), Disturbance and resilience in the Luquillo Experimental Forest, *Biological Conservation*, 253, 108891, doi:<https://doi.org/10.1016/j.biocon.2020.108891>.

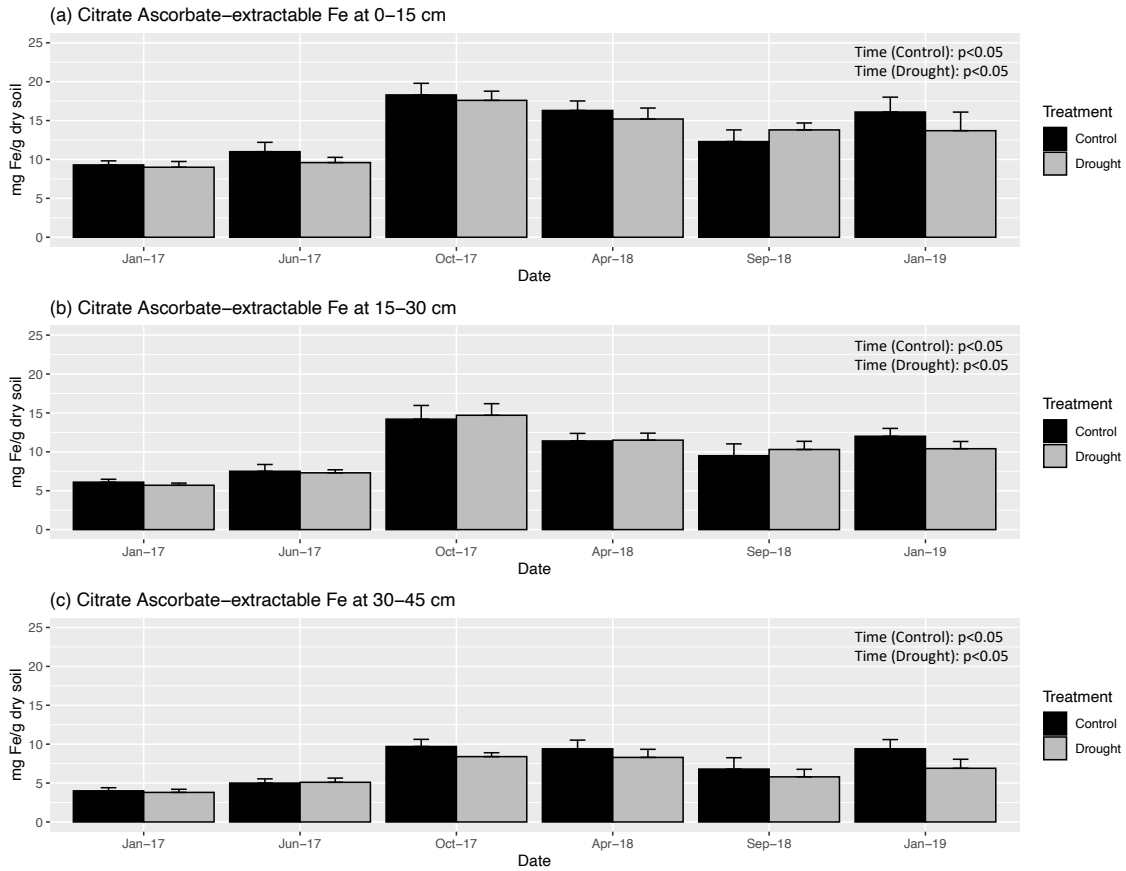
Supplementary Figures



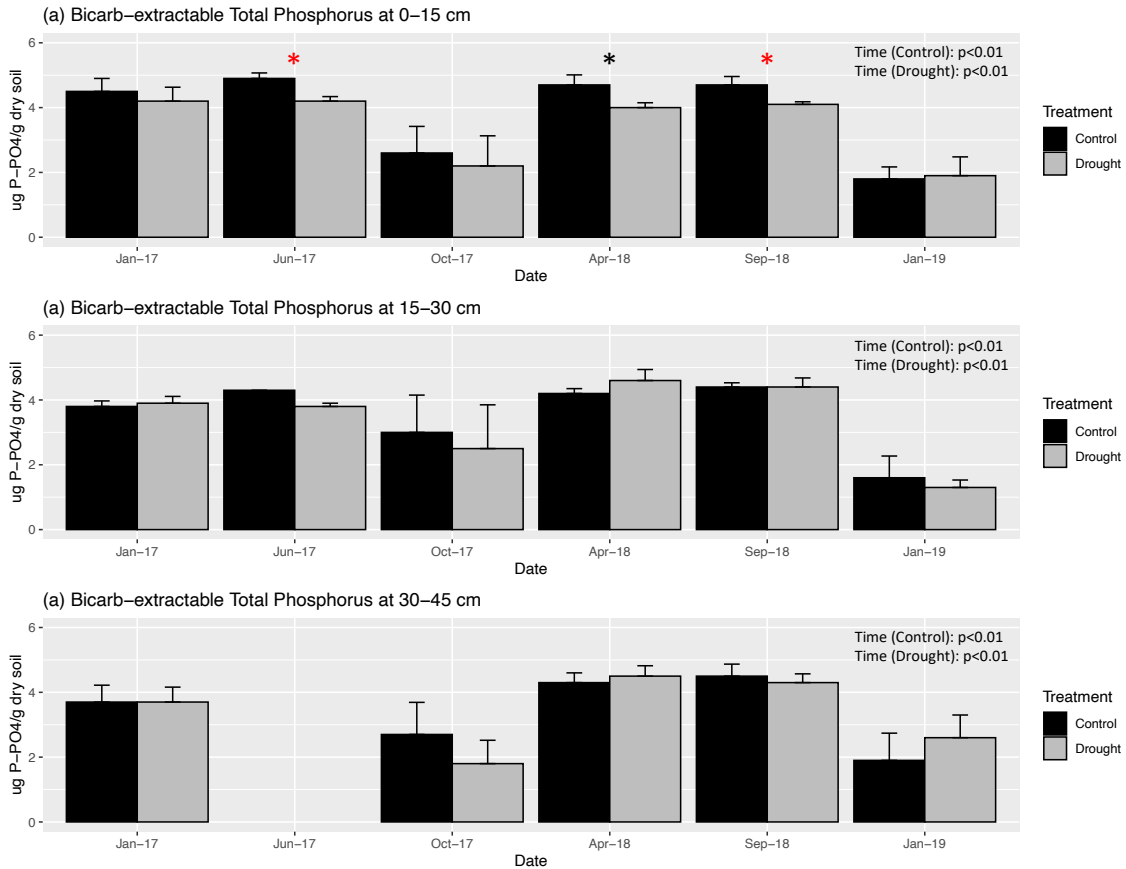
Supplementary Figure 1a-c. Mean HCl-extractable Fe²⁺ (+ SE, n = 5) by treatment at a) 0-15 cm, b) 15-30 cm, and c) 30-45 cm.



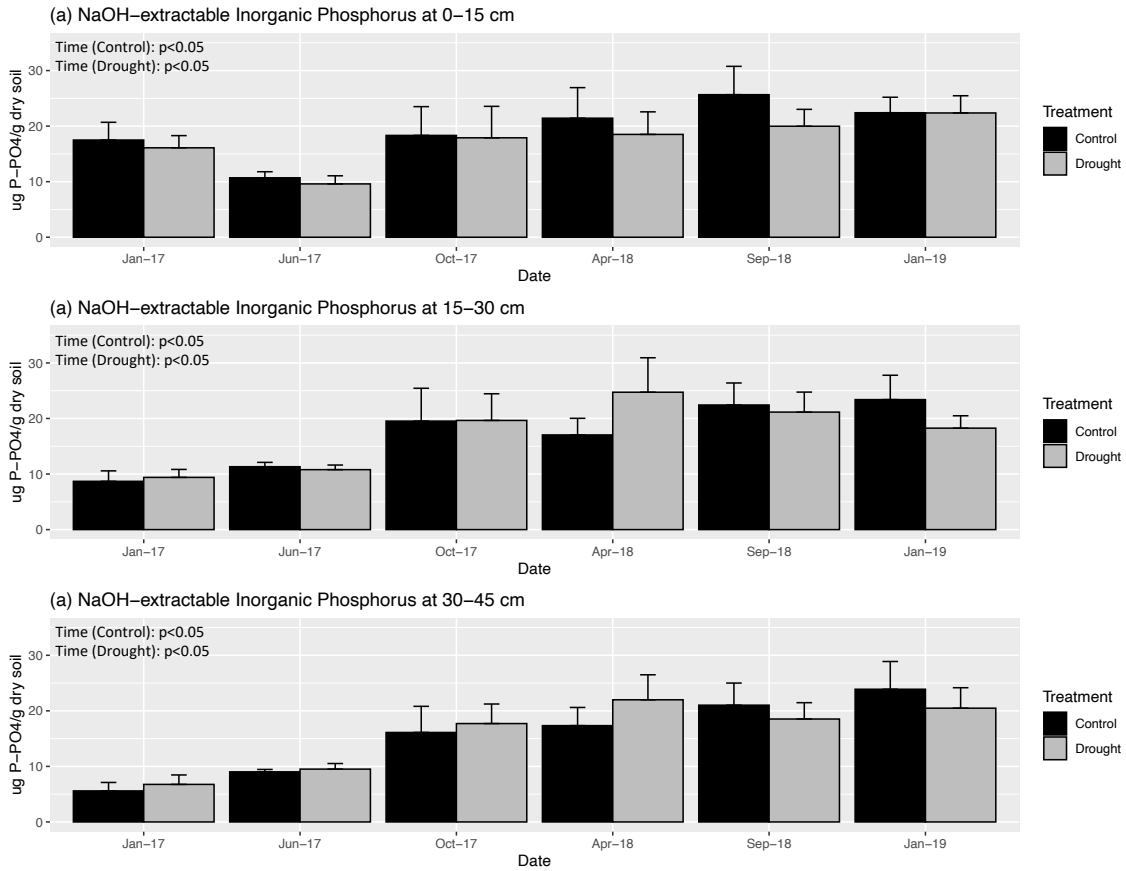
Supplementary Figure 2a-c. Mean HCl-extractable total Fe (+ SE, n = 5) by treatment at a) 0-15 cm, b) 15-30 cm, and c) 30-45 cm.



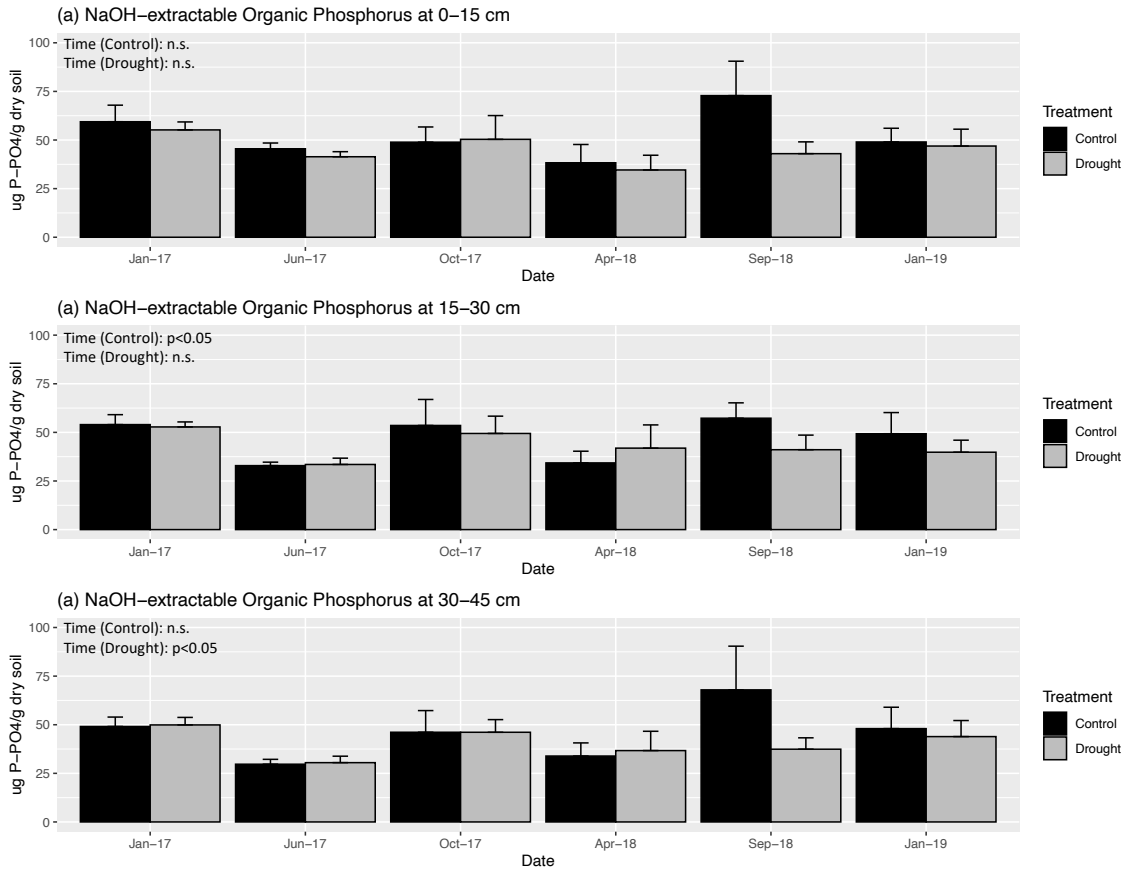
Supplementary Figure 3a-c. Mean citrate ascorbate-extractable Fe (+ SE, n = 5) by treatment at a) 0-15 cm, b) 15-30 cm, and c) 30-45 cm.



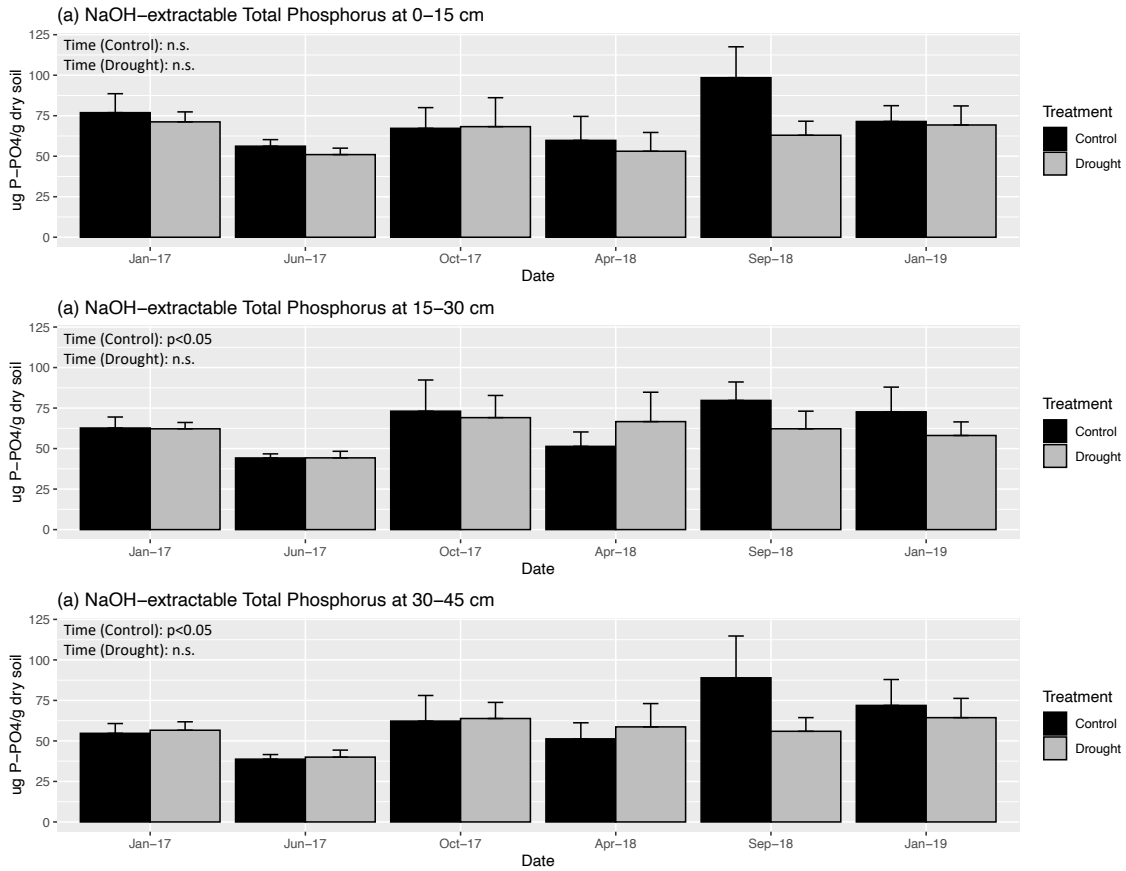
Supplementary Figure 4a-c. Mean NaHCO₃-extractable soil phosphorus (+ SE, n = 5) by treatment at a) 0-15 cm, b) 15-30 cm, and c) 30-45 cm. Red and black asterisk indicate significance at $p < 0.05$ or $p < 0.1$, respectively.



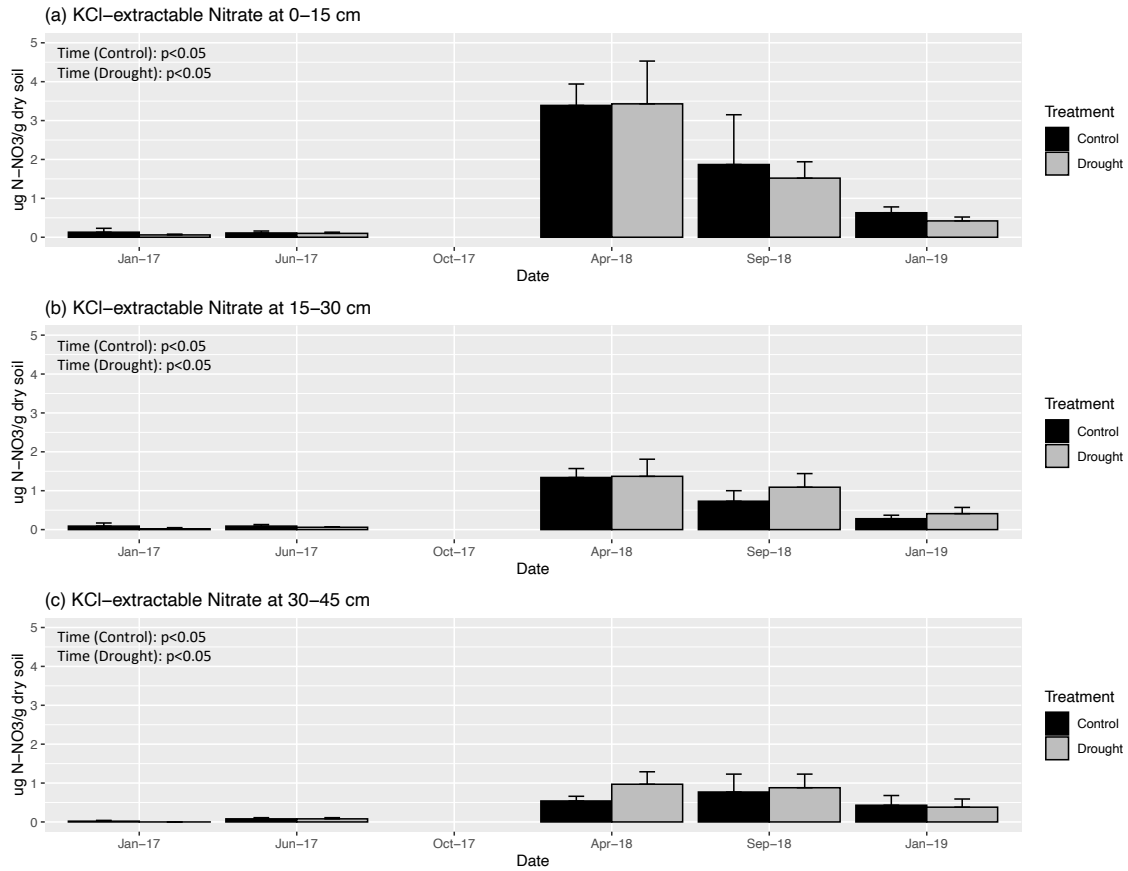
Supplementary Figure 5a-c. Mean NaOH-extractable inorganic soil phosphorus (+ SE, $n = 5$) by treatment at a) 0-15 cm, b) 15-30 cm, and c) 30-45 cm.



Supplementary Figure 6a-c. Mean NaOH-extractable organic soil phosphorus (+ SE, n = 5) by treatment at a) 0-15 cm, b) 15-30 cm, and c) 30-45 cm.



Supplementary Figure 7a-c. Mean NaOH-extractable total soil phosphorus (+ SE, n = 5) by treatment at a) 0-15 cm, b) 15-30 cm, and c) 30-45 cm.



Supplementary Figure 8a-c. Mean KCl-extractable soil nitrate (+ SE, n = 5) by treatment at a) 0-15 cm, b) 15-30 cm, and c) 30-45 cm.

Concluding section

The three chapters that make up this dissertation provide a comprehensive understanding of the soil biogeochemical responses to disturbance events in a wet tropical forest, and provide a indicators for detecting the ongoing changes provoked by intensifying disturbance regimes. The study of hurricane effects at different spatial and temporal scales, and making use of multiple research approaches (i.e., experimental, modelling), revealed the major role of debris deposition as a driver for both short-term and long-term responses of soil biogeochemistry. More importantly, it was also demonstrated that soil carbon and nutrient pools tend to be more resilient to repeated hurricane disturbances than forest biomass, with significant future shifts in the relative proportion of forest C stocks. The third chapter was focused on drought responses, which revealed the critical role of soil microclimate as a driver of soil biogeochemical dynamics. Despite the focus on the throughfall exclusion experiment in the third chapter, the occurrence of Hurricane María in 2017 provided an invaluable opportunity to study the interaction between disturbances at yet another spatial and temporal scale. Together, these chapters represent a significant contribution to our understanding of the soil biogeochemical impacts of climate change-induced shifts in disturbance regime on the form and function of wet tropical forests.